12-22-2016

The Role of One-Carbon Metabolism in the Development and Prevention of Colorectal Cancer

Matthew P. Hanley
University of Connecticut, hanley@uchc.edu

The Role of One-Carbon Metabolism in the Development and Prevention of Colorectal Cancer

Matthew Patrick Hanley, Ph.D.

University of Connecticut, 2017

Colorectal cancer (CRC) is the 3rd most common form of cancer in the United States, and the 2nd most common cause of cancer-related death. CRC incidence has declined over the past several decades, however, there is a continued need for improved methods of CRC detection and prevention. Methyl group homeostasis, which is dysregulated in CRC and impacts several fundamental biological processes, represents a promising target for novel CRC detection and prevention strategies. DNA methylation is influenced by methyl group homeostasis and is known to be frequently dysregulated in CRC. However, less is known about the extent of aberrant methylation in early colonic neoplasia. We utilized reduced representation bisulfite sequencing (RRBS) to identify cancer-associated methylation changes in 10 *KRAS*-mutant human aberrant crypt foci (ACF), the earliest precursor to CRC, and 10 primary CRCs. Using this approach, extensive methylation changes were identified in both ACF and CRCs, including hypermethylation of homeobox genes and Polycomb repressive complex 2 (PRC2) gene targets. Furthermore, we show that intergenic binding sites for the transcription factor AP-1 undergo significant hypomethylation. Importantly, 75% of the methylation changes identified in ACF were also present in CRC samples. These data identify epigenomic features of early colonic neoplasia that may provide new targets for CRC detection and prevention.

Folate one-carbon metabolism (FOCM), which regulates methyl group homeostasis, has been proposed as a target for CRC prevention strategies. The present work shows that dietary restriction of the methyl donors folate, choline, methionine and vitamin B12 provides long-lasting tumor protection to the

intestine. Tumor protection was associated with persistent remodeling of intestinal morphology, inhibition of crypt fission, reduced crypt cell mitosis, and increased apoptosis in both normal crypts and tumors. MDD also reduced numbers of crypt cells expressing Dclk1, which have tumor-initiating potential. In a follow-up study, we used untargeted metabolomic profiling to identify MDD-associated changes to several metabolic pathways, including the methionine cycle, the transsulfuration pathway, secondary bile acid synthesis, and fatty acid β-oxidation (FAO). Together, these results indicate that temporary MDD can provide long-lasting tumor protection and identify several pathways that may serve as novel targets for CRC chemoprevention.

The Role of One-Carbon Metabolism in the Development and Prevention of Colorectal Cancer

Matthew Patrick Hanley

B.S., Union College, 2011

A Dissertation

Submitted in Partial Fulfillment of the

Requirements for the Degree of

Doctor of Philosophy

at the

University of Connecticut

2017

2017

APPROVAL PAGE

Doctor of Philosophy Dissertation

The Role of One-Carbon Metabolism in the Development and Prevention of Colorectal Cancer

Presented by

Matthew Patrick Hanley, B.S.

Major Advisor _____
Daniel W. Rosenberg

Associate Advisor _____
Charles Giardina

Associate Advisor _____
Blanka Rogina

Associate Advisor _____
Marc Lalande

University of Connecticut

2017

In memory of

Stephen M. Hanley

and

Robert L. Sullivan

ACKNOWLEDGMENTS

I would like to thank my advisor, Dr. Daniel Rosenberg, for the opportunity to conduct my doctoral research in his laboratory, where I was given the direction and support needed to pursue these challenging projects. I am grateful to have been given independent responsibility for my research, freedom to pursue my own ideas, and the opportunity to explore diverse aspects of science and medicine.

I would also like to thank the members of my committee, Drs. Charles Giardina, Blanka Rogina, Marc Lalande, and Gerd Pfeifer, for their support throughout the course of my studies. Your insight and guidance has been invaluable to the completion of this work.

Special thanks to Dr. Thomas Devers and the members of the GI department, whose tireless labor enabled the clinical research described herein. Additionally, thanks to Margaret Toro and Christopher Sampson for their efforts to ensure our continuous regulatory compliance.

I would like to thank the current and former members of the Rosenberg lab for their support and camaraderie. In particular, David Drew, Allen Mo, Huakang Huang, and Masako Nakanishi have been colleagues and friends without whom I could not have completed this process.

Finally, I'd like to thank my friends and family for their encouragement and understanding throughout this process, and for providing opportunities for respite and reflection. An enormous debt of gratitude is owed for the love and support of Julie Hanley and Caroline Minehan, whose faith in me never wavered.

TABLE OF CONTENTS

LIST OF FIGURES

LIST OF TABLES

Chapter 1: Introduction

1.1 Colorectal Cancer

Together, cancers of the colon and rectum, collectively referred to as "colorectal cancer" (CRC), are the third most commonly diagnosed cancer in the United States (1). In 2016, there were ~130,000 new cases and ~50,000 deaths due to CRC in the US, making this disease the second most common cause of cancer-related death in the country. Incidence and mortality associated with CRC have declined over the past several decades (2), primarily due to improvements in the development and implementation of effective screening modalities. However, the risk of CRC increases dramatically with age (3) and it is anticipated that CRC incidence will increase as the average age of the US population increases (4). Survival rates for CRC remain low; the 5-year survival rate for CRC is 65% overall, and only 11% for cancers detected in Stage IV (1). Thus, there is a continued need for improvements in the early detection and prevention of CRC.

CRC develops slowly, arising *via* a series of precursor lesions in a step-wise progression known as the adenoma-carcinoma sequence. Development of sporadic CRC begins with the acquisition of an "initiating" mutation within a single colonic epithelial cell. The progression of a transformed epithelial cell to carcinoma is driven by the acquisition of molecular aberrations that alter protein structure and function. These molecular changes result in several phenotypic hallmarks, including uncontrolled proliferation, resistance to cell death, and the induction of new vascular growth. Pathologically, this progression is characterized by the growth of small neoplastic foci into larger adenomatous polyps, a subset of which are able to develop into CRC. In cases of sporadic CRC, the mutation that initiates this process is acquired spontaneously as the result of exposure to a mutagen or an error in cellular replication. However, in certain hereditary CRC syndromes, such as Familial Adenomatous Polyposis (FAP), this initiating mutation is passed from generation to generation, greatly increasing an affected individual's risk of CRC. For many reasons, current pharmacological and surgical therapies fail to eliminate advanced tumors (5). An

alternative strategy, which has led to significant reductions in CRC mortality, is to prevent the development of CRC altogether by arresting or reversing the progression of precursor lesions.

1.2 Genetics and Molecular Biology of Colorectal Cancer

1.2.1 Genetic Mutations

The development of CRC is characterized by the accumulation of mutations within tumor suppressors and proto-oncogenes. A tumor suppressor gene is a gene that protects a cell from carcinogenesis by preventing uncontrolled cellular growth. Tumor suppressor genes frequently code for proteins involved in the negative regulation of proliferation and mitosis, the DNA damage response, and the initiation and execution of programmed cell death ("apoptosis"). Inactivation or loss of a tumor suppressor gene enables carcinogenesis by eliminating these important protective mechanisms. In contrast, oncogenes are created by the activation of "proto-oncogenes", normal genes which gain the ability to cause cancer *via* mutation or overexpression. Proto-oncogenes very often code for proteins that are involved in the positive regulation of cell growth and differentiation, and their activation frequently leads to abnormal increases in these processes. Proto-oncogenes are frequently involved in intracellular signaling pathways, especially those regulating mitogenesis. Following mutation, oncogenes promote abnormal activation of mitogenic signaling pathways, increase cellular proliferation, and actively drive tumor growth. Cancers typically harbor multiple mutations, and it is generally accepted that changes to tumor suppressors and oncogenes cooperate to promote oncogenesis.

While a variety of genes can be mutated in CRC, a fairly limited set of genes are mutated with high enough frequency to be considered classical "drivers" of colonic oncogenesis. According to the adenoma-carcinoma sequence originally proposed by Vogelstein (6), inactivating mutations in the tumor suppressor gene *Adenomatous polyposis coli (APC)* are the most common initiating event in colorectal carcinogenesis. This proposal is supported by the observation that *APC* is mutated in up to 80% of CRCs (7). Furthermore,

the hereditary cancer syndrome FAP, which carries a nearly 100% lifetime risk of CRC, is caused by a heritable *APC* mutation (8). APC's primary function is to regulate activation of the mitogenic Wnt-signaling pathway, which is normally involved in the development and regeneration of the intestinal epithelium (9). When the Wnt pathway is inactive, APC forms a "destruction complex" with the proteins Axin, casein kinase 1α (CK1α), and glycogen synthase kinase 3β (GSK3β) that binds the protein β-catenin and targets it for proteasomal degradation (9). When the Wnt pathway is activated, this destruction complex dissociates and β-catenin is able to accumulate within the cytoplasm. At a critical concentration, β-catenin is translocated to the nucleus, where it acts as a coactivator for the TCF/LEF family of transcription factors and upregulates the expression of genes that promote cellular proliferation and migration (9). Loss or inactivation of APC prevents assembly of the destruction complex, leading to constitutive activation of the Wnt signaling pathway and uncontrolled cellular proliferation. In CRC, mutations to *APC* are typically point or frame-shift mutations that lead to the production of a non-functional protein. For sporadic CRC, the majority of these mutations (95%) are located within the "mutational cluster region" (MCR) (10), which is located in exon 15 and spans from codon 1286 to 1580. In hereditary CRC, only 23% of *APC* mutations fall within the MCR.

Another tumor suppressor gene that is commonly mutated in CRC is *TP53*, which codes for tumor protein p53 (p53), a critical regulator of DNA repair, cell cycle progression, and apoptosis that has been described as the "guardian of the genome" (11). *TP53* mutations have been reported in up to 50% of CRCs (11) and are thought to arise late in the adenoma-carcinoma sequence. Normally, p53 is activated by a wide range of cellular stressors including DNA damage, oxidative stress, heat or osmotic shock, and oncogene activation (12). Following activation, p53 induces arrest of the cell cycle at the G1/S checkpoint. If DNA repair is impossible, p53 can also initiate programmed cell death to eliminate the damaged cell (12). Inactivation of p53 leads to the loss of these protective mechanisms and significantly increases the risk of genomic damage and neoplastic transformation. In CRC, inactivation of p53 occurs most frequently

as a result of loss of heterozygosity (LOH) of the short arm of chromosome 17 (11) followed by somatic mutation of the remaining allele. 45% of the "second hits" to p53 occur within 5 "hotspots" (codons 175, 245, 248, 273, and 282) and are C->T transitions thought to result from the deamination of 5-methylcytosine (11).

The majority of proto-oncogenes associated with CRC are involved in the mitogen-activated protein kinase (MAPK) signaling pathway (13). The MAPK pathway is a signal transduction pathway that communicates a mitogenic signal from cell-surface receptors to the nucleus in order to promote cell division (14). Normally, signaling through this pathway is initiated by binding of an extracellular mitogen to the cell-surface epidermal growth factor receptor (EGFR). EGFR activation facilitates the dissociation of GDP from the small GTPase RAS, enabling GTP binding and RAS activation (14). RAS then activates the kinase RAF, which phosphorylates MEK, which in turn activates MAPK. Finally, MAPK activates transcription factors, such as MYC, which are translocated to the nucleus and effect changes to cell physiology, including increased cell division (14). The MAPK pathway genes most commonly mutated in CRC are *KRAS* and *BRAF*, which code for the small GTPase K-ras and the serine/threonine kinase B-raf. *KRAS* and *BRAF* are mutated in 50% and 25% of human CRCs, respectively (13,15). These mutations are thought to arise subsequent to *APC* mutations in the adenoma-carcinoma sequence (16). *KRAS* mutations typically take the form of G>A transitions or G>T transversions (17) and impair GTPase activity, leading to constitutive activation of K-ras. Similarly, BRAF mutations are typically T>A transversions in codon 600 that cause valine to be substituted with glutamate (V600E) in the protein activation domain, leading to constitutive activation of B-raf (18). Mutations in both *KRAS* and *BRAF* lead to constitutive activation of the MAPK signaling pathway and uncontrolled cellular proliferation.

While *APC, TP53, KRAS* and *BRAF* are among the genes most commonly mutated in human CRC, there are mutations to many other genes that have been shown to be associated with human CRC (19). Other frequently mutated genes include cell division control protein 4 (*CDC4*), an inhibitor of cell cycle

progression, transforming growth factor beta 2 receptor (*TGFβ2R*) (20), and "deleted in colon cancer" (*DCC*) (21). However, contributory mutations have been detected in a wide variety of genes, and it is possible for CRCs to develop without acquiring the aforementioned mutations. In fact, a recent genome-wide analysis by Vogelstein *et al.* (22) indicates that the average colorectal tumor carries between 2 and 8 mutations within a set of ~140 genes, all of which contribute directly to a selective growth advantage. Furthermore, this study demonstrated that while these mutations affected three core cellular processes (cell fate determination, cell survival, and genome maintenance), no two tumors shared identical mutational profiles (22).

1.2.2 Epigenetic Alterations

In addition to the established series of mutational events that accompany the adenoma-carcinoma sequence, a number of epigenetic aberrations have been identified in CRC, including altered DNA methylation and covalent histone modifications (23). Furthermore, cancer-associated DNA methylation changes have been found within normal colonic mucosa in patients without tumors, suggesting that certain epigenetic defects may be characteristic of an epithelium that is predisposed to neoplastic transformation (24,25). In CRC, aberrant DNA methylation predominantly takes two forms: global hypomethylation, especially of transposable elements (26–28), and hypermethylation of CpG islands within gene promoter regions (29,30). Global hypomethylation was the first cancer-associated epigenetic defect to be discovered and is now recognized as a common feature of CRC (16). Cancer-associated DNA hypomethylation decreases overall genomic stability by increasing the risk of double-stranded DNA breaks, promoting the instability of repetitive sequences, and reactivating transposable elements (31). In this way, DNA hypomethylation directly contributes to an increased mutational load.

Although global hypomethylation was discovered earlier, gene-specific promoter hypermethylation has been studied in CRC more extensively (29,30). Hypermethylation of CpG islands

within gene promoter regions inhibits the binding of transcription factors and promotes the recruitment of chromatin-remodeling complexes that cause the stabilization of condensed chromatin (32). These changes lead to the transcriptional downregulation of genes coded within these chromatin regions in a process known as "epigenetic silencing" (33). Several key tumor suppressor genes, including *CDKN2A*, *hMLH1*, and *CDH1* have been shown to be epigenetically silenced in CRC (29). Furthermore, preclinical studies have demonstrated the requirement for *de novo* DNA methylation during intestinal adenoma development (34,35). Deletion of DNA methyltransferase 1 and 3a (DNMT1, DNMT3a) has been shown by Eads *et al.* (34) and Weis *et al.* (35), respectively, to prevent intestinal tumor formation in $Apc^{Min/+}$ mice. Site-specific hypermethylation can also cause gene expression imbalances by inducing loss of imprinting (LOI) of parentally-imprinted loci (36). For example, Insulin-like Growth Factor 2 (IGF2), which is normally expressed only from the paternal allele, is frequently overexpressed in CRC due to hypermethylation of the IGF2/H19 imprinting control region (ICR) on the maternal allele, leading to aberrant transcriptional activation (36). Thus, *de novo* methylation directly contributes to colorectal tumorigenesis both by silencing tumor suppressors and by activating proto-oncogenes.

A subset of CRCs that exhibit hypermethylation of a particular set of genes have been described as displaying a CpG island methylator phenotype (CIMP) (37). CIMP-associated CRCs appear to have distinct molecular features (such as frequent *BRAF* mutation) (38), distinct histology (such as serrated hyperplasia) (39), and distinct epidemiology (40), suggesting that they represent a clinically and etiologically distinct class of tumor (40). The observation that many of the genes hypermethylated in CIMP-positive CRCs have important tumor-suppressive functions led to the suggestion that CIMP tumors arise *via* a pathway driven by promoter hypermethylation and epigenetic, rather than genetic, inactivation of tumor suppressor genes (41,42). This "alternative pathway" (42) of colorectal carcinogenesis is now generally accepted, and is believed to have implications for CRC prevention and therapy.

CIMP is defined by hypermethylation of specific sets of genes that are referred to as "CIMP panels". The classical CIMP panel examines methylation of the genes *MINT1, MINT2, MINT31, hMLH1,* and *CDKN2A* (43) and a tumor is considered to be CIMP-positive if it displays hypermethylation at ≥3 of these loci. CIMP positivity has been shown to be associated with the presence of a *BRAF* mutation, proximal tumor location, instability of microsatellite repeats (MSI) and a poor prognosis (44). Attempts to refine the original CIMP panel have led to the development of a "new" CIMP panel that is comprised of the genes *CACNA1G, IGF2, NEUROG1, RUNX3,* and *SOCS1* (44)**.** This new panel has been shown to be superior to the classical panel in the identification of CRCs harboring *BRAF* mutations and MSI, but has inferior prognostic power (44). Notably, it has been shown that the prognostic power of both CIMP panels is maximized when they are combined with analysis of MSI (44). While CIMP analysis has the potential to improve personalized management of CRC, there is currently no consensus on a standardized panel for the clinical identification of CIMP (44).

While epigenetic modifications in CRC have been thoroughly investigated, less is known about their role in early neoplastic progression. Several studies have demonstrated aberrant DNA methylation in colorectal adenomas (45,46). As shown by Luo *et al.* (45)*,* adenomas exhibit considerable epigenetic heterogeneity, but can be broadly classified into those with high-frequency methylation and those with low-frequency methylation. Adenomas with a high frequency of aberrant methylation exhibited methylation signatures similar to those of advanced CRC and had a low frequency of *APC* mutations, suggesting that they might arise *via* a WNT-independent pathway (45). Studies from our laboratory (47) and others (46,48,49), have even identified methylation defects associated with a limited set of genes within human ACF. Chan *et al*. (48) showed that *MINT1*, *MINT2*, *MINT31*, and the tumor suppressor gene *CDKN2A*, were frequently methylated in ACF from patients with synchronous CRC and that these epigenetic modifications were strongly associated with *KRAS* codon 12 mutations. We later demonstrated that the tumor suppressor gene *RASSF1A* is silenced by promoter hypermethylation in distal colon ACF,

even in the absence of synchronous tumors (47). More recently, Inoue *et al.* (46) demonstrated that 6 genes are frequently hypermethylated in *BRAF*-mutant ACF, sessile serrated polyps (SSPs) and cancers located in the proximal colon, providing additional evidence for the role of aberrant methylation in the serrated pathway to CRC. Together, these observations suggest that aberrant DNA methylation patterns may be established prior to adenoma formation and may be important for the promotion of early colonic neoplasia. However, our limited understanding of the epigenetic alterations present in premalignant lesions represents an important barrier to the development of new cancer detection and prevention strategies.

1.2.3 Metabolic Reprogramming

While the first observations of dysregulated metabolism in cancer cells were made nearly a century ago, studies over the last decade have revealed that tumorigenesis is dependent on extensive reprogramming of cellular metabolism (50). This reprogramming affects many distinct metabolic pathways, but a common consequence is a shift towards the generation of biosynthetic building blocks and the ability to acquire necessary nutrients from a frequently nutrient-poor environment (50). These changes enable a cancer cell to fulfill the biosynthetic demands associated with rapid proliferation (50). A number of specific metabolic changes have been detected in CRCs with high frequency (51).

The first metabolic change to be identified in cancer cells was the increased uptake of glucose and the preferential use of glycolysis to produce lactate, a phenomenon known as the “Warburg effect” (52). Glycolysis is an inefficient means of ATP generation compared to oxidative phosphorylation, and so this phenotype was originally thought to represent a defect in the mitochondrial machinery required for oxidative energy production (53). However, recent studies have demonstrated that cancer cells have only a modest increase in ATP consumption relative to their need for biosynthetic precursor molecules and reducing equivalents in the form of NADPH (50). Glucose metabolism is a robust source of these

molecules, while the tricarboxylic acid (TCA) cycle, which generates ATP and NADH, is the major negative regulator of glycolysis (54). Thus, uncoupling of glycolysis from the TCA cycle by converting glucose into lactate prevents TCA cycle-mediated inhibition of glycolysis and enables the robust production of biosynthetic precursors. This phenomenon has been observed in most cancer types, including CRC (55), and has been used as the basis for several new imaging and therapeutic approaches.

Cancer cells upregulate the generation of biosynthetic precursors by diverting glycolytic intermediates into several pathways that branch off from glycolysis. The first of these branching pathways is the pentose phosphate pathway (PPP), which generates NADPH and ribose-5-phosphate, a critical structural component of nucleotides (56). Proteins involved in the PPP have been shown to be almost ubiquitously upregulated in CRC samples (57), suggesting that this pathway is enhanced in CRC. Furthermore, pharmacologic inhibition of the PPP has been shown to be a viable strategy for CRC therapy (57). Perhaps the best studied of the pathways that shunt metabolites out of glycolysis is the use of 3-phosphoglycerate in the synthesis of serine as a means to generate methyl groups (50). Metabolic flux studies have suggested that cancer cells may use as much as 50% of glucose-derived carbon in this pathway (58). Proliferation of CRC cell lines has been shown to be inhibited by withdrawal of serine from the culture media, and the growth of CRC xenografts is inhibited when mice are fed a serine- and glycine-free diet (59), suggesting an increased demand for serine in these cells. Serine has a unique role as a substrate for folate one-carbon metabolism (FOCM), which generates purine nucleotides and S-adenosylmethionine (SAM), the main methyl donor used in DNA methylation reactions (60). Under normal conditions, cells use methionine as the primary substrate for the generation of SAM, but are also able to use serine to generate methionine *via* homocysteine remethylation under conditions of methionine starvation (61). However, recent studies have shown that CRC cells utilize serine for the generation of methionine regardless of methionine availability in the microenvironment, suggesting increased flux through FOCM and the methionine cycle in CRC (61). Interestingly, methylene tetrahydrofolate dehydrogenase 2 (MTHFD2), a

component of the FOCM arm used to generate nucleotides, was shown to be among the top three most frequently overexpressed metabolic enzymes in all cancers (62), suggesting that alterations in FOCM may be universal in tumorigenesis.

CRCs have also been shown to dysregulate various aspects of fatty acid metabolism. Early studies of cancer cell lipid utilization revealed a shift towards the *de novo* synthesis of fatty acids (63) (which is required for plasma membrane synthesis), cell growth, and proliferation. Using broad-spectrum metabolite profiling, Williams *et al.* (64) have demonstrated that primary CRCs exhibit significantly increased levels of many fatty acids, including phosphatidylcholine (PC), the primary plasma membrane constituent. More recent evidence suggests that cancer cells are also capable of utilizing fatty acid oxidation (FAO) as a means of energy production and that certain cancers, including CRC, may use this mechanism preferentially (65,66). FAO is comprised of cyclical reactions that result in the shortening of fatty acid hydrocarbon chains and the production of NADH, $FADH_2$, and Acetyl-CoA in each round of oxidation (66). NADH and $FADH_2$ subsequently enter the electron transport chain (ETC) to produce ATP, and Acetyl-CoA can be used in a variety of biosynthetic processes (66). By mass, fatty acids provide twice as much energy as carbohydrates and are therefore the preferred substrate in situations that require increased ATP production. This is exemplified by cancer cells undergoing loss of attachment (LOA) during metastasis, in which glycolysis is inhibited and levels of ATP and NADPH are depleted (66). As shown by Schafer *et al.* (67), activation of FAO increases levels of ATP and protects cancer cells from anoikis. FAO dependence has been thoroughly documented in certain types of cancer, such as prostate cancer, and has been validated as a viable therapeutic target (68). However, our understanding of the role of FAO in CRC development is currently incomplete.

1.3 Colorectal Cancer Prevention

1.3.1 Risk Factors

There are many genetic and environmental characteristics that can increase an individual's lifetime risk of developing CRC; these characteristics are referred to as "risk factors". Risk factors can be largely classified as "unmodifiable", which are characteristics inherent to the individual that cannot be changed, and "modifiable", which can. Unmodifiable risk factors, such as a personal or family history of CRC, a diagnosis of inflammatory bowel disease or an inherited cancer syndrome, and an individual's ethnic background, can all increase CRC risk. On the other hand, modifiable risk factors are typically behaviors or consumption habits in which an individual knowingly (or sometimes unknowingly) partakes. Habits such as cigarette smoking and heavy alcohol consumption are both strongly associated with CRC incidence, and cessation of both behaviors is associated with clear reductions in risk (69,70). Obesity and a lack of physical exercise have also been shown to increase CRC risk considerably (71,72). Finally, diet has been shown to have a significant effect on the development of CRC, with diets high in fat, refined sugars, and red meat increasing risk, and diets high in fruits and vegetables significantly decreasing risk (73).

The link between the consumption of foods that contain known carcinogens (e.g. alcohol and n-nitroso compound-containing red meat) and CRC risk is particularly well established (74), and it has been estimated that approximately 35% of human CRCs can be attributed to pro-carcinogenic compounds present in the average diet (74). However, it is also known that an individual's diet can be cancer protective (75,76), and just as there are dietary components which are associated with an increased risk of CRC, epidemiological studies have identified a large number of dietary constituents which are associated with a decreased risk of CRC (77). Inverse relationships between intake of selenium, Vitamin D_3 and folic acid and CRC risk have been previously demonstrated (78,79). It has been proposed that dietary components such as these may be useful as the basis for novel chemoprevention strategies (80).

1.3.2 CRC Screening

CRC develops slowly over the course of several decades. This slow development provides the opportunity for the detection and removal of precancerous lesions and early-stage cancers. Currently, the American College of Gastroenterology recommends routine endoscopic screening every 10 years, beginning at age 50 (81). More frequent screening beginning at a younger age is recommended for individuals with a personal history of CRC or adenoma, a first-degree relative with a history of CRC, a diagnosis of IBD, or a hereditary cancer syndrome (81). Increased utilization of screening colonoscopy has significantly reduced the incidence of CRC in the US, as well as associated morbidity and mortality, over the last several decades (82). One study of approximately 2,600 individuals undergoing colonoscopy between 1980 and 1990 found that mortality due to CRC was reduced by 53% after an average follow-up period of 15.8 years (82). Colonoscopy is currently the preferred screening method due to its ability to directly prevent CRC by the removal of precursor lesions (81).

Because CRC is rare in the average screening population, the most common positive outcome of screening colonoscopy is the detection of a polyp, which is typically removed. Patients are stratified into CRC risk categories according to the histopathologic features of polyps identified during colonoscopy. In 2012, the United States Multi-Society Task Force on CRC issued guidelines for postpolypectomy surveillance (83), which updated a previous 2006 guideline. Patients with no polyps, or with only small hyperplastic polyps in the rectum or distal colon, are instructed to return for surveillance colonoscopy after 10 years (83). Patients in whom 1-2 small tubular adenomas or a single sessile serrated polyp are detected are instructed to return in 5 years (83). All other patients, including those with >3 polyps, one or more large tubular adenoma, one or more villous adenoma, one or more large sessile serrated adenoma, or any polyp with high-grade dysplasia, are instructed to return for follow-up colonoscopy in 3 years' time (83). Finally, individuals with a diagnosis of FAP or HNPCC, or those who fit the clinical criteria for serrated

polyposis syndrome, are recommended to undergo annual surveillance colonoscopy due to their high risk of developing CRC (83).

Many additional approaches have been evaluated for their ability to reduce CRC morbidity and mortality. Many of these alternate approaches are non-invasive and are thus the screening method preferred by patients (84). Furthermore, these tests do not require the same degree of medical expertise as colonoscopy and can frequently be self-administered, dramatically reducing costs associated with screening. Thus, while routine colonoscopy remains the screening tool preferred by the American College of Gastroenterology (81), it is thought that the availability of alternative approaches may encourage the screening of individuals who might otherwise choose to dispense with screening altogether (81). Stool blood tests, such as the fecal occult blood test (FOBT) and the fecal immunochemical test (FIT), are the most commonly used non-invasive screening tests. These tests rely on the detection of CRC biomarkers– measurable substances whose presence is indicative of a colonic tumor. The FOBT and FIT are used to detect blood in the stool that is not detectable by eye. Blood detected in this way is non-specific, but may indicate the presence of a tumor. The sensitivity of the FOBT is between 20 and 50%, but it has been estimated that use of the FOBT reduces CRC mortality by 33% (85). More recently, tests designed to detect cancer-specific molecular biomarkers have been approved by the FDA. Cologuard, a DNA test which detects the presence of *NDRG4* and *BMP3* DNA methylation, as well as *KRAS* mutations, has shown efficacy in CRC detection (86), though the long-term effects of this test on CRC morbidity and mortality remain to be seen. Typically, a positive result of one of these tests requires follow-up colonoscopy to confirm the presence of a tumor.

1.3.3 Aberrant crypt foci as surrogate markers for CRC

Aberrant crypt foci (ACF) are the earliest detectable abnormality in the colon and putative precursors to CRC (87–89). ACF were originally discovered by Bird (90) in the colons of mice treated with the chemical

carcinogen azoxymethane (AOM), and were later identified in humans during endoscopy (91). Subsequent study of ACF revealed that they share many histologic and molecular features with adenomas and CRC (47,48,88,89,91). ACF exhibit many of the same genetic abnormalities that are found in more advanced lesions, including the mutations that are traditionally thought to arise early in the adenoma carcinoma sequence. For these reasons, ACF are a promising candidate biomarker for CRC risk.

The histopathological characteristics of ACF can be variable, but ACF are broadly classified into two categories: hyperplastic and dysplastic. Dysplastic ACF are characterized by abnormal proliferation within the upper crypt, nuclear disorganization, and nearly complete loss of goblet cells differentiation (92). Dysplastic ACF frequently exhibit *KRAS* mutations (88,93), and at least one study has reported a high frequency of APC mutations (94), although this frequency may be exaggerated by the inclusion of FAP patients in the study. Because of these histological and molecular features, dysplastic ACF are generally accepted as the earliest precursor to CRC. Hyperplastic ACF display characteristics similar to hyperplastic polyps and exhibit a high incidence of *KRAS* and *BRAF* mutations (88,93). Hyperplastic ACF can be further sub-classified based on the presence or absence of serrated histology. Serrated ACF are defined by a stellate luminal shape in cross-section with a prominent component of columnar crypts with microvesicular cytoplasm (88). While hyperplastic ACF as a whole exhibit both *KRAS* and *BRAF* mutations, *BRAF* alterations have been shown to be the predominant mutation associated with serrated hyperplastic ACF, while *KRAS* mutations are more frequent in non-serrated ACF (88). While hyperplastic ACF were once thought to lack *APC* mutations, it has recently been shown that *APC* mutations can be detected within serrated ACF (94). Interestingly, serrated hyperplastic ACF have previously been shown to be associated with cigarette smoking (95), suggesting a role for this risk factor in the etiology of serrated neoplasia. While dysplastic ACF are generally accepted as a precursor to CRC, there is controversy surrounding the role of hyperplastic ACF in colorectal carcinogenesis. Thus, it will be important to fully characterize the genetic alterations that are present in hyperplastic ACF to better understand the myriad pathways to CRC.

1.3.4 Chemoprevention of CRC

While screening and surveillance remain the most effective strategies for CRC prevention, there has been growing interest in the use of chemoprevention as a complementary strategy for CRC risk reduction. Chemoprevention is the use of pharmacologic or natural agents to inhibit the development of carcinoma by preventing the neoplastic transformation of normal cells, or by arresting or reversing the progression of existing premalignant cells. A large number of natural and synthetic agents have been evaluated for their ability to prevent CRC including non-steroidal anti-inflammatory drugs (NSAIDs), folic acid, calcium, vitamin D, and various anti-oxidants (96). The chemopreventive efficacy of most of these agents remains controversial (96), however, there is good evidence to support the use of certain agents within specific contexts. NSAIDs, especially those that inhibit the enzyme cyclooxygenase-2 (COX-2), such as aspirin, have shown the ability to reduce the incidence of adenomas and CRC in the general population (96) and have been shown to reduce polyp recurrence in individuals with FAP (96). Recently, the United States Preventive Services Task Force (USPSTF) issued a recommendation that aspirin be used for the prevention of CRC in individuals over the age of 50 who are also at an increased risk of cardiovascular disease (97). There is also evidence that calcium supplementation may reduce the risk of adenoma recurrence in individuals with increased risk of CRC, such as those with a personal history of adenoma (96).

Unfortunately, many chemopreventive agents have failed to show efficacy in randomized controlled trials (RCTs), or have had positive RCT results called into question by large meta-analyses. These failures have caused some to question the validity of cancer chemoprevention, even going so far as to claim that chemoprevention causes more harm than good (98). However, advocates of chemoprevention argue that the failure of chemopreventive interventions in large RCTs of human subjects pulled from the general population underscores the need to test the right agents, in the right doses, in the right populations (99). In fact, many chemoprevention trials have failed to examine the efficacy of a given agent

in a population that reflects the preclinical model in which that agent originally demonstrated promise (99). It will be important for future chemoprevention studies to match interventions to the specific subpopulations who stand to benefit most. Furthermore, it will be important to understand how the best chemoprevention strategy for a particular individual may change over time in order to adapt to changes in diet, age, and personal history of neoplasia. In order to fully realize the potential of CRC chemoprevention, novel strategies should be tailored to an individual's unique risk profile.

1.4 Folate One-Carbon Metabolism (FOCM)

1.4.1 FOCM and CRC Risk

Over the last few decades there has been increased interest in how an array of dietary components may affect cancer progression and whether any of these components have potential for use as chemopreventive agents. Folate, also known as vitamin B_9, has been the subject of numerous studies seeking to understand its role in cancer progression (100–105). This is due, in part, to the 1996 mandate by the United States Food and Drug Administration (FDA) requiring the supplementation of wheat, rice, bread, cereals, pasta and other grain products with folic acid in an effort to reduce the incidence of neural tube birth defects (106). Following this mandate, several studies were published that put forth conflicting findings regarding the influence of folate supplementation on colorectal cancer (CRC) progression; nearly two decades later the debate over whether folate promotes or prevents CRC continues. The controversy surrounding the influence of folate on tumorigenesis is likely due to its position at the center of a complex metabolic network that controls a variety of biological processes including nucleotide synthesis, DNA integrity, and epigenetic regulation of gene expression (107,108). It is because of folate's involvement in many biological processes relevant to cancer development, and its potential to modulate these processes, that it has been widely considered for its potential chemopreventive benefit. However, despite significant

potential and a large body of research into its multifaceted functions, understanding of the intricate effects of folate intake and supplementation on cancer risk remains elusive.

The earliest investigations into the relationship between folate and CRC risk were epidemiological case-control studies examining associations between CRC incidence and folate intake determined from dietary questionnaires. Three such studies that were among the first to report on folate intake and CRC risk demonstrated an inverse relationship between folate consumption and CRC incidence (101,109–111). Importantly, all three of these studies were conducted in countries that, at the time, had not implemented folic acid fortification programs and were therefore more likely to have higher incidence of inadequate folate intake. For the most part, studies of folic acid intake and the risk of colorectal neoplasia conducted in the United States after the implementation of the national fortification program have also supported an inverse relationship between intake and risk in the general population (112–114). However, several key studies have challenged this long-standing paradigm. A recent meta-analysis of 50,000 individuals enrolled in 13 different folate supplementation trials failed to show a significant effect of folate intake on CRC risk in the general population (115). Furthermore, several randomized controlled trials of folate supplementation have suggested that elevated folic acid intake may actually *increase* CRC risk in certain high-risk subpopulations (116,117). As shown by Cole and Baron (118), folic acid supplementation (1mg/d) in individuals with a history of colorectal adenoma significantly increases the incidence of advanced lesions at 3-year follow-up. Additionally, a more recent meta-analysis of six large folic acid supplementation trials has concluded that folic acid supplementation is associated with an increased risk of cancer (119).

In contrast to many epidemiologic studies, studies in rodent models have suggested that folate deficiency *slows* tumor progression when it is initiated after the establishment of preneoplasia (120–122). As a result, it has been suggested that folic acid may have a “dual modulatory effect” on carcinogenesis (123); prior to the establishment of neoplastic lesions, high folate intake decreases the risk of cancer,

while high folate intake *after* the establishment of neoplasia drives progression. Thus, within the context of folate-based chemoprevention strategies, careful consideration of dosage and timing with respect to carcinogenic initiation are critical determinants of the safety and efficacy of an intervention. Furthermore, these data suggest that certain high-risk human populations, such as individuals with a personal history of colonic neoplasia, or those with a heritable CRC syndrome, may benefit from reduced folate intake. Thus, improved understanding of the effects of dietary folate modulation on CRC pathogenesis may lead to the development of novel strategies for CRC prevention and treatment.

1.4.2 **Molecular Biology of FOCM**

Folic acid metabolites are used as substrates in the biosynthesis of both thymidylate and purine nucleotides. Once folate has entered the cell, it is reduced to tetrahydrofolate (THF), which acts as the central nexus of FOCM (**Figure 1-1**). THF undergoes a series of enzymatic conversions, with each step in the pathway giving rise to an intermediate that serves a unique role. The most important folate derivatives for nucleotide metabolism are 5,10-Methylene THF and N^{10}-Formyl THF. 5,10-Methylene THF is the substrate for the enzyme thymidylate synthase (TS) which transfers a methyl group from 5,10-Methylene THF to deoxyuridine monophosphate (dUMP) to generate thymidine monophosphate (dTMP) (124). N^{10}-Formyl THF, on the other hand, is the substrate for two enzymes involved in separate steps in the biosynthesis of purine nucleotides: Phosphoribosylglycinamide formyltransferase (GART) and phosphoribosylaminoimidazolecarboxamide formyl transferase (AICARFT) (125,126). GART transfers a methyl group from N^{10}-formyl THF to glycinamide ribonucleotide (GAR) to generate the purine intermediate N-formylglycinamide ribonucleotide (FGAR). Later in the purine biosynthetic pathway, AICARFT transfers another carbon from N^{10}-formyl THF to AICAR to generate the purine intermediate 5-formamidoimidazole-4-carboxamide ribonucleotide (FAICAR) (**Figure 1-1**) (127). Thus, the supply of folate is incredibly important for nucleotide biosynthesis, as it is the primary source of crucial structural carbons

Figure 1-1. Folate One-Carbon Metabolism (A) Overview of folate metabolism. Dietary folate is converted into several key metabolites by a series of enzymatic conversions. (B) 5,10-Methylene Tetahydrofolate is used as the substrate for thymidylate synthesis, where a methyl group is donated to deoxyuridine monophosphate (dUMP) to form deoxythymidine monophosphate (dTMP). (C) 10-Formyl Tetrahydrofolate performs a similar function in the synthesis of the purine nucleotide precursor, inosine monophosphate (IMP). Initially, 10-FTHF donates a formyl group to convert glycinamide ribonucleotide (GAR) to N-formylglycinamide ribonucleotide (FGAR). In a later step, 10-FTHF donates a formyl group to convert 5-Aminoimidazole-4-carboxamide ribonucleotide (AICAR) into 5-Formamidoimidazole-4-carboxamide ribotide (FAICAR). (D) Methyl groups can be shuttled from 5-Methyl Tetrahydofolate (5-MTHF) to the homocysteine cycle, where they are used to regenerate the "universal methyl donor", S-adenosyl methionine (SAM). SAM in turn serves as the substrate for the DNA methyltransferase enzymes, which transfer a methyl group from SAM to cytosine, resulting in the formation of 5-methylcytosine.

Figure 1-1

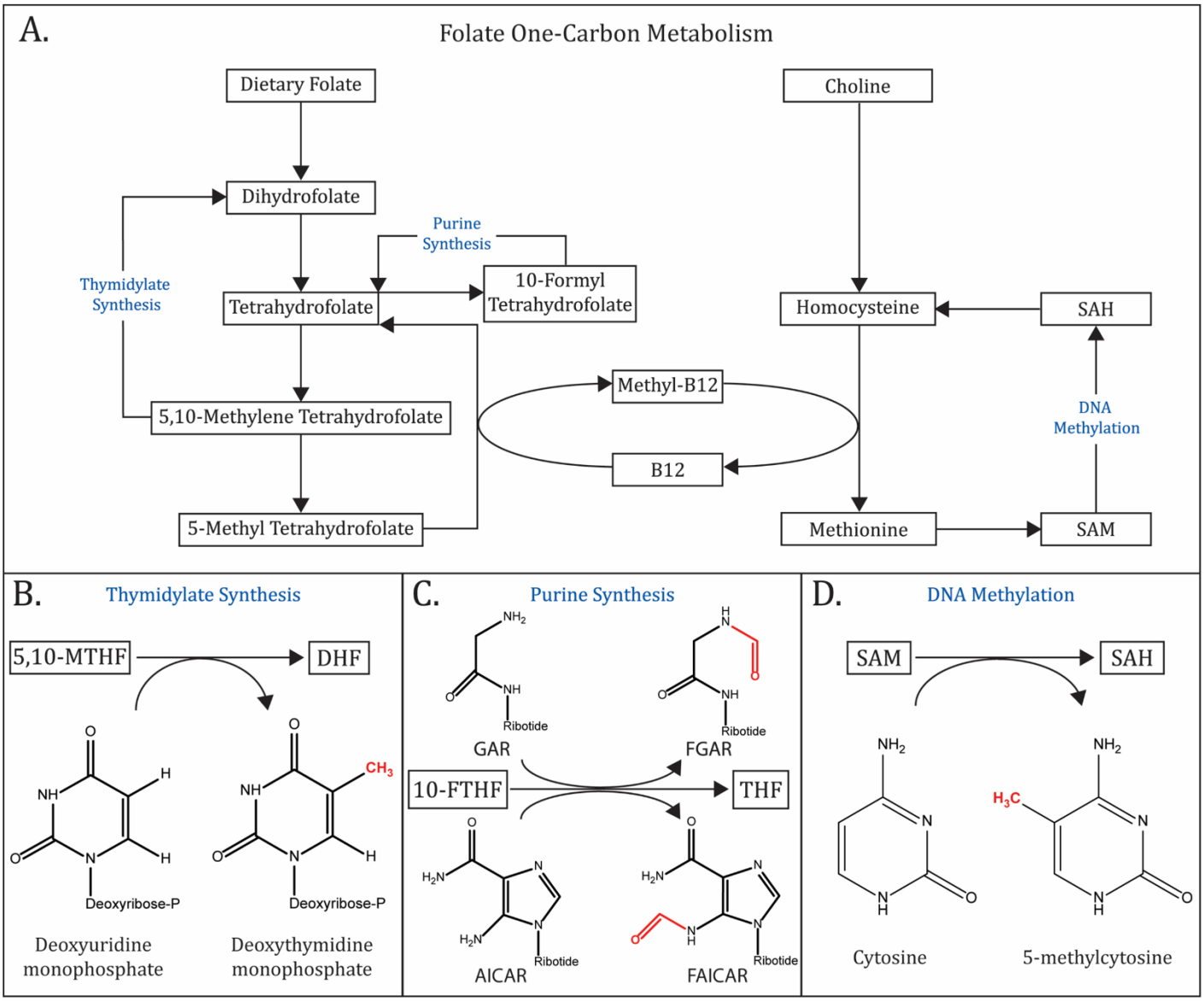
A.
Folate One-Carbon Metabolism
Dietary Folate
Dihydrofolate
Purine Synthesis
Thymidylate Synthesis
Tetrahydrofolate
10-Formyl Tetrahydrofolate
5,10-Methylene Tetrahydrofolate
5-Methyl Tetrahydrofolate
Methyl-B12
B12
Choline
Homocysteine
SAH
DNA Methylation
Methionine
SAM
B.
Thymidylate Synthesis
5,10-MTHF
DHF
Deoxyribose-P
Deoxyuridine monophosphate
Deoxythymidine monophosphate
C.
Purine Synthesis
Ribotide
GAR
FGAR
10-FTHF
THF
AICAR
FAICAR
D.
DNA Methylation
SAM
SAH
Cytosine
5-methylcytosine

in purine precursors and of the carbon that is necessary to convert dUMP to dTMP. Imbalances in these key folate metabolites have previously been detected in colorectal tumors, underscoring the relevance of this metabolic pathway to colon carcinogenesis (128).

It is folic acid's role in nucleotide metabolism that has made it an interesting chemopreventive candidate from a mechanistic standpoint. It has been hypothesized that folate deficiency causes DNA damage by reducing the availability of nucleotide synthesis precursors and thus causing an imbalance in nucleotide pools (129). However, this same mechanism might help to explain the inhibitory effect of folate deficiency on the growth of established neoplasia. Cells which have undergone transformation tend to have a higher rate of replication and a higher demand for nucleotides than their comparatively slow-replicating normal counterparts. In transformed cells, low folate status places a severe restriction on nucleotide biosynthesis, inhibiting DNA replication and slowing tumor growth (130). A recent study by Witherspoon (131) revealed that the chemopreventive agent α-difluoromethylornithine (DFMO) exerts its protective effects by altering the availability of folate derivatives, supporting this hypothesis.

A second mechanism through which folate intake has been proposed to offer chemopreventive benefit is the modulation of DNA methylation. The supply of one-carbon groups used in methylation reactions is dependent on metabolic flux through the methionine cycle (132), which generates SAM, the "universal methyl donor". Dietary folic acid is eventually converted to the metabolite 5-methyltetrahydrofolate (5-MTHF); a methyl group is then transferred to homocysteine to generate methionine, which reacts with ATP to generate SAM. SAM is the substrate for DNMTs, which transfer a methyl group to DNA CpGs, converting SAM to S-adenosyl homocysteine (SAH) and the target cytosine to 5-methylcytosine (**Figure 1-1**) (133). The availability of SAM and SAH are important regulators of DNMT activity and the maintenance of patterns of DNA methylation. Considering the importance of folate for homocysteine metabolism and DNA methylation, it has been suggested that folate-based chemoprevention may help to maintain normal patterns of methylation (108,134,135).

While nucleotide biosynthesis and DNA methylation are the best-characterized folate-dependent molecular mechanisms, steps still need to be taken to understand how the role of FOCM in cancer risk changes throughout the carcinogenic process. As a cell acquires more genomic changes and progresses towards cancer its metabolic demands change. This should be taken into account when considering a biosynthesis-based mechanism of folate chemoprevention.

1.5 Specific Aims

Aim 1: **To characterize the landscape of aberrant DNA methylation in human colonic preneoplasia**

ACF are the earliest detectable abnormality in the colon and putative precursors to CRC that share many histologic and molecular abnormalities with colonic adenomas and carcinomas. While extensive epigenetic modifications are a common feature of CRC, their role in early neoplastic progression is less well defined. To address this deficit, we will use an integrative genomic approach to identify functional DNA methylation changes in human ACF. We will combine laser-capture microdissection (LCM) with reduced-representation bisulfite sequencing (RRBS) and whole-genome RNA sequencing (RNA-Seq) to characterize changes to DNA methylation and gene expression in a set of 10 ACF and 10 Stage III-IV primary CRCs. These data will contribute to a more in-depth understanding of the DNA methylation changes that are present in early colonic neoplasia, and may lead to the identification of new targets for CRC detection and prevention.

Aim 2: **To evaluate the preventive efficacy of temporary dietary methyl donor deficiency**

Folate one-carbon metabolism (FOCM) is the metabolic system that converts a group of nutrients referred to as "methyl donors" into one-carbon moieties that are used in nucleotide biosynthesis and DNA methylation. Disruption of FOCM has been used successfully for many years as a strategy to treat CRC. However, less is known about how disruption of FOCM *via* manipulation of dietary methyl donors can be used to *prevent* colorectal carcinogenesis. We have previously shown that a diet deficient in the methyl donors folate, choline, methionine and vitamin B12 is able to suppress tumor formation in $Apc^{Min/+}$ mice. In this aim, we will extend our previous studies by examining the effects of dietary methyl donor deficiency (MDD) in a mouse model with an *Apc* truncation mutation more typical of that found in human cancers and a higher prevalence of colon tumor development. Furthermore, we will specifically determine

whether temporary MDD, followed by re-feeding with a methyl donor sufficient (MDS) diet, is capable of providing long-lasting tumor protection while reversing unwanted side effects.

Aim 3: **To define the metabolic changes associated with MDD cancer protection**

We have previously demonstrated that a MDD diet protects against tumor formation in $Apc^{Min/+}$ mice. At present, the metabolic pathways through which the MDD diet affects changes to the intestinal epithelium and reduces CRC risk are unknown. We will use an untargeted metabolomic profiling platform to quantify ~400 biochemicals within samples of colonic mucosa collected from mice in Aim 2. We will then employ pathway analysis to identify the specific metabolic pathways that are critical to the protective effects of MDD. In addition, we will identify any metabolic changes that persist beyond temporary administration of the MDD diet. These data will provide clues to the molecular changes underlying MDD-induced tumor protection and identify metabolomic features of the MDD diet that may provide new targets for CRC prevention.

Chapter 2: Genome-wide methylation profiling reveals cancer-associated changes within human early colonic neoplasia

2.1 Introduction

Colorectal cancer (CRC) is the second-leading cause of cancer-related deaths in the U.S (1). In addition to the established series of mutational events that accompany the adenoma-carcinoma sequence, a number of epigenetic aberrations have been identified in CRC, including altered DNA methylation and covalent histone modifications (23). Global DNA hypomethylation, first identified in cancers more than three decades ago, is now recognized as a common genetic feature of CRC (26). DNA hypomethylation promotes genomic instability (27), in many cases leading to an increased mutational load and activation of proto-oncogenes (27). On the other hand, gene-specific promoter hypermethylation has been shown to promote CRC by silencing the expression of key tumor suppressor genes such as *CDKN2A*, *hMLH1* and *CDH1* (29).

While extensive epigenetic modifications are a common feature of CRC, their role in early neoplastic progression is less well defined. As reviewed by Sakai et al. (30), changes to DNA methylation have been found at early stages of cancer development, particularly in colorectal adenomas. Specific DNA methylation changes have even been found within normal colonic mucosa of patients with CRC (24,25), suggesting the possibility that epigenetic defects may predict subsequent cancer risk. Aberrant crypt foci (ACF) are the earliest morphologically identifiable mucosal abnormality in the colon, a subset of which may be precancerous and contribute to a "field defect" within the mucosa (136). Studies from our laboratory (47) and others (48,49) have identified methylation defects associated with human ACF, including the silencing of tumor suppressor genes by promoter hypermethylation. An early study by Chan *et al*. (48) showed that *MINT1*, *MINT2*, *MINT31*, and the tumor suppressor gene *CDKN2A*, were frequently methylated in ACF from patients with synchronous CRC. This study further reported that increased DNA methylation in ACF was strongly associated with the presence of *KRAS* codon 12 mutations (48). We later

demonstrated that the tumor suppressor gene *RASSF1A* is silenced by promoter hypermethylation in distal colon ACF, even in the absence of synchronous tumors (47). These observations suggest that aberrant DNA methylation patterns may be established prior to adenoma formation and may be important for the promotion of early colonic neoplasia.

Our limited understanding of the molecular alterations present in premalignant lesions represents an important barrier to the development of new cancer detection and prevention strategies (137). To address this issue, the present study was undertaken to develop a more in-depth understanding of the DNA methylation changes that are present in human ACF. To achieve the requisite sensitivity for analysis of isolated colonic epithelial cells, we combined reduced representation bisulfite sequencing (RRBS) with laser-capture microdissection (LCM) of ACF harboring mutations in exon 2 of the *KRAS* oncogene. RRBS is an efficient, high-throughput sequencing technique that combines sodium bisulfite conversion of unmethylated cytosines with *MspI* restriction digestion to enrich samples for CpG-rich regions of the genome (138). Using this approach, we have shown that *KRAS*-mutant ACF harbor extensive DNA methylation changes, many of which are also present in primary CRCs. ACF-associated methylation changes were enriched for genes involved in cellular identity and differentiation, a set of genes targeted by the Polycomb Repressive Complex 2 (PRC2), and genomic regions containing AP-1 transcription factor binding sequences. These observations extend the scope of aberrant methylation in the earliest stages of colonic neoplasia and define features of an epigenomic landscape that may provide new targets for CRC detection and chemoprevention.

2.2 Materials and Methods

Subject selection and human tissue collection

All ACF subjects included in this study were enrolled in an ongoing clinical study at John Dempsey Hospital (UConn Health). All patients who met the Amsterdam criteria for familial adenomatous polyposis

(FAP) or hereditary non-polyposis CRC (HNPCC) were excluded from this study. In order to control for the effects of age and smoking on DNA methylation, all selected subjects were non-smokers between the ages of 50 and 65. 10 ACF were biopsied from the distal colons of individual subjects as previously described (88). Briefly, ACF were identified and biopsied during high-definition, magnifying chromoendoscopy using indigo carmine dye-spray (88). For each subject, a sample of normal-appearing mucosa was also obtained from the distal colon. Biopsies were immediately embedded in OCT freezing medium (Neg 50, ThermoFisher Scientific), flash-frozen, and stored at -80°C. Frozen tissues were sectioned onto polyethylene naphthalate (PEN, ThermoFisher Scientific) membrane slides using a Leica CM1900 Cryostat. Frozen sections were stained with hematoxylin and eosin (H&E) and routine histologic analyses were performed**.** All biopsies collected from ACF subjects were histologically confirmed by a board-certified human gastrointestinal pathologist blinded according to previously established criteria (88).

Ten Stage III-IV CRCs resected from the distal colons of individual subjects were obtained from the City of Hope frozen tumor bank. In addition, 10 histologically-confirmed matched normal samples, collected from the margins on either side of the resected tumor, were obtained. Tissue sections were stained with H&E and reviewed by a board-certified pathologist to confirm the presence and histopathology of the lesions. This study was conducted with the written informed consent of each subject, as well as Institutional Review Board approval from both the University of Connecticut Health and City of Hope (IRB Protocols IE-10-068OSJ-3 and 97134, respectively).

Laser-capture microdissection

LCM of ACF and matched normal biopsies was performed as previously described (88). Briefly, an ArcturusXT Laser Capture Microdissection system was used to isolate a minimum of 1 mm^2 of tissue (~5000 cells) from 12 µm-thick frozen serial sections. LCM caps were stored at -80°C until nucleic acid extraction.

DNA methylation profiling and mutation screening

Genomic DNA was isolated from laser-captured colonic crypt epithelium using phenol/chloroform extraction. *KRAS* Exon 2 was amplified by PCR using targeted primers (5'GGTCCTGCACCAGTAATATG and 5'AACCTTATGTGTGACATGTTCTAA) and sequenced at the City of Hope Integrative Genomics Core using Sanger sequencing. Only ACF and cancer samples with a mutation in *KRAS* Exon 2 ($KRAS^{G12D}$ or $KRAS^{G12V}$) were selected for further analysis by RRBS. RRBS was done as previously described (139). Briefly, purified DNA was digested by overnight incubation with MspI at 37°C. Following restriction digest, DNA fragments were subjected to end repair and A-tailing, followed by linker ligation. Bisulfite conversion was done using the EZ DNA Methylation-Gold Kit (Zymo Research) according to the manufacturer's instructions. RRBS libraries were sequenced on the HiSeq 2500 (Illumina) using 100 bp paired-end sequencing according to the manufacturer's protocol. A minimum of 14 million reads/sample were aligned to human reference genome assembly hg19. For RRBS analysis, genomic regions were defined as sequences containing a minimum of 2 CpGs separated by no more than 100 bp. Differentially methylated regions (DMRs) were defined as genomic regions exhibiting an average change in methylation ≥15% compared to matched normal, with a false discovery rate (FDR)-adjusted p-value < 0.05. Bootstrapping analysis was performed as a control for the identification of overlapping DMRs by generating 1,000 sets of 811 randomly selected DMRs, calculating the average number of overlapping DMRs in these sets and comparing the expected value to the observed number of overlapping DMRs. As shown in **Figure 2-1**, data obtained using RRBS from independent sequencing runs were highly reproducible.

A

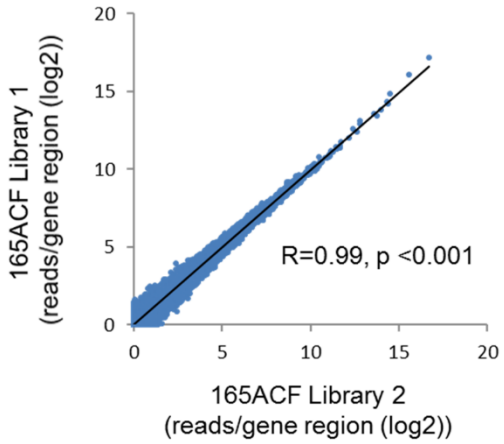

B

Comparison of Independent Sequencing Runs	Pearson's Correlation Coefficient
20ACF Run 1 vs 20ACF Run 2	0.98
20N Run 1 vs 20N Run 2	0.98
2ACF Run 1 vs 2ACF Run 2	0.97
2N Run 1 vs 2N Run 2	0.98

Figure 2-1. Internal controls for reduced representation bisulfite sequencing and RNA-Seq analysis. (A) Parallel RNA sequencing runs of two independent library preparations from the same ACF sample show a high correlation between the number of successfully mapped reads per genomic region. (B) Correlation between multiple sequencing runs from the same library for 2 ACF and 2 samples of normal colonic mucosa. Correlation coefficients were calculated for the total number of successfully mapped reads for individual CpGs with a minimum of 10 mapped reads, excluding those within *Msp1* restriction sites (CCGG).

Transcriptome profiling

RNA was isolated from cancer samples using the mirVana miRNA Isolation Kit (Ambion) and from laser-captured ACF samples using the Arcturus PicoPure Frozen RNA Isolation Kit (ThermoFisher) according to the manufacturers' instructions. Sequencing libraries were prepared from RNA isolated from cancer samples using the TruSeq Stranded Total Library Preparation Kit and the RiboZero Gold rRNA Removal Kit (Illumina). For RNA extracted from ACF, depletion of rRNA was done using the RiboZero Magnetic Kit according to the "Protocol for Removal of rRNA from Small Amounts of Total RNA" (Clontech). Subsequently, dscDNA library preparation and amplification were done using the SMARTer Stranded RNA-Seq Kit (Clontech) according to the manufacturer's protocol. RNA sequencing for both sample types was done on the HiSeq 2500 (Illumina) using 40-bp paired-end sequencing according to the manufacturer's protocol. A minimum of 40 million reads/sample were aligned to the human reference genome assembly hg19. As shown in **Figure 2-1**, data obtained using RNA-seq from two independent library preparations were highly reproducible

Bioinformatics Analysis

Gene ontology (GO) analysis was conducted using the Database for Annotation, Visualization, and Integrated Discovery (DAVID) according to standard protocol (140). Briefly, GO analysis was done using the statistical overrepresentation test with Bonferroni correction for multiple testing. Gene set enrichment analysis (GSEA) was performed by calculating the overlap of gene sets of interest with annotated gene sets stored in the Molecular Signatures Database (MSigDB) version 5.1 (Broad Institute, Cambridge MA)(141). Comparison of DMRs to H3K27Ac-marked enhancer regions was done using ENCODE dataset ENCSR327XTS. Hypergeometric Optimization of Motif EnRichment (HOMER) analysis (142) was used to evaluate the enrichment of known transcription factor binding motifs located within differentially methylated regions of the genome. Bootstrapping analysis was performed as a control for

HOMER by generating 1,000 sets of 297 randomly selected intergenic regions, calculating the expected percent enrichment for motifs of interest and comparing this value to the observed percent enrichment.

Statistical Analysis

The set of genomic regions with frequently altered DNA methylation was subjected to complete linkage clustering using a Euclidean distance measure. Correlation between changes in promoter methylation and changes in gene expression were estimated by Pearson's correlation analysis. Statistical analyses of differentially methylated regions (DMRs) and differentially expressed genes were performed using Student's *t*-test followed by false discovery rate (FDR) correction using the Benjamini-Hochberg procedure. Principal component analysis (PCA) and biplot generation were done using the R programming language and software environment.

2.3 Results

Genome-wide DNA methylation changes in colon cancers and ACF

To investigate the epigenomic landscape of early colonic neoplasia, RRBS analysis was used to identify DNA methylation changes in stage III-IV CRCs and ACF biopsied from the distal colon; representative images of an ACF visualized during endoscopy and its histological appearance are shown in **Figure 2-2A**. Differentially methylated regions (DMRs), defined as genomic regions exhibiting an average change in methylation ≥ 15% compared to matched normal that achieved a false-discovery-adjusted p-value < 0.05, were used for all subsequent analyses. The heat-map shown in **Figure 2-2B**, generated by unsupervised clustering, shows DMRs identified in CRC. A total of 23,745 DMRs were identified, consistent with previous reports that aberrant DNA methylation is a common feature of CRC (30). 5,995 (25%) of these DMRs were hypermethylated, while 17,750 (75%) were hypomethylated.

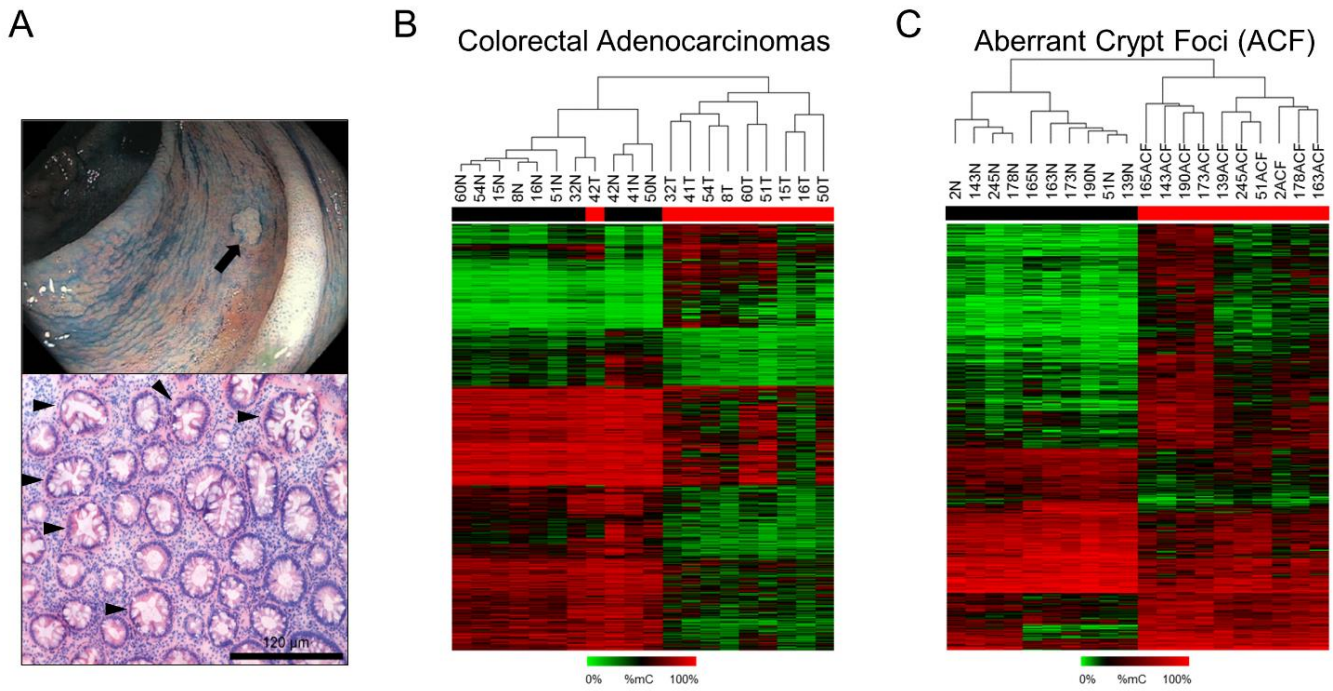

Figure 2-2. DNA methylation patterns in Stage III-IV CRCs and ACF. (A) (Top) Gross appearance of a human ACF during endoscopic screening. (Bottom) H&E-stained slide showing an ACF biopsy with serrated morphology. Serrated crypts, characterized by star-shaped lumen in cross section, are indicated with black arrows. (B) Heat-map depicting differentially methylated regions (DMRs), defined as genomic regions with a change in methylation relative to matched normal >15% and a FDR-adjusted P-value<0.05, in colon cancer samples. In general, tumor samples are segregated from normal mucosa by unsupervised clustering, indicating distinct methylation profiles. Of the 23,745 DMRs detected in cancer samples, 5,995 (25%) were hypermethylated while 17,750 (75%) were hypomethylated, indicating a trend towards decreased global methylation. (C) Heat-map depicting DMRs in ACF. In general, ACF are segregated from normal mucosa samples by unsupervised clustering, indicating distinct methylation profiles. 811 DMRs were identified, 537 (66%) of which were hypermethylated and 274 of which (34%) were hypomethylated, indicating a trend towards increased global methylation that contrasts the global methylation status of cancer samples.

Methylation changes were also found in ACF (**Figure 2-2C**); 811 regions were differentially methylated compared to matched normal mucosa. However, in ACF, 537 (66%) of these DMRs were hypermethylated, while only 274 (34%) were hypomethylated, indicating an *increase* in global methylation. The difference in net methylation change between ACF and CRC suggests that a shift in global methylation status may be important for progression from early neoplasia to invasive CRC.

To gain a better understanding of the functional significance of methylation changes found in ACF, GSEA was used to compare the set of all ACF DMRs to annotated functional gene sets stored in the Molecular Signatures Database (Broad Institute, Cambridge, MA) (141). GSEA identified enrichment for transcription factors involved in intestinal development, including *CBFA2T2, FOXF1, NKX2-3, NOTCH1, PAX6,* and *PDGFA* (**Figure 2-3**) (143–148). In addition, this set of genes was enriched for targets of PRC2 identified in human embryonic stem cells (hESCs) (149). PRC2 is a chromatin-remodeling complex involved in the maintenance of stem cell plasticity (150). Furthermore, ACF-associated DMRs showed enrichment for genes known to be trimethylated at lysine 27 of histone subunit 3 (H3K27me3, the "polycomb mark") in normal adult colonic mucosa (151). Finally, genes with frequent methylation changes in ACF contained a number of HOX genes (*HOXA3, HOXC9, HOXC10, HOXC11,* and *HOXC13*), a family of early developmental regulators whose aberrant expression has previously been implicated in human carcinogenesis (152). These findings demonstrate that genes involved in normal intestinal development and genes targeted by PRC2 in embryonic stem cells frequently exhibit methylation changes in human ACF and suggest a role for the epigenetic disruption of these genes in the establishment of early neoplasia.

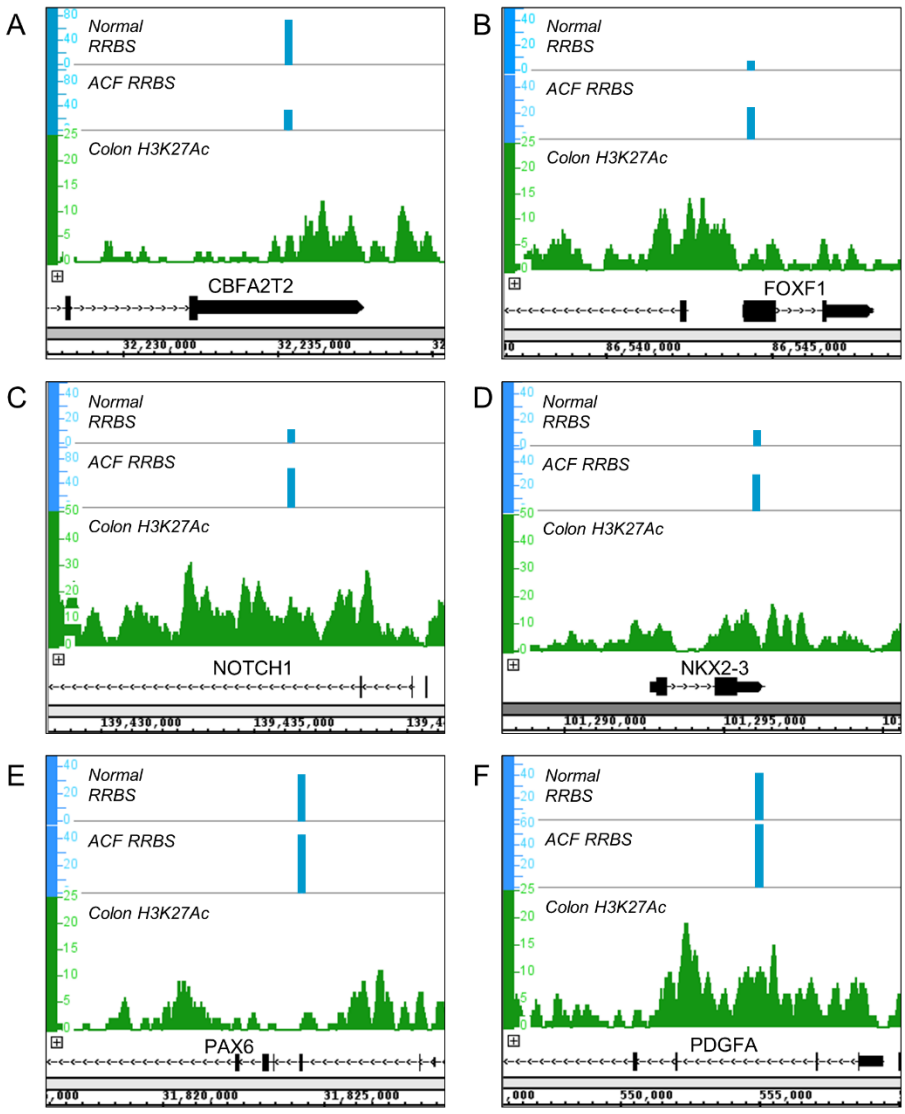

Figure 2-3. Representative sequencing tracks showing aberrant methylation of genes involved in normal intestinal development. DMRs associated with these genes tended to overlap with H3K27Ac peaks identified in normal colonic mucosa, suggesting that they occur within active enhancer regions. H3K27Ac data was obtained from the ENCODE project (Accession: ENCSR327XTS).

Cancer-associated methylation changes are present in ACF

In the following analyses, methylation profiles of DMRs present in CRCs and ACF samples were normalized to matched normal-appearing mucosa. As shown in **Figure 2-4A**, data were clearly separated by PCA, indicating distinct methylation profiles, although ACF showed tighter overall clustering than tumors. Despite segregation by PCA, a subset of genomic regions was classified as DMRs in both cancer and ACF samples (**Figure 2-4B**). Of these shared DMRs, the majority exhibited methylation changes in the same direction (66% hypermethylated, 32% hypomethylated) and are referred to as "overlapping" DMRs. In general, these methylation changes were of greater magnitude in cancers than in ACF, regardless of the direction of change or the genomic location of the altered region.

As shown in **Figure 2-5A**, 592 DMRs were classified as overlapping. Bootstrapping analysis confirmed that this degree of overlap between ACF and CRC DMRs was highly significant (**Figure 2-5B**). Approximately 75% of all DMRs identified in ACF overlapped with CRC DMRs. Hypermethylated overlapping DMRs were evenly distributed among promoters (139, 35%), gene bodies (147, 37%) and intergenic regions (113, 28%) (**Figure 2-5C**). In contrast, hypomethylated overlapping DMRs occurred mainly within gene bodies (84; 44%) and intergenic regions (104; 53%); only 5 (3%) were located in promoter regions (**Figure 2-5C**). As shown in **Figure 2-6A**, GSEA revealed that overlapping DMRs were frequently associated with homeobox genes. As shown in **Figure 2-6B**, overlapping DMRs associated with homeobox genes were frequently hypermethylated.

Non-promoter DMRs undergo a switch in methylation status during cancer development

To better define the methylation landscape of early and late colonic neoplasia, all DMRs were separated according to their genomic location into gene body, intergenic, and promoter DMRs. 8,849 (37%) cancer-associated DMRs were located within gene bodies, 12,170 (51%) were located in intergenic

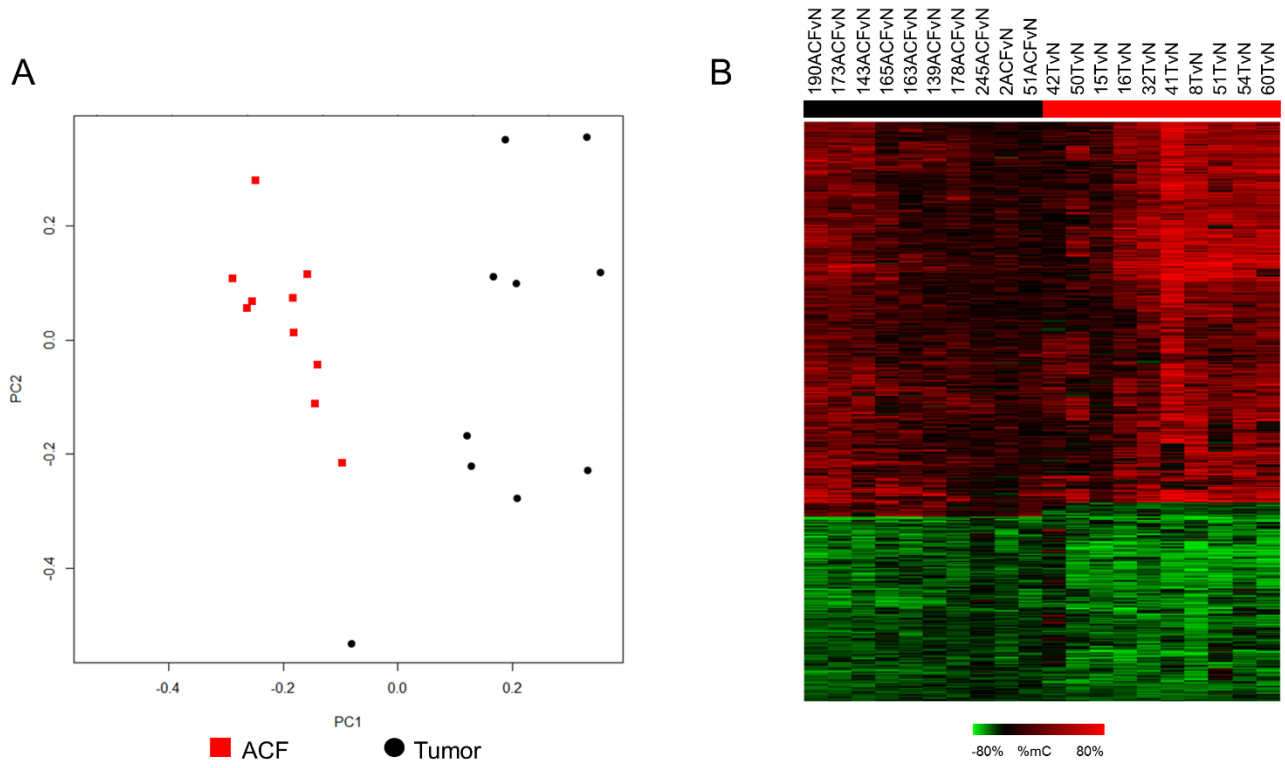

Figure 2-4. Direct comparison of DNA methylation changes in Stage III-IV CRCs and ACF. (A) Principal component analysis (PCA) biplot of DNA methylation changes demonstrates a clear segregation of ACF (red) and tumor samples (black), indicating distinct aberrant methylation profiles. CRC samples are less tightly clustered than ACF samples, suggesting greater variability within cancer samples. (B) Heat-map depicting DMRs detected in both ACF and CRC. Of 608 shared DMRs, 66% were hypermethylated and 32% were hypomethylated; a small subset of DMRs (2%) were hypermethylated in ACF but hypomethylated in cancer. Notably, the magnitude of these overlapping changes was typically greater in CRC than in ACF.

Figure 2-5. Genomic distribution of "overlapping" DMRs. (A) 592 DMRs exhibited a methylation change in the same direction in both stage III-IV cancers and ACF; these DMRs are referred to as "overlapping" DMRs (B) Histogram depicting the results of bootstrapping control analysis for overlapping DMR analysis. On average, randomly generated genomic region sets contained 9.6 ± 3.1 overlapping DMRs, significantly fewer than the 592 observed real overlapping DMRs ($P<0.001$), indicating that the probability of identifying these overlapping DMRs by random chance is very low. (C) Distribution of the genomic location of DMRs with altered methylation identified in both ACF and CRC. Overlapping hypermethylated DMRs were evenly distributed amongst promoters (35%), gene bodies (37%) and intergenic regions (28%). Overlapping DMRs exhibiting hypomethylation were rarely located within promoters (3%), but were common in gene bodies (44%) and intergenic regions (53%). (D) Distribution of the genomic location of all DMRs (increased and decreased methylation) in ACF and CRC. While the genomic distribution of DMRs identified in ACF was very similar to the distribution of all sequenced regions, DMRs identified in cancer samples exhibited a bias towards non-promoter localization.

Figure 2-5

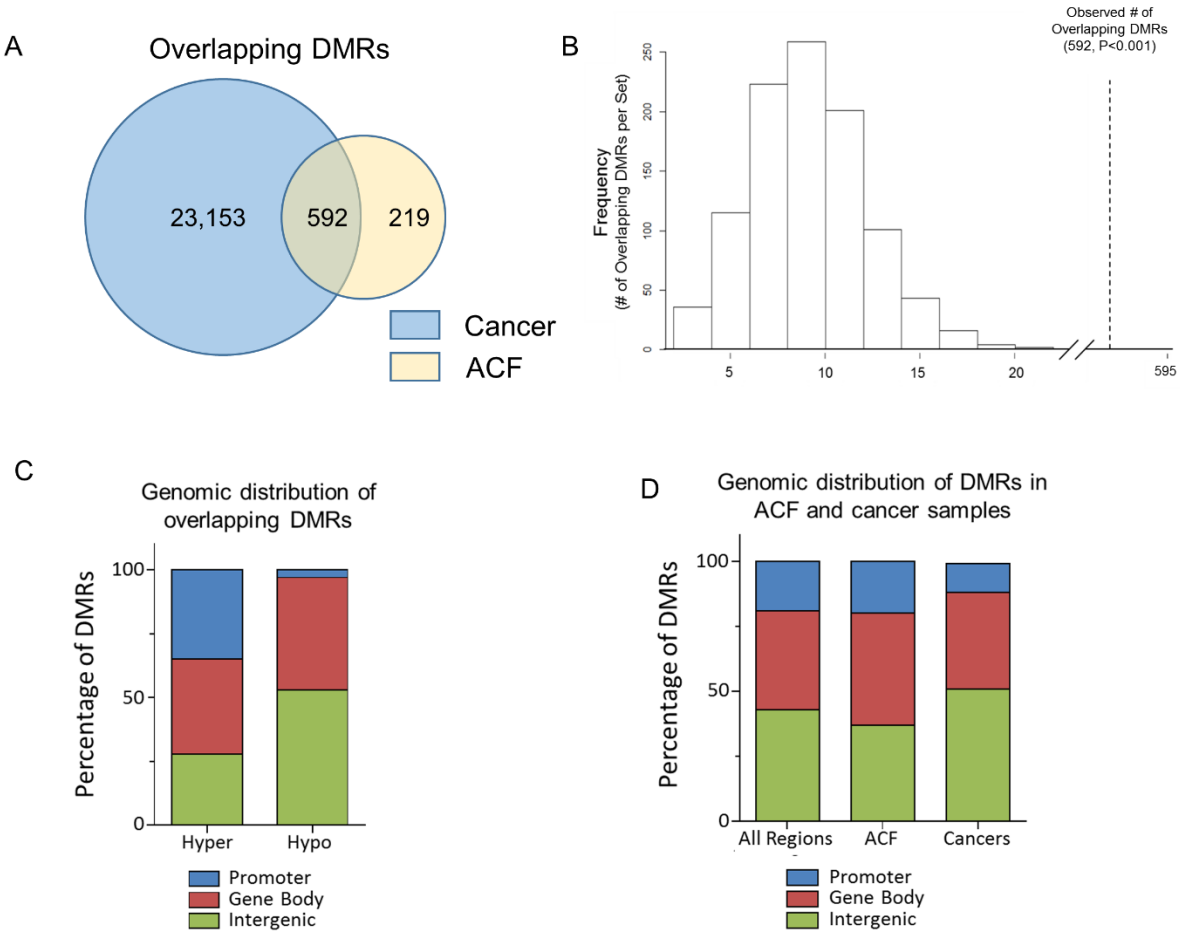
A
Overlapping DMRs
23,153
592
219
Cancer
ACF
B
Observed # of Overlapping DMRs (592, P<0.001)
Frequency (# of Overlapping DMRs per Set)
0
50
100
150
200
250
5
10
15
20
595
C
Genomic distribution of overlapping DMRs
Percentage of DMRs
0
50
100
Hyper
Hypo
Promoter
Gene Body
Intergenic
D
Genomic distribution of DMRs in ACF and cancer samples
Percentage of DMRs
0
50
100
All Regions
ACF
Cancers
Promoter
Gene Body
Intergenic

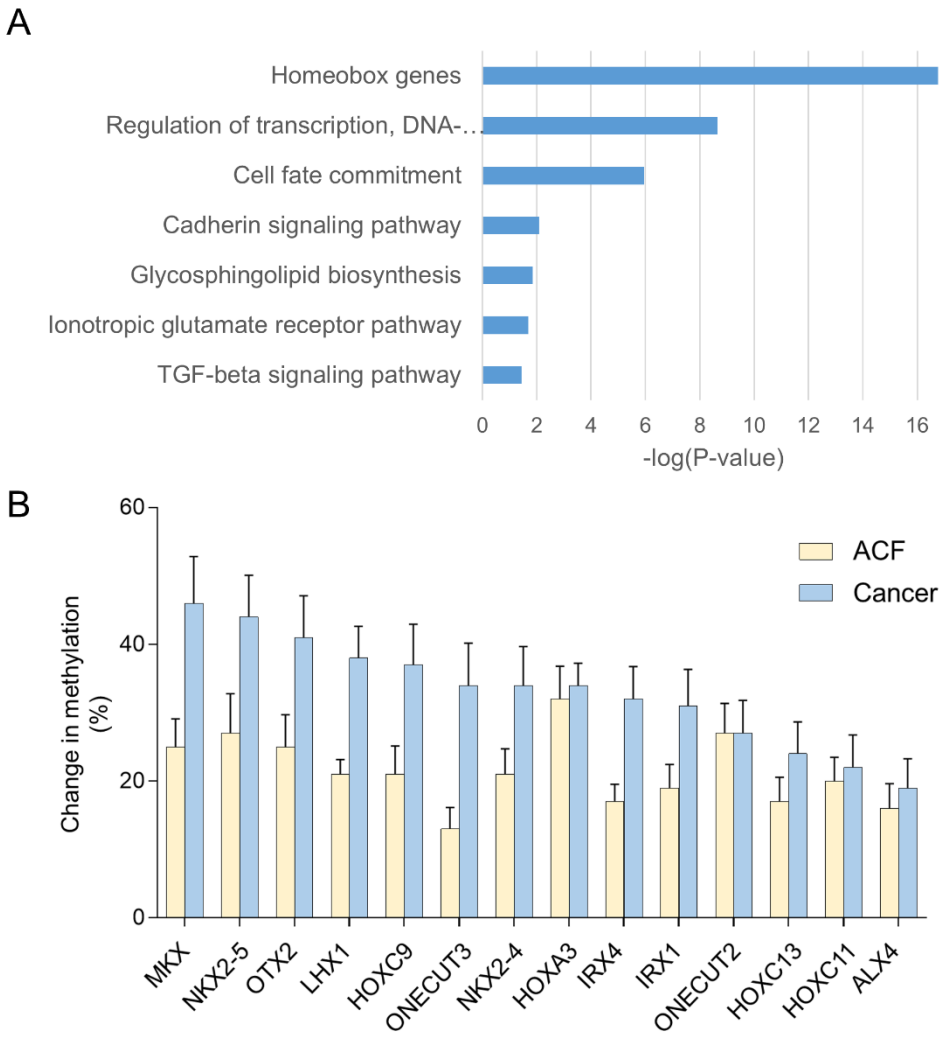

Figure 2-6. Functional enrichment analysis of overlapping DMRs. (A) GO results for overlapping DMRs. Overlapping DMRs were significantly enriched (FDR-adjusted P-value <0.05) for homeobox genes, as well as genes involved in the regulation of transcription and cell fate commitment. (B) Selected representative homeobox genes with increased methylation in both ACF and cancer. All of the genes shown here exhibit significantly increased methylation in both ACF and cancer samples compared to matched normal tissues; notably, the magnitude to which methylation is increased tends to be greater in cancer than in ACF. Error bars represent SEM.

regions, and 2,726 (11%) were located within known promoter regions, indicating more extensive methylation changes within non-promoter regions in CRC (**Figure 2-5D**). Similarly, of the 811 DMRs found in ACF, 349 (43%) were located within gene bodies, 297 (37%) were located in intergenic regions, and 165 (20%) were located within promoters (**Figure 2-5D**).

In cancers, DMRs in non-promoter regions were primarily hypomethylated compared to matched normal; 6,591 (74%) gene body-associated DMRs were hypomethylated (**Figure 2-7A**) and 10,401 (85%) intergenic DMRs were hypomethylated (**Figure 2-7B**). In contrast, 213 (61%) gene body-associated DMRs were hypermethylated (**Figure 2-7A**) and 168 (57%) intergenic regions were hypermethylated (**Figure 2-7B**) in ACF samples. Together, these results suggest that genome-wide DNA hypomethylation occurs during later stages of CRC progression. In contrast to gene bodies and intergenic regions, the majority of promoter DMRs in both cancers (1,968, 72%) and ACF (165, 95%) were hypermethylated (**Figure 2-7C**).

Intergenic DMRs are enriched for AP-1 family transcription factor binding motifs

As shown in **Figure 2-5D** and **Figure 2-7B**, a significant fraction of ACF and cancer DMRs were located in noncoding intergenic regions of the genome. To determine whether these DMRs were enriched for regulatory features, we used Hypergeometric Optimization of Motif EnRichment (HOMER) analysis (142) to identify sequence elements within DMRs that correspond to known transcription factor binding motifs. As shown in **Figure 2-8A**, intergenic DMRs in CRCs were enriched for 103 motifs, including 6 that were also enriched in ACF intergenic DMRs. Furthermore, a number of motifs were also enriched in DMRs located within gene bodies in cancer samples. As shown in **Figure 2-8B**, bootstrapping analysis indicated that these results were highly statistically significant. As shown in **Figure 2-8C**, 5 of the 6 motifs enriched in ACF intergenic DMRs corresponded to binding sequences for AP-1 family transcription factors. The majority of DMRs enriched for AP-1 motifs were hypomethylated in both ACF and cancer samples (**Figure 2-8D**); however, a greater number of AP-1 sites were affected in cancer samples than in ACF. Furthermore,

Figure 2-7. Volcano plots depicting DMRs in colon cancers and ACF grouped by genomic region. DMRs identified in ACF and colon tumors were segregated according to genomic location, and the methylation changes in gene bodies (GBs), intergenic regions, and promoter regions were examined; DMRs are depicted as blue dots. (A) Gene body-associated DMRs in ACF and colon tumors. In ACF, of the 349 Gene body-associated 136 (39%) were hypomethylated while 213 (61%) were hypermethylated, indicating a net increase in methylation. The opposite pattern was observed in colon tumors; of the 8,849 Gene body-associated DMRs in colon tumors, 6,591 (74%) were hypomethylated while only 2,258 (26%) were hypermethylated. (B) Intergenic DMRs in ACF and colon tumors. Of the 297 intergenic DMRs identified in ACF 129 (43%) were hypomethylated, while 168 (57%) were hypermethylated, again indicating a net increase in methylation. Again, the opposite pattern was observed in intergenic DMRs detected in colon tumors; 10,401 (85%) intergenic DMRs were hypomethylated while only 1,769 (15%) were hypermethylated. Together, these observations indicate that non-promoter DMRs undergo a switch in methylation status during cancer progression. (C) Promoter-associated DMRs in ACF and Stage II colon tumors. Of 165 promoter-associated DMRs identified in ACF, only 9 (5%) were hypomethylated, while 156 (95%) were hypermethylated. The same pattern was observed in promoter-associated DMRs identified in colon tumors, 758 (28%) were hypomethylated while 1,968 (72%) were hypermethylated. Thus, in both ACF and Stage II colon tumors, promoter-associated DMRs exhibit a net increase in methylation.

Figure 2-7

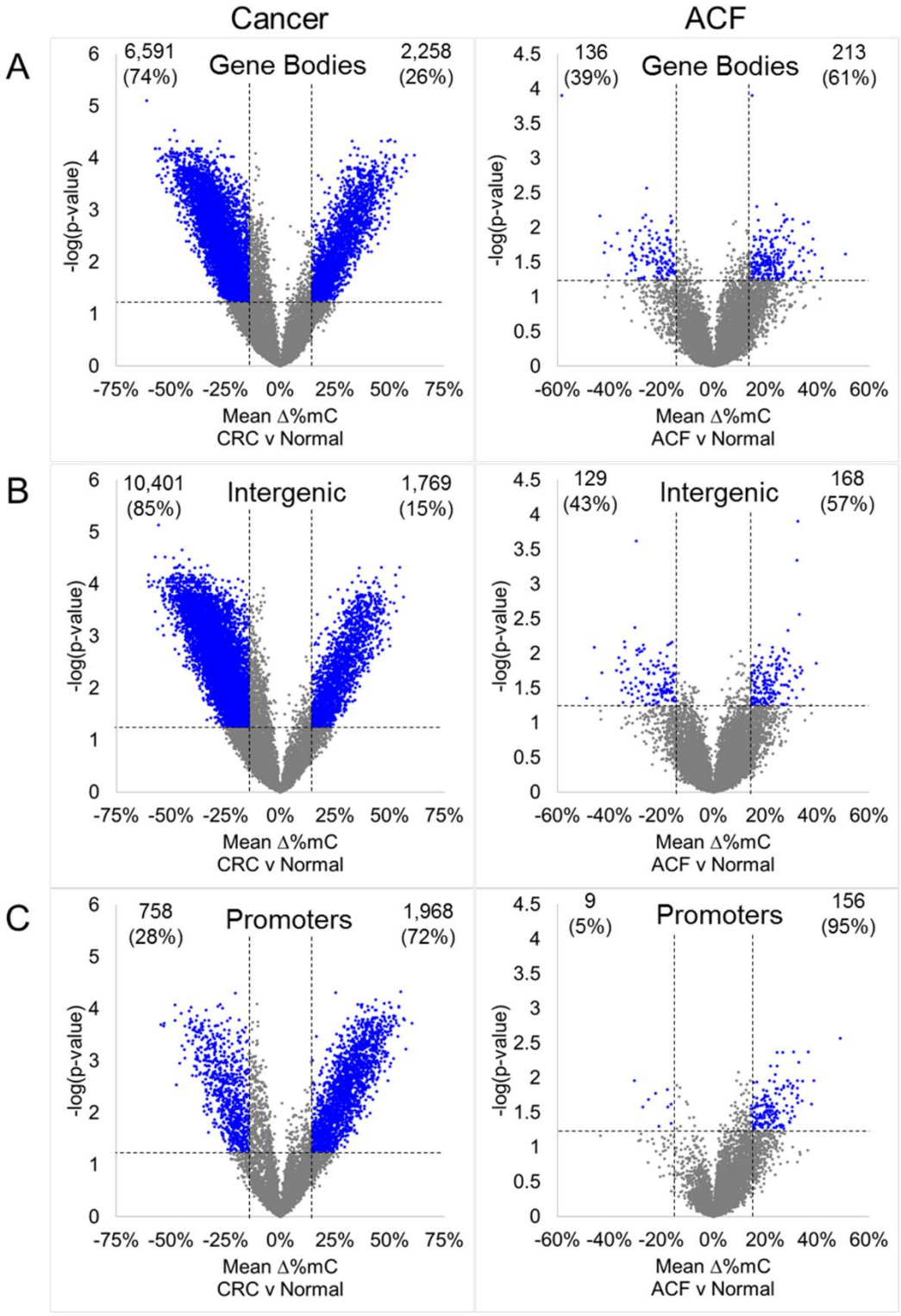
Cancer
ACF
A
6,591 (74%)
Gene Bodies
2,258 (26%)
136 (39%)
Gene Bodies
213 (61%)
B
10,401 (85%)
Intergenic
1,769 (15%)
129 (43%)
Intergenic
168 (57%)
C
758 (28%)
Promoters
1,968 (72%)
9 (5%)
Promoters
156 (95%)
-log(p-value)
Mean Δ%mC
CRC v Normal
Mean Δ%mC
ACF v Normal

Figure 2-8. Enrichment of AP-1 binding motifs in intergenic DMRs. DMRs from ACF and cancers were subjected to Hypergeometric Optimization of Motif EnRichment (HOMER) analysis to determine whether they were enriched for known regulatory elements. (A) In ACF, intergenic DMRs were found to be heavily enriched for sequences corresponding to the binding motifs of AP-1 transcription factor family members, indicated with an asterisk. No motifs were significantly enriched in gene body or promoter DMRs in ACF. (B) Density plot of motif scores for AP-1 family binding motifs generated *via* bootstrapping analysis. Asterisks indicate the actual enrichment score for each motif observed in intergenic ACF DMRs. (C) 103 motifs were found to be enriched in intergenic DMRs in cancers, including the 6 motifs previously identified as enriched in ACF intergenic DMRs, indicating that the enrichment of intergenic DMRs for AP-1 binding motifs is a cancer-associated phenomenon. (D) Change in methylation of DMRs enriched for AP-1 binding motifs in ACF and cancer. In both sample types, the DMRs containing AP-1 binding motifs were significantly hypomethylated compared to their respective matched normal samples. This pattern was particularly prominent in cancer samples, where 95% of AP-1 enriched DMRs were hypomethylated. Furthermore, a greater number of AP-1 sites were affected in cancer than in ACF. (E) Average change in percent methylation of DMRs enriched for AP-1 family motifs. Intergenic DMRs containing AP-1 binding motifs exhibited a ~15% reduction in methylation in ACF and a ~25% reduction in cancer. Bars represent average change in methylation of all DMRs containing the indicated motif. Error bars represent SEM.

Figure 2-8

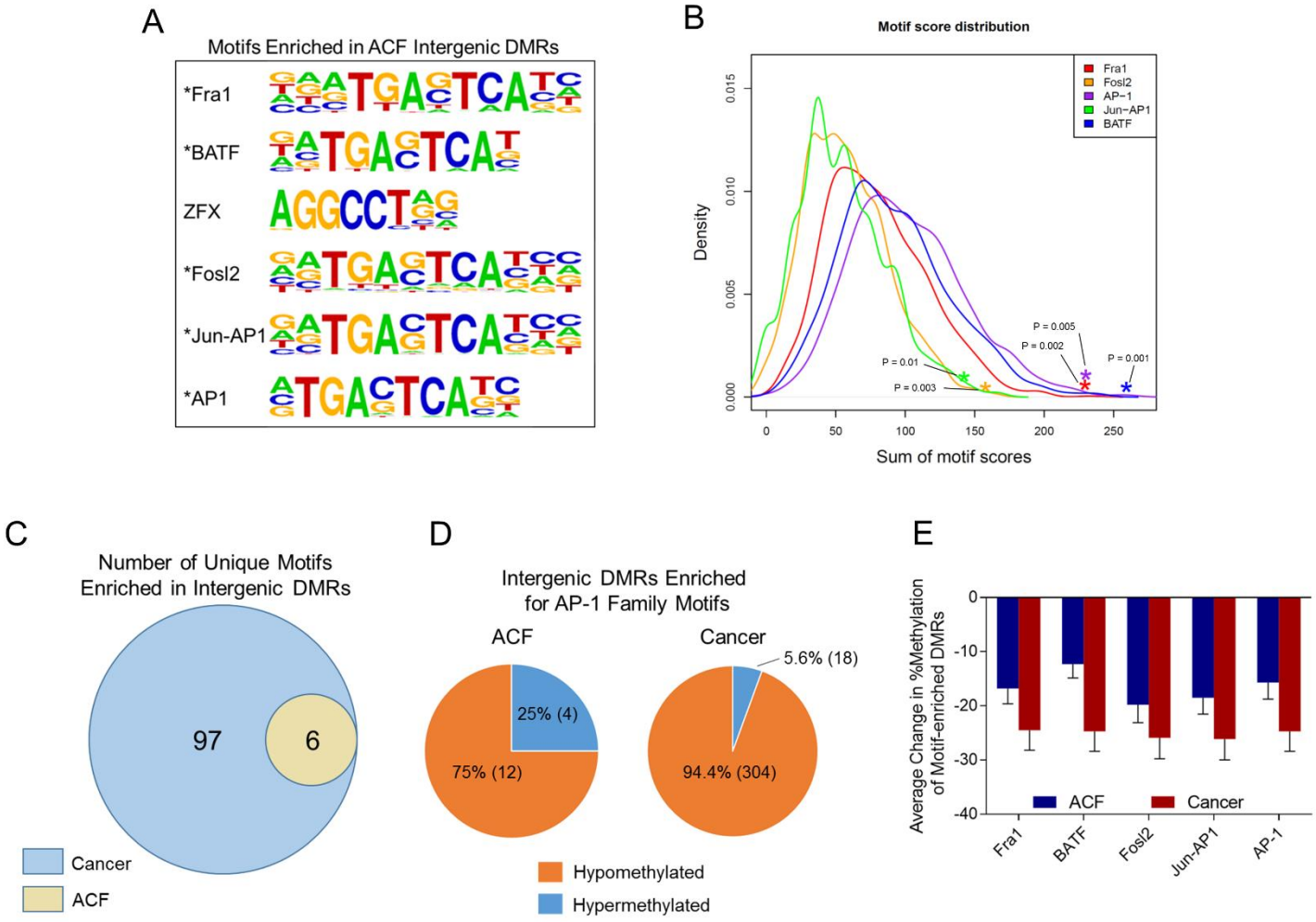
A
Motifs Enriched in ACF Intergenic DMRs
*Fra1
*BATF
ZFX
*Fosl2
*Jun-AP1
*AP1
B
Motif score distribution
Fra1
Fosl2
AP-1
Jun-AP1
BATF
Density
0.000
0.005
0.010
0.015
P = 0.005
P = 0.002
P = 0.001
P = 0.01
P = 0.003
0
50
100
150
200
250
Sum of motif scores
C
Number of Unique Motifs
Enriched in Intergenic DMRs
97
6
Cancer
ACF
D
Intergenic DMRs Enriched
for AP-1 Family Motifs
ACF
Cancer
25% (4)
75% (12)
5.6% (18)
94.4% (304)
Hypomethylated
Hypermethylated
E
Average Change in %Methylation
of Motif-enriched DMRs
0
-10
-20
-30
-40
ACF
Cancer
Fra1
BATF
Fosl2
Jun-AP1
AP-1

as shown in **Figure 2-8E**, the average degree of hypomethylation at AP-1 motif-associated DMRs was greater in cancers than in ACF.

Aberrant DNA methylation is associated with altered gene expression in colon cancers

Promoter methylation is an important mechanism for regulating gene expression (29). To assess the functional consequences of aberrant promoter methylation, genome-wide RNA-Seq analysis was performed on CRC and ACF samples. Scatter-plots depicting the correlation between promoter methylation and gene expression are shown in **Figure 2-9**. In CRCs, promoter methylation was negatively correlated with gene expression (Pearson's correlation coefficient = -0.55) (**Figure 2-9A**), consistent with the transcriptional silencing commonly found in advanced neoplasia (29). However, when ACF were subjected to a similar analysis, there was no correlation observed between promoter methylation status and changes in gene expression (Pearson's correlation coefficient = -0.07) (**Figure 2-9B**).

This lack of correlation between promoter methylation and gene expression in ACF may be related to the magnitude of methylation changes. To address this possibility, 12 genes with promoter hypermethylation in both CRC and ACF, but reduced expression in CRC only, were selected for further analysis of their promoter methylation statuses. As shown in **Figure 2-10A**, the expression of *GSG1L, DPP6, NEFL, GRIN2A, SORCS1, NPTX1, SFRP1, ST8SIA5, ADCYAP1R1, SNAP25* and *GABRB3* were each significantly reduced by at least 3-fold in Stage III-IV cancers, but had no significant change in expression in ACF. These genes showed an average increase in promoter methylation of ~40% in CRCs, but an increase of only ~20% in ACF (**Figure 2-10B**), suggesting that the extent of promoter methylation in early neoplasia is insufficient to alter gene expression.

Overexpression of EZH2, the catalytic subunit of PRC2, has been identified in CRC and is frequently associated with a poor prognosis (153). To determine whether the enrichment of ACF DMRs for PRC2 targets may be due to the overexpression of components of the PRC2 complex, we interrogated our RNA-

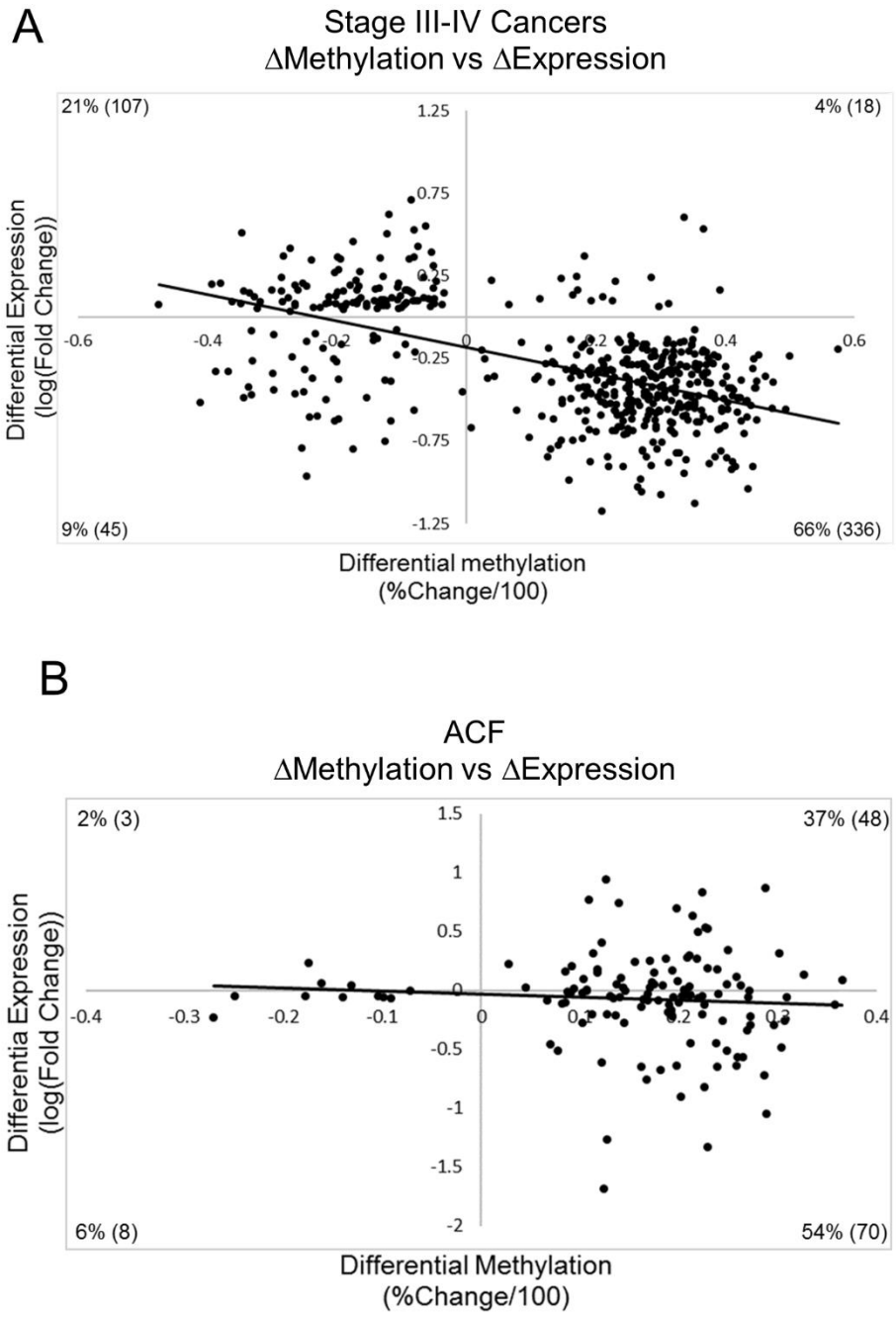

Figure 2-9. Promoter methylation is correlated with gene expression in CRCs but not ACF. (A) Scatter-plot depicting the correlation between changes in promoter methylation and gene expression in CRCs (Pearson's correlation coefficient = -0.55), indicating increased promoter methylation associated with gene silencing. (B) Scatter-plot depicting the lack of correlation between changes in promoter methylation and gene expression in ACF (Pearson's correlation coefficient = -0.07).

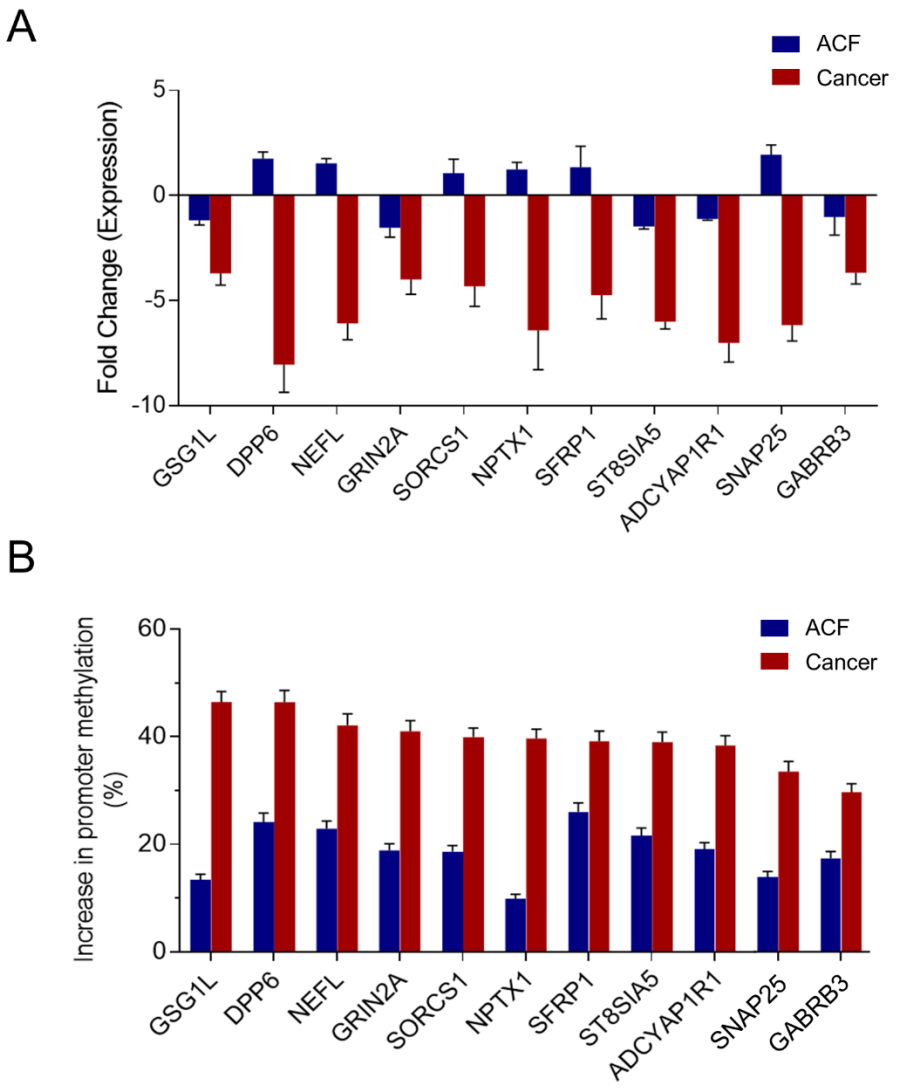

Figure 2-10. Relationship between DNA methylation and expression for selected genes. (A) Selected genes with promoter DMRs identified in both cancer and ACF. GSG1L, DPP6, NEFL, GRIN2A, SORCS1, NPTX1, SFRP1, ST8SIA5, ADCYAP1R1, SNAP25, and GABRB3 were significantly downregulated in cancer samples (at least 3-fold reduction in expression), but not significantly altered in ACF. (B) These same genes exhibit promoter hypermethylation in both cancer and ACF, but the degree of increased methylation is greater in cancer (~40% increase) than in ACF (~20% increase). Bars represent average percentage change in methylation of promoter DMRs for indicated genes across samples. Error bars represent 95% confidence interval and SEM in (A) and (B), respectively.

Seq data for changes in expression of the Polycomb genes *EZH2*, *SUZ12*, and *EED*. As shown in **Figure 2-11A**, *EZH2* was overexpressed in Stage III-IV CRCs (1.55-fold increase, p=0.03), but not in ACF (**Figure 2-11B**). We also interrogated the RNA-Seq dataset for the expression levels of the DNA methyltransferases (DNMTs), a group of genes (*DNMT1, DNMT3A* and *DNMT3B*) that are often up-regulated in CRC (154). As shown in **Figure 2-11A&B**, *DNMT1* and *DNMT3B* are overexpressed in cancer samples, but not in ACF. Taken together, these results suggest that while overexpression of EZH2, DNMT1 and DNMT3B may promote hypermethylation and cancer progression, their overexpression is not required for the establishment of early colonic neoplasia. Alternatively, higher expression of DNMT1, DNMT3B and EZH2 may accompany increased cell proliferation in CRC but may not be causative for the DNA methylation changes.

2.4 Discussion

The disruption of DNA methylation patterns has been shown to play an important role in the pathogenesis of CRC (30). However, the epigenomic landscape at the earliest stages of colonic neoplasia has not been clearly defined. Several studies have demonstrated methylation defects within a limited set of genes in ACF and the normal colonic mucosa from patients with CRC (24,25,47,48). However, a systematic genome-wide investigation of DNA methylation changes occurring in early human colonic neoplasia has not yet been reported. In the present study, we have applied a highly sensitive genome-wide approach by combining LCM with RRBS to compare DNA methylation changes present in early colonic neoplasia with the extensive modifications found in advanced CRC.

As expected, the majority of DMRs identified in Stage III-IV cancers were hypomethylated. This global loss of DNA methylation was particularly common within intergenic regions, in which ~85% of DMRs were hypomethylated. These findings are consistent with previous reports of genome-wide hypomethylation in a number of different human cancers (26,155). DNA hypomethylation also occurs in

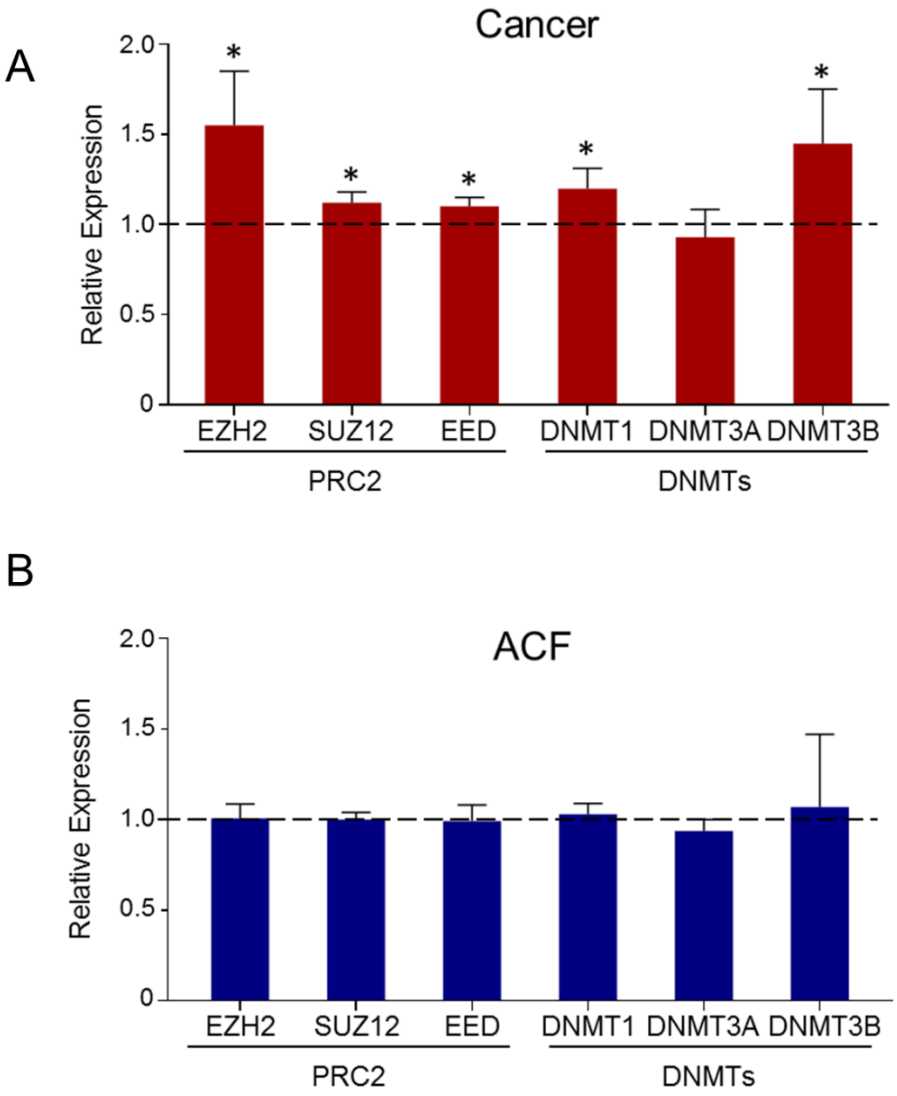

Figure 2-11. Expression of PRC2 components and DNA methyltransferases in cancer and ACF samples. (A) Significant overexpression of the PRC2 components EZH2 (1.55-fold, P<0.05), SUZ12 (1.12-fold, P<0.05) and EED (1.1-fold, P<0.05) were detected in cancer samples. Furthermore, overexpression of the DNA methyltransferase enzymes DNMT1 (1.2-fold, P<0,05) and DNMT3B (1.45-fold, P<0.05) were detected in cancers. (B) Despite similarities in the patterns of aberrant methylation in cancer and ACF, including the enrichment of promoter DMRs for PRC2-target genes in ACF, no change in the expression of any PRC2 component or DNMT enzyme was detected in ACF samples.

low-grade adenomas (155,156), indicating that this epigenetic alteration precedes the development of more advanced malignancies. However, our present study has uncovered an unexpected finding; the majority of DMRs (across all genomic locations) in ACF samples are *hypermethylated*, indicating a global gain of DNA methylation at the earliest stages of tumor initiation. Since the majority of ACF are self-limiting and unlikely to progress to malignancy (93)**,** genome-wide hypermethylation may in fact provide a mechanism for restricting ACF progression, in part by reducing the likelihood of genomic instability associated with DNA hypomethylation (27).

Promoter DMRs in both CRC and ACF were enriched in genes known to be targeted by PRC2 in embryonic stem cells (ESCs). PRC2 is a histone-modifying complex expressed in ESCs that plays an important role in maintaining 'stemness' (150) by repressing genes required for differentiation *via* the methylation of histone H3K27 (157). Since many genes targeted by PRC2 in human ESCs become hypermethylated in CRC and other cancers (158,159), it is thought that PRC2 occupancy and/or histone methylation will increase the susceptibility of genes to aberrant hypermethylation (160,161). Widschwendter *et al.* (159) hypothesized that cancer-associated promoter hypermethylation of PRC2 targets originates in stem cells during the earliest stages of carcinogenesis, and predisposes these cells to neoplastic transformation by "locking in" a stem cell phenotype. Our data support the timing of this hypothesis by demonstrating that hypermethylation of PRC2 targets occurs as early as the ACF stage. While H3K27 methylation of PRC2 targets was originally thought to be restricted to ESCs, Rada-Iglesias *et al.* (162) and Hahn *et al*. (163) showed that this modification is also found in normal adult colonic epithelial cells. Together, these observations suggest that DNA hypermethylation in ACF is directed by the Polycomb complex, or its associated histone marks that are present in normal cells prior to early neoplastic initiation.

In addition, the present study has uncovered extensive promoter and gene body hypermethylation of homeobox genes in both cancers and ACF, many of which belong to the HOX

family. The expression of homeobox genes, which is regulated to a large extent by epigenetic modifications (164,165), contributes to the maintenance of cellular identity and adult tissue morphology (166). Aberrant hypermethylation of homeobox-containing genes has been described in breast and lung cancers, and several HOX genes (HOXA7, HOXA9, and HOXB13) are reportedly hypermethylated in CRC (158,167,168). However, the large number of differentially methylated homeobox genes identified in our panel of primary Stage III-IV cancers (**Figure 2-6**) is an unexpected result. A subset of homeobox genes was also hypermethylated in ACF, suggesting that this epigenetic change is an early event in colonic neoplasia. CpG islands associated with homeobox genes are commonly hypermethylated in early stage ductal carcinomas (DCIS) and early-stage lung carcinomas (158,168), suggesting that this change is an early event in other tissues as well. Together, these results suggest that dysregulation of homeobox genes *via* hypermethylation occurs more extensively in CRC than previously thought, and that this epigenetic aberration is established in early neoplasia.

Finally, our results indicate that aberrant DNA methylation commonly occurs within non-transcribed, intergenic regions in both ACF and CRCs. Upon further analysis, we have found that intergenic DMRs are enriched for transcription factor binding sites, especially those corresponding to members of the AP-1 transcription factor family. AP-1 is a nuclear transcription factor that controls many critical cellular functions, including proliferation, differentiation and apoptosis (169). AP-1 also plays an important role in oncogenesis; activating mutations in the *KRAS* gene are thought to promote tumor development by increasing AP-1 activity, with concurrent up-regulation of proliferative and anti-apoptotic genes (170). Notably, all of the ACF and CRC samples examined in this study contained mutant *KRAS*. Recent evidence indicates that transcriptional activation by AP-1 is controlled, in part, by DNA methylation (171). As shown by Park *et al.* (171), the DNA binding activity of AP-1 is significantly reduced when CpGs in close proximity to its DNA binding motif are methylated. A genome-wide methylation study of a single *KRAS*-mutant stage III colon adenocarcinoma by Berman *et al.* (172) suggested that epigenetic regulation of AP-1 is disrupted

in cancer by demonstrating that genomic regions with cancer-specific hypomethylation are significantly enriched for AP-1 binding motifs. Our study has confirmed this observation in a larger panel consisting of 10 *KRAS*-mutant colon cancers, substantiating a role for hypomethylation of AP-1 sequences in CRC. Furthermore, our data extend this hypothesis by demonstrating that a small number of AP-1 sites are hypomethylated in ACF, suggesting that this epigenetic phenomenon begins early in the neoplastic process. However, the number of affected AP-1 sites, and the average degree of hypomethylation at these sites, was significantly greater in cancer samples than in ACF. These observations suggest that the expansion of AP-1 site hypomethylation may promote neoplastic progression.

In summary, the present study demonstrates that cancer-associated DNA methylation changes are more abundant in ACF than previously thought. These changes frequently affect genes involved in cellular identity and differentiation, suggesting that disrupted regulation of cell fate determination may contribute to the establishment of early colonic neoplasia. Methylation of these genes, including those targeted by PRC2 or containing homeobox sequences, may be useful targets for novel chemopreventive interventions. Furthermore, the present study identifies epigenetic changes specifically associated with advanced neoplasia, including a switch in the global methylation status of non-promoter regions, which may serve as useful biomarkers for cancer risk. Our results provide new insights into the role of DNA methylation in the development of early colonic neoplasia, and provide target candidates for the use of epigenetic profiling in CRC detection and prevention.

Chapter 3: Dietary methyl donor deficiency suppresses intestinal adenoma development

3.1 Introduction

Many epidemiological studies and follow-up meta-analyses suggest that folate deficiency increases the risk of developing colorectal cancer (CRC) (173–176). Consistent with this observation, several small cohort and case-control studies have suggested that folate has a small protective effect against CRC (177), although a more recent meta-analysis of 13 supplementation trials comprised of 50,000 individuals found no significant effect of folate on cancer incidence in the general population (115). However, data from several recent clinical trials suggest that folate supplementation may actually *increase* cancer risk in certain high-risk subpopulations (116,117). These findings are particularly troubling when considered within the context of the USDA-mandated folate supplementation program that requires cereals, flour and other grain products in the US to be fortified with folic acid. This program was initiated to reduce the incidence of neural tube birth defects (NTDs) in newborns, and although highly successful (178)**,** it has had the unintended consequence of significantly raising blood folate levels within the general population (179).

Subsequent studies of folate intake and disease risk have raised concern about the effects of this widespread folate fortification on populations at low risk for NTDs, but high risk of cancer. A randomized, placebo-controlled clinical trial by Cole and Baron (118) found that men with a personal history of colorectal adenoma who received 1 mg/d supplemental folic acid were more likely to present with an advanced colonic lesion at a 5-year follow-up examination. This finding may be of particular concern for individuals with hereditary CRC syndromes, such as familial adenomatous polyposis (FAP), who develop multiple neoplastic foci at a young age (180) and thus may be more susceptible to the potential cancer-promoting effects of folic acid supplementation. In addition, the prevalence of colorectal polyps in individuals over the age of 50 is estimated to be as high as 45% (181–183); these individuals, who are unlikely to become pregnant and are therefore not concerned with NTDs, could in fact be harmed by folic

acid supplementation. An analysis of folate consumption before and after the implementation of mandatory fortification revealed that men and women over the age of 50 experienced the largest increase in folic acid intake (184).

Folate is a key component of folate one-carbon metabolism (FOCM). In addition to folate and its derivatives, the nutrients choline, methionine and vitamin B12 are also fundamental components of this metabolic pathway; these nutrients are collectively referred to as 'methyl donors'. Through FOCM, one-carbon moieties are utilized in nucleotide biosynthesis and methylation reactions, although these processes are regulated by two distinct arms of the FOCM pathway (185). In one arm, nucleotide biosynthesis is directly dependent upon the availability of folate and its derivatives. In the other arm, protein and DNA methylation reactions are dependent upon the generation of S-adenosylmethionine from choline, homocysteine and methionine. Vitamin B12 serves as a link between these two key arms of the pathway by transferring methyl groups from the folate cycle to the methionine cycle (186).

The fundamental cellular processes controlled by FOCM illustrate the importance of maintaining methyl donor homeostasis; inhibition of FOCM flux can have severe consequences for DNA stability, gene expression and cell survival. Under normal conditions, it is important for cells to have an adequate supply of methyl donor nutrients. However, rapidly replicating cancer cells have an increased demand for folate, making FOCM an ideal target for anti-cancer interventions (187). Anti-folates, a class of chemotherapeutic agents that disrupt key steps in FOCM, have had a long history of success in the clinic (188). Less is known, however, about whether dietary manipulation of methyl donor nutrients can be used to prevent carcinogenesis.

We recently reported the effects of combined dietary depletion of folate, methionine, choline and vitamin B12 on tumor development in *Apc*$^{Min/+}$ mice, a model of Wnt-driven intestinal cancer (122,189). *Apc*$^{Min/+}$ mice, maintained on a methyl donor deficient (MDD) diet beginning at 5 weeks of age, were significantly protected against intestinal tumorigenesis (~96% reduction in tumor number; $P<0.01$). This

reduction in tumor burden was associated with a broad decline in immune cell populations and decreased expression of pro-inflammatory cytokines (122). In the present study, the effects of dietary MDD are examined in greater detail in the $Apc^{\Delta 14/+}$mouse, a mouse model with an *Apc* truncation mutation more typical of that found in human cancers and a higher prevalence of colon tumor development (190). An 11-week period of methyl donor restriction started prior to tumor initiation is shown to afford long-lasting tumor protection, even when mice are returned to dietary repletion. Protection is accompanied by significant morphological changes to the intestinal crypt architecture, including altered cell turnover and a reduction in the number of cryptal Dclk1-positive cells. Finally, the undesirable effects associated with methyl donor restriction are shown to be transient and readily reversible following methyl donor repletion. Taken together, these results indicate that temporary dietary methyl donor restriction in adenoma-prone mice can induce persistent changes to the intestinal epithelium and provide long-lasting tumor protection. These data also suggest that transient reductions in dietary methyl donor consumption should be considered when studying the impact of folate on colon cancer risk in humans.

3.2 Materials and Methods

Animal treatment

$Apc^{\Delta 14/+}$ mice on a C57BL/6 background were generated and kindly provided by Dr. Christine Perret as previously described (190). All mice were maintained in a temperature-controlled, light-cycled room and allowed free access to drinking water. Animal experiments were conducted with approval from the Institutional Animal Care and Use Committee (UConn Health). Genotyping of *Apc* was performed by PCR using DNA from mouse tail biopsies. Dietary studies used two amino-acid defined experimental diets: the Methyl Donor Sufficient (MDS; TD.99366, Harlan Laboratories, Madison WI) diet and the Methyl Donor Deficient (MDD; TD.00605) diet, which was identical to the MDS diet except for the depletion of folate, choline, methionine and vitamin B12, and the addition of homocysteine. Diet compositions are

detailed in **Table 3-1.** *Apc*$^{\Delta 14/+}$ mice were randomized at 4 weeks of age and placed into four experimental groups; each group was placed on a specific dietary regimen for 18 weeks, as depicted in **Figure 3-1**. Group I (MDS, n=28) mice were fed the MDS diet *ad libitum* for the entire 18-week period. Group II (MDD, n=19) mice were fed the MDD diet *ad libitum* for 18 weeks. Group III (MDS-PF, n=27) mice were pair-fed the MDS diet in an amount equivalent to levels consumed by Group II mice. Finally, mice in Group IV (MDD:MDS, n=28) were placed on the MDD diet for 11 weeks, and then switched to the MDS diet for the remaining 7 weeks. All mice were sacrificed at 22 weeks of age. Mice were examined weekly for changes in body weight, rectal prolapse, or bleeding indicating intestinal obstruction or anemia associated with tumors. Individual body weights and average food consumption were recorded weekly.

Tissue processing and analysis of tumor burden

Upon sacrifice, the entire small intestine, colon, liver, spleen and kidneys were harvested. The small intestine and colon were flushed with ice-cold PBS and opened longitudinally. Specimens were fixed flat in 10% neutral buffered formalin solution and stored in 70% ethanol. Tissues were stained with 0.2% methylene blue and the numbers, size and location of tumors were scored under a dissecting microscope. Size was measured as tumor diameter at its widest point.

Histological and Morphometric Analyses

After tumor quantification, tissues were processed and paraffin-embedded for subsequent histological analyses. Paraffin-embedded tissues were sectioned onto glass slides at a thickness of 5-µm and stained with hematoxylin and eosin (H&E). Liver and kidneys were also stained with Masson's trichrome stain to visualize collagen deposition. All tissues were examined for histological abnormalities using an Olympus BX60 light microscope. H&E-stained small intestine and colon tissue sections were used

Diet Components	MDS (g/kg)	MDD (g/kg)
L-Alanine	3.5	3.5
L-Arginine HCl	12.1	12.1
L-Asparagine	6	6
L-Aspartic Acid	3.5	3.5
L-Cystine	3.5	3.5
L-Glutamic Acid	40	40
Glycine	23.3	23.3
L-Histidine HCl, monohydrate	4.5	4.5
L-Isoleucine	8.2	8.2
L-Leucine	11.1	11.1
L-Lysine HCl	18	18
L-Methionine	8.2	0
L-Phenylalanine	7.5	7.5
L-Proline	3.5	3.5
L-Serine	3.5	3.5
L-Threonine	8.2	8.2
L-Trytophan	1.8	1.8
L-Tyrosine	5	5
L-Valine	8.2	8.2
Sucrose	351.68	366.1
Corn Starch	150	150
Maltodextrin	150	150
Soybean Oil	80	80
Cellulose	30	30
Mineral Mix, AIN-93M-MX (94049)	35	35
Calcium Phosphate, monobasic, monohydrate	8.2	8.2
Choline Bitartrate	2.5	0
THBQ, antioxidant	0.02	0.02
Niacin	0.039	0.039
Calcium Pantothenate	0.0208	0.0208
Pyridoxine HCl	0.0091	0.0091
Thiamin HCl	0.0078	0.0078
Riboflavin	0.0078	0.0078
Folic Acid	0.0026	0
Biotin	0.0003	0.0003
Vitamin B12 (0.1% in mannitol)	0.0325	0
Vitamin E DL-alpha tocopheryl acetate	0.195	0.195
Vitamin A Palmitate	0.0104	0.0104
Vitamin D3, cholecalciferol	0.0026	0.0026
Vitamin K12, phylloquinone	0.001	0.001
Homocysteine	0	9

Table 3-1. Nutritional composition of MDD and MDS diets.

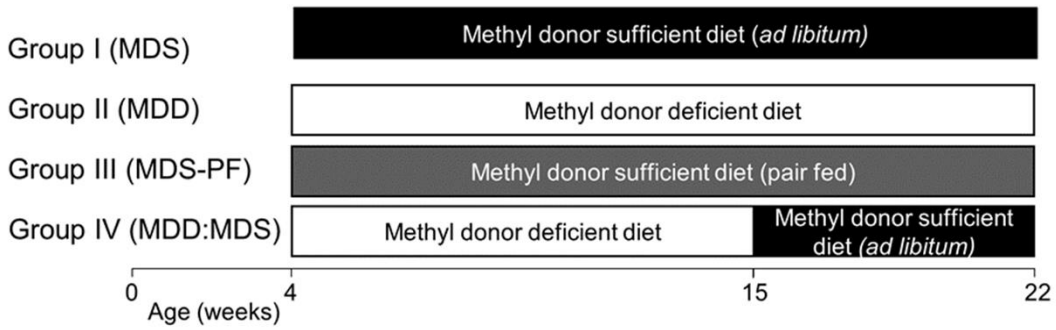

Figure 3-1. Dietary methyl donor deficiency study design. At 4 weeks of age, a total of 102 mice were randomized and placed into 4 experimental groups. Group 1 (MDS *ad lib.,* n=28) received MDS diet *ad libitum*, group 2 (MDS pair fed, n=27) received MDS diet pair fed with group 3 (MDD, n=19) which received the MDD diet; all mice in groups 1, 2, and 3 received their respective diets for 18 weeks, starting at 4 weeks of age. In addition, mice in group 4 (MDD:MDS, n=28) were placed on the MDD diet for 11 weeks, starting at 4 weeks of age, before being transferred to the MDS diet for an additional 7 weeks. All mice were sacrificed at 22 weeks of age.

for morphometric analysis. Crypt length was measured using ImageJ image processing software calibrated using an ocular micrometer. Four 20x regions per animal (n=4/group) were randomly selected in the ileum and colon, and a minimum of 5 crypts was measured per region. Data are reported as the mean crypt length in micrometers. Crypt branching index (CBI) was calculated by averaging the total number of branched crypts in 3 H&E sections per animal (n=4/group).

Immunohistochemistry and Quantification of Immunostaining

Immunostaining was performed as previously described (191). Sections were subjected to sodium citrate antigen retrieval; for cleaved caspase-3 antigen retrieval 0.05% Tween-20 was added to the sodium citrate buffer. Sections were incubated overnight at 4°C with anti–Ki-67 (1:600; Cell Signaling Technology, Inc.), anti–phospho-Histone H3 (PHH3; 1:200; Cell Signaling Technology, Inc.), anti-cleaved caspase-3 (CC3; 1:400; Cell Signaling Technology, Inc.), or anti-DCAMKL1 (Dclk1; 1:50; Abcam). All sections were then incubated with SignalStain Boost IHC Detection Reagent (Mouse, HRP, Cell Signaling Technology, Inc.). For quantification of Ki-67 staining in normal tissue, 30 crypts with complete longitudinal sections were randomly selected from 4 mice per group. Ki-67 index was calculated as the average percent Ki-67–positive cells per crypt. Ki-67 staining in tumors was quantified in a minimum of 2,000 cells from five fields per mouse (40x). For quantification of PHH3 and Dclk1 staining in normal tissue, 150 crypts with complete longitudinal sections were chosen at random from 4 mice per group. The total number of positive-stained cells per crypt were counted, averaged, and reported as the percent positive cells per crypt. For tumor tissue, a minimum of ten fields (40x) was selected and PHH3-index was calculated as the average number of $PHH3^+$ cells per field. CC3 staining was quantified in normal and tumor tissue by averaging the total number of CC3-positive cells in ten fields (40x).

Statistical Analysis

Comparisons of small intestine and colon tumor multiplicity were made using the Kruskal-Wallis test with Dunn's Multiple Comparisons post-test. Comparisons of small intestine and colon crypt length, and crypt branching indices, were made using one-way ANOVA with Bonferroni's post-test. Individual comparisons of tumor size, Ki-67, PHH3, CC3 and Dclk1 immunostaining were made using Fisher's exact test, or one-way ANOVA with Bonferroni's post-test when appropriate. For all analyses, a *P*-value < 0.05 was considered to be statistically significant.

3.3 Results

Methyl donor deficiency induces a sustained reduction in intestinal tumor formation

Our recent study in $Apc^{Min/+}$ mice showed dramatic tumor protection by restricting the consumption of diet-derived methyl donors (122). To extend these results to a second *Apc*-dependent mouse tumor model, the following study was conducted in $Apc^{\Delta 14/+}$ mice, in which tumor formation is driven by the deletion of *Apc* exon 14 (190). $Apc^{\Delta 14/+}$ mice were maintained on four experimental diets, as depicted in **Figure 3-1**. As shown in **Figure 3-2A**, tumor multiplicity was evaluated in the small intestine. Methyl donor restriction significantly reduced the total number of polyps by 78% (70.2 ± 24.6 vs. 15.4 ± 14.7 in MDS and MDD, respectively; P<0.01). A group of MDS mice were also pair-fed to the MDD mice to match their reduced food consumption and lower calorie intake (MDS-PF). Pair-fed mice showed an intermediate reduction (37%; P<0.05) in intestinal tumor multiplicity (**Figure 3-2A**), consistent with our earlier study (122), indicating that reduced calorie consumption cannot fully account for the protection afforded by the MDD diet**.**

To determine whether tumor protection persists beyond the period of active methyl donor restriction, an additional group of mice was methyl donor depleted for an initial 11 weeks, beginning at 4 weeks of age, and then returned to a methyl donor replete diet for an additional 7 weeks (MDD:MDS). As

shown in **Figure 3-2A**, the number of small intestinal tumors was significantly reduced (68%, P<0.01) in the MDD:MDS mice compared to MDS mice (22.2 ± 18.8 versus 70.2 ± 24.6, respectively). There was also no significant difference in the number of small intestinal tumors between MDD:MDS and MDD mice, indicating that tumor protection is maintained even after dietary repletion of methyl donors. There was a downward shift in the size distribution of tumors in the MDD and MDS-PF groups, with the most pronounced shift present in mice maintained on the MDD diet throughout the entire 18-week study (**Figure 3-2B**). In the colon, methyl donor restriction significantly reduced the total number of tumors by 50% (3.0 ± 2.1 versus 1.5 ± 1.9 in MDS and MDD, respectively; P<0.01), an effect that was not observed in the pair-fed mice. MDD:MDS displayed a moderate (23%), but non-significant (P=0.19) reduction in tumors (**Figure 3-2C**). The size distribution of colon tumors was shifted downward in the MDD-fed mice, but this downward shift was not present in the MDD:MDS group (**Figure 3-2D**).

Methyl donor deficiency alters crypt morphology and cell turnover

Interventions that reduce intestinal cancer risk are frequently accompanied by reduced crypt length, decreased cell proliferation, decreased crypt branching and increased apoptosis (192). The MDD diet produced each of these changes, and these alterations persisted even after dietary methyl donors were replenished. As shown in **Figure 3-3A**, small intestinal crypt length was reduced in both the MDD (26%; P<0.01) and MDS pair-fed mice (15%; P<0.01) compared to MDS controls. This effect was also observed in the MDD:MDS mice (16%; P<0.01), indicating that compacted crypt morphology is maintained after methyl donor repletion. In the colon, average crypt lengths were significantly reduced in both the MDD (20%; P<0.01) and MDD:MDS mice (6%; P<0.05) (**Figure 3-3B**).

Intestinal epithelial growth can be controlled *via* crypt fission (193). Furthermore, crypt fission acts as a pathway for *Apc*-mutant crypts to clonally expand, thereby increasing the risk of tumor formation (194). As shown by Fischer *et al.* (194), reduced crypt fission is associated with diminished tumor burden

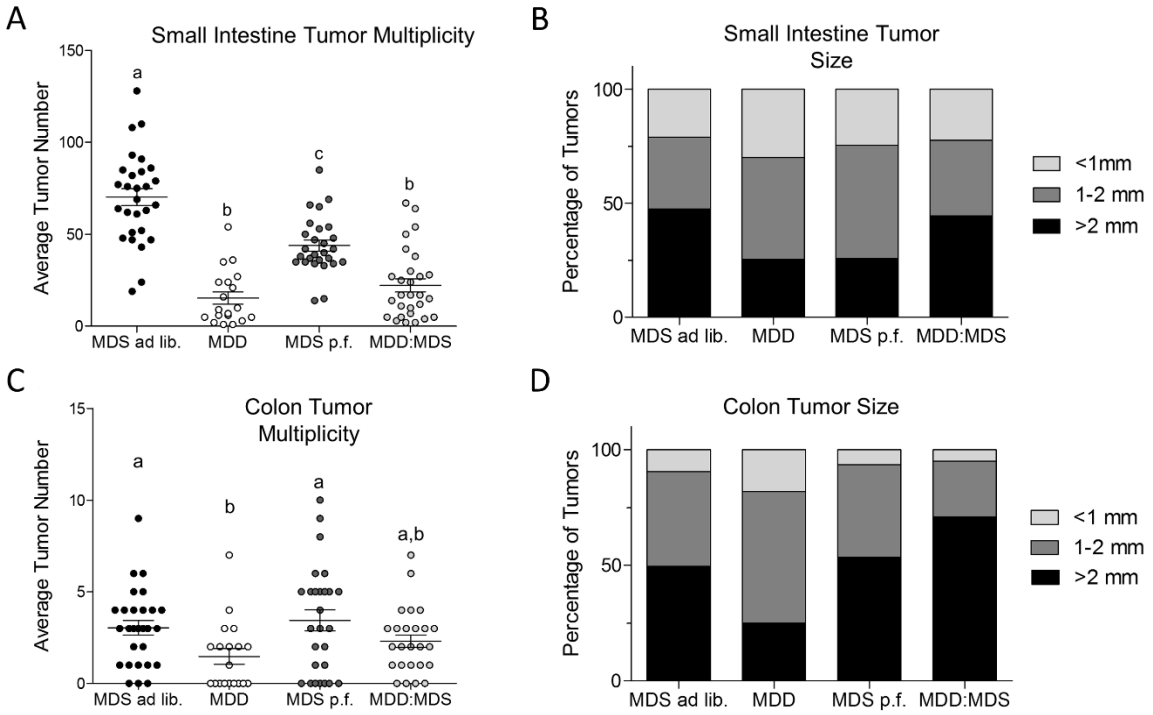

Figure 3-2. Intestinal tumor burden. (A) Total number of tumors per mouse in the small intestine. Caloric restriction (MDS pair fed) causes a modest reduction (37 ± 4.2%, P<0.05) in tumor multiplicity, while MDD causes a larger reduction (78 ± 5%, P<0.01). Note, there is no significant difference in tumor number in the MDD and MDD:MDS groups, indicating that protection from tumor formation induced by 11 weeks of MDD persists through at least 7 weeks of methyl donor repletion. (B) Distribution of small intestine tumor sizes. Caloric restriction and MDD both cause a downward shift in the distribution of intestinal tumor sizes. (C) Total number of tumors per mouse in the colon. MDD causes a reduction (51 ± 14%, P<0.01) in the average number of colon tumors; however, caloric restriction does not have an effect on colon tumor multiplicity. (D) Distribution of colon tumor sizes. MDD causes a downward shift in colonic tumor size distribution; however, caloric restriction does not. Thus, even when tumors are able to form, their growth is inhibited by MDD. Error bars indicate means ± SEM. Statistically significant differences (P<0.05) between groups, measured by the Kruskal-Wallis test with Dunn's Multiple Comparisons post-test, are indicated within dot plots by differences in the letter placed above each group.

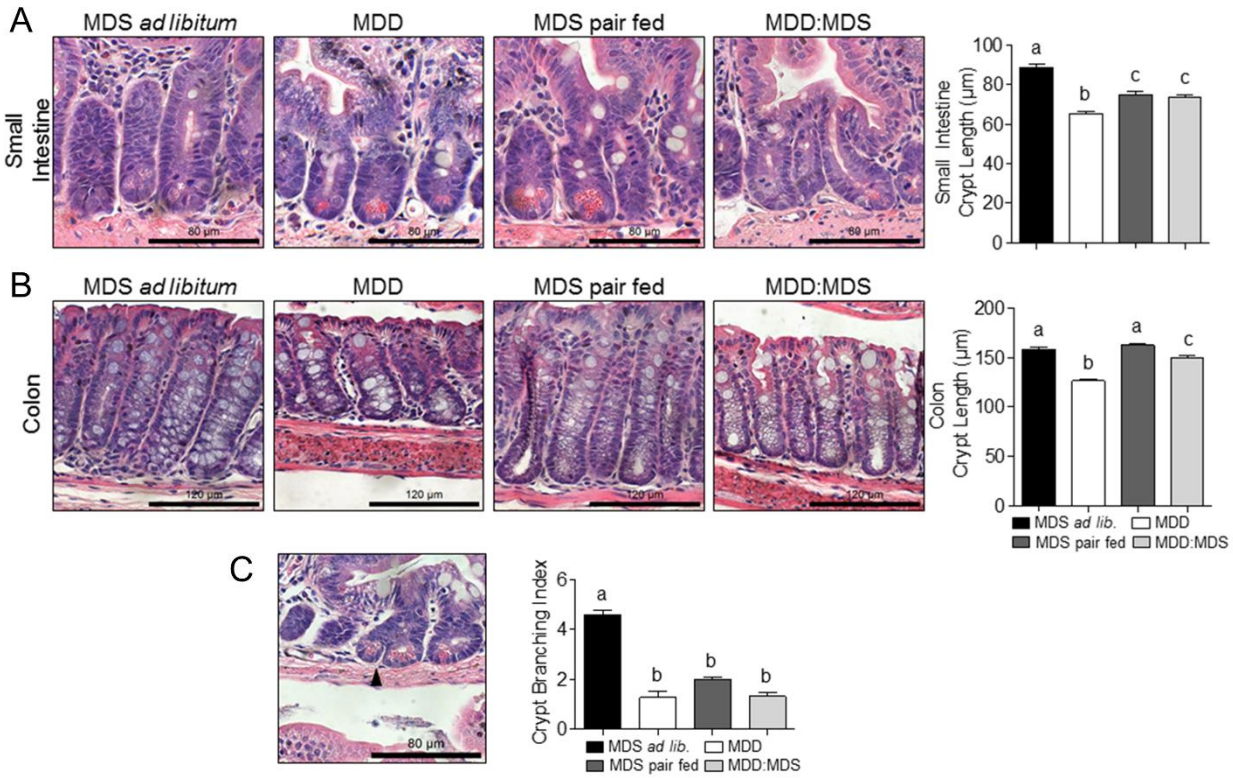

Figure 3-3. Intestinal and colonic crypt length and fission rates. (A) Representative images of normal small intestine crypts used for morphometric analysis, with quantification. MDD was associated with an approximately 25% reduction ($P<0.01$) in the average length of normal small intestine crypts. Average crypt length is also reduced in MDD:MDS mice (16% reduction, $P<0.01$), suggesting long-term changes to crypt homeostasis. (B) Representative images of normal colon crypts used for morphometric analysis, with quantification. MDD was associated with an approximately 20% reduction ($P<0.01$) in average crypt length. (C) Small intestine crypt branching index (CBI) was reduced in the MDD mice (73%, $P<0.01$), indicating a reduced rate of crypt fission under conditions of dietary methyl donor restriction. Error bars indicate means ± SEM. Statistically significant differences ($P<0.05$) between groups, measured by ANOVA with Bonferroni's post-test, are indicated within bar graphs by differences in the letter placed above each group. Scale bars, 80 and 120 µm.

in *Apc*-mutant mice. To determine whether MDD diet decreases crypt fission, the intestinal crypt branching index (CBI), a measure of the rate of crypt fission (195), was assessed. A representative image of a small intestine crypt from the MDS mice undergoing crypt fission is shown in **Figure 3-3C**. Although already a rare event in normal mucosa (193), the CBI was further reduced in both the MDD (73%; P<0.01) and MDS-PF (56%; P<0.01) groups (1.25 ± 0.5 and 2 ± 0.14 versus 4.6 ± 0.4 branched crypts per section, respectively). The CBI in MDD:MDS mice remained significantly reduced (71%; P<0.01) relative to MDS controls (1.3 ± 0.3 versus 4.6 ± 0.4 branched crypts per section), indicating that impaired crypt fission continues after methyl donor repletion. Similar changes did not occur in the colon (data not shown).

Diet can also influence intestinal cancer development through the modulation of cell proliferation and apoptosis (196). As shown in **Figure 3-4A,** Ki-67 staining was significantly reduced in both MDD (12%, P<0.01) and MDD:MDS (6%, P<0.01) mice. In addition, Ki-67$^+$ cell numbers in extant tumors were also reduced in MDD (24%, P<0.01) and MDD:MDS mice (6%, P<0.01) (**Figure 3-4B**). Apoptotic cells were identified by immunostaining for CC3. As shown in **Figure 3-5A**, CC3$^+$ cells were intermittently present within the upper portion of small intestinal villi, tending to cluster towards the villus tip and rarely found within the crypt compartment. MDD significantly increased (4.9-fold; P<0.01) the average number of CC3$^+$ cells per field (**Figure 3-5A**). However, increased numbers of apoptotic cells did not persist upon methyl donor repletion (MDD:MDS, **Figure 3-5A**). Similar patterns of apoptosis were observed in intestinal tumors, regardless of size or location (**Figure 3-5B**). There were no differences observed in CC3 staining in colon tumors or normal colonic mucosa of mice from each of the experimental groups (data not shown). An increased rate of apoptosis is therefore unlikely to contribute to adenoma risk reduction in the MDD:MDS mice.

The effects of methyl donor status on mitosis were also evaluated within the intestinal mucosa. As shown in **Figure 3-6A**, methyl donor restriction (MDD) significantly reduced the frequency of PHH3$^+$ cells per crypt by 53% (P<0.01). Reduced numbers of mitotic cells were also present within the small

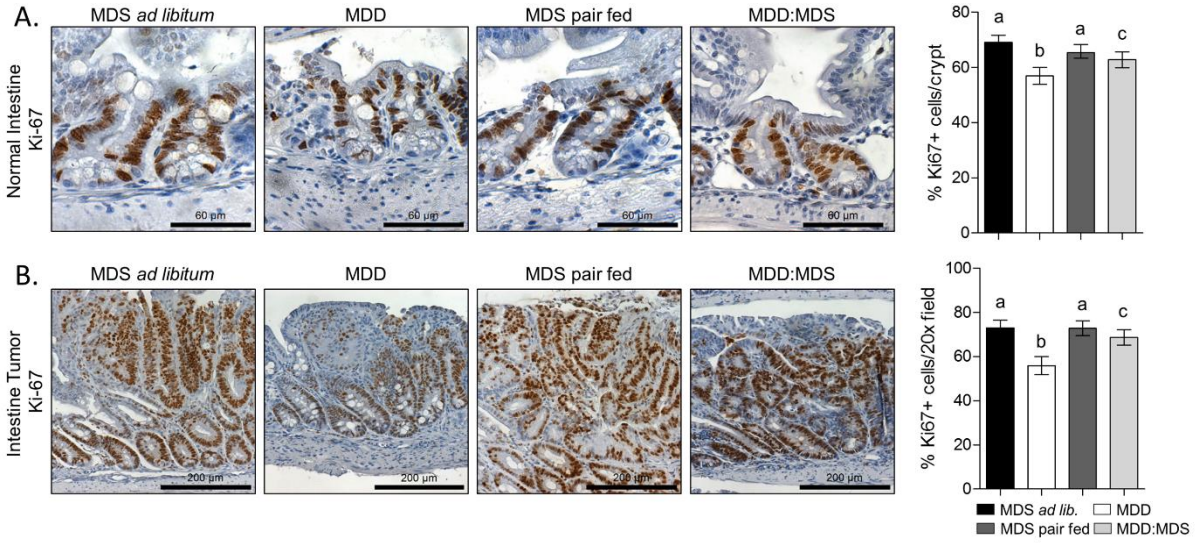

Figure 3-4. Immunohistochemical staining of Ki-67 in normal crypts and tumors of the small intestine.

(A) Representative images of Ki-67 staining in normal crypts, with quantification. MDD caused a small reduction (12%, $P<0.01$) in the average percentage of Ki-67$^+$ cells per crypt. MDD:MDS mice exhibited a small (6%, $P<0.01$), but significant, reduction in the average percentage of Ki-67$^+$ cells per crypt, possibly indicating that MDD-induced inhibition of proliferation persists during methyl donor repletion in normal crypts. (B) Representative images of Ki-67 staining in tumors, with quantification. Tumor proliferative index was determined by calculating the average percentage of Ki-67$^+$ cells in 5 40x fields per mouse (minimum 2000 cells counted). MDD induced a modest reduction (17%, $P<0.01$) in proliferative index in tumors of the small intestine. There was no reduction in proliferative index in tumors from MDD:MDS mice, indicating that MDD-induced reductions in proliferation are reversed by repletion with MDS diet. Bars indicate means ± SEM. Statistically significant differences ($P<0.05$) between groups, measured by ANOVA with Bonferroni's post-test, are indicated within bar graphs by differences in the letter placed above each group. Scale bars, 80 and 200 µm.

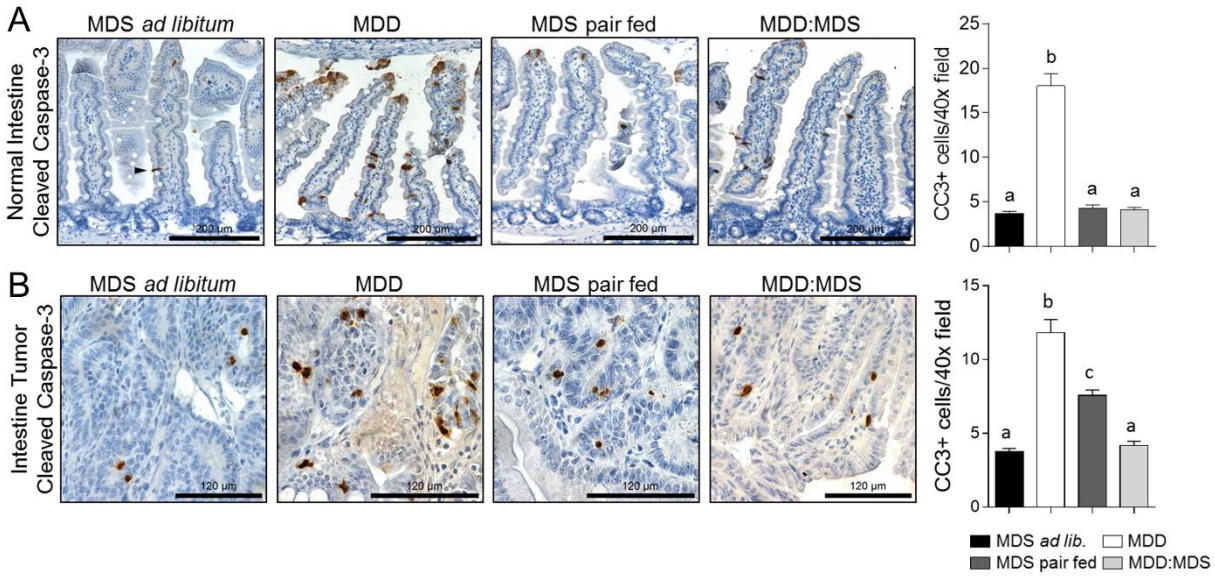

Figure 3-5. Immunohistochemical staining of Cleaved Caspase-3 (CC3) in normal crypts and tumors of the small intestine. (A) CC3 staining in normal tissue, with quantification. Apoptotic index was determined by calculating the average number of apoptotic cells in 10 40x fields of view per mouse. MDD caused an approximately 5-fold increase ($P<0.01$) in apoptotic index in normal tissue. Apoptotic cells were primarily located in the villi and tended to cluster towards the villous tip. (B) Representative images of CC3 staining in tumors of the small intestine, with quantification. Caloric restriction (MDS pair fed) and MDD caused 2-fold ($P<0.01$) and 3.1-fold ($P<0.01$) increases in apoptotic index, respectively. Apoptotic cells were scattered throughout the tumor with no obvious localization. Bars indicate means ± SEM. Statistically significant differences ($P<0.05$) between groups, measured by ANOVA with Bonferroni's post-test, are indicated within bar graphs by differences in the letter placed above each group. Scale bars, 200 and 120 µm.

Figure 3-6. Immunohistochemical staining of phospho-Histone H3 (PHH3) in normal crypts and tumors of the small intestine. (A) Representative images of PHH3 staining in normal small intestine, with quantification. MDD induced a large reduction in the average number of $PHH3^+$ cells per crypt in the small intestine on (53%, $P<0.01$), suggesting an inhibition of mitosis. The average number of $PHH3^+$ cells per crypt was also reduced in the MDD:MDS mice (35% reduction, $P<0.01$), suggesting that mitotic inhibition in normal crypts persists through at least 7 weeks of methyl donor repletion. (B) Representative images of PHH3 staining in tumors, with quantification. Tumor mitotic index was calculated by averaging the number of $PHH3^+$ cells in 10 40x microscope fields; MDD caused a large reduction (81%, $P<0.01$) in tumor mitotic index. Mitotic index was also reduced in tumors from MDDMDS mice (31%, $P<0.05$), indicating that mitotic inhibition in tumors persists, to a lesser degree, at least 7 weeks beyond methyl donor repletion. (C) Representative images of PHH3 staining in normal colon crypts, with quantification. MDD induced a large reduction in the average number of $PHH3^+$ cells per crypt in the colon (48%, $P<0.01$, respectively), suggesting an inhibition of mitosis. Bars indicate means ± SEM. Statistically significant differences ($P<0.05$) between groups, measured by ANOVA with Bonferroni's post-test, are indicated within bar graphs by differences in the letter placed above each group. Scale bars, 80 and 120 μm.

Figure 3-6

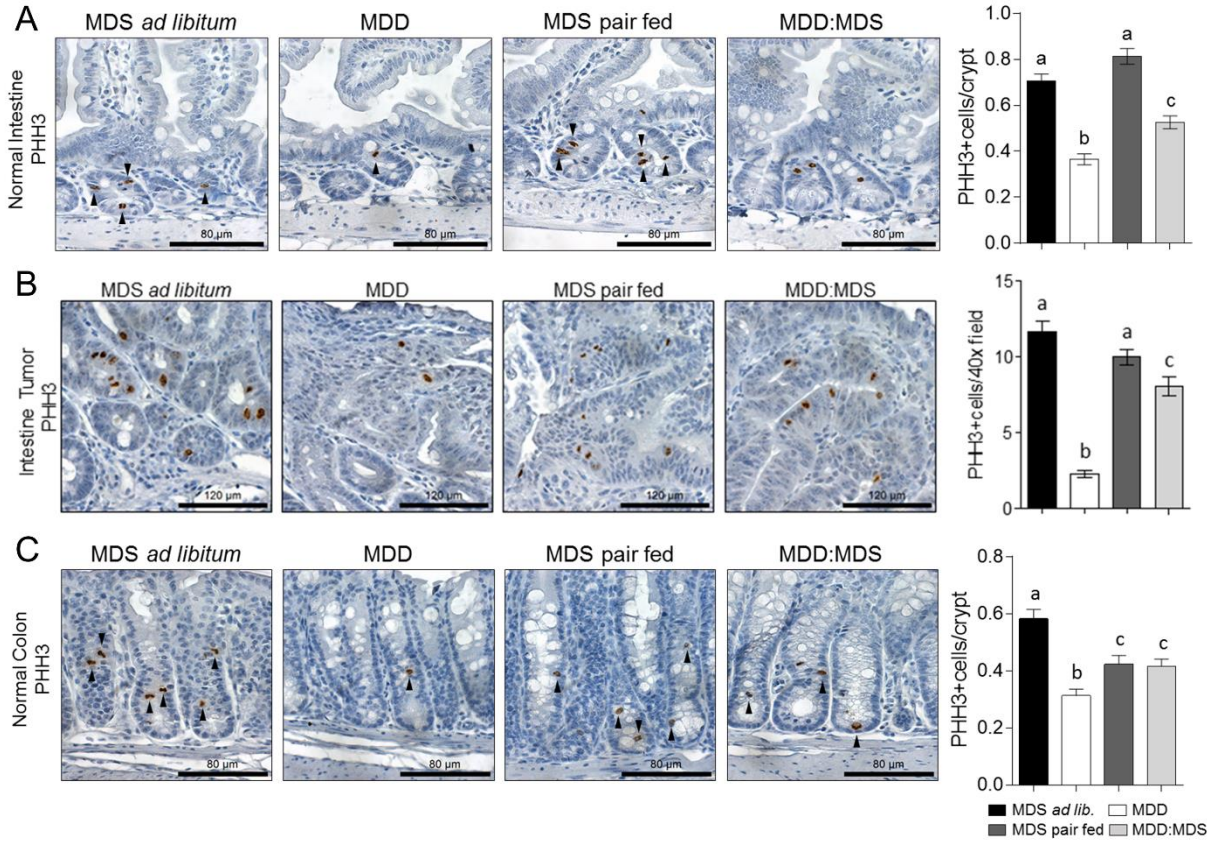
A
MDS *ad libitum*
MDD
MDS pair fed
MDD:MDS
Normal Intestine PHH3
80 µm
PHH3+cells/crypt
1.0
0.8
0.6
0.4
0.2
0.0
a
b
a
c
B
MDS *ad libitum*
MDD
MDS pair fed
MDD:MDS
Intestine Tumor PHH3
120 µm
PHH3+cells/40x field
15
10
5
0
a
b
a
c
C
MDS *ad libitum*
MDD
MDS pair fed
MDD:MDS
Normal Colon PHH3
80 µm
PHH3+cells/crypt
0.8
0.6
0.4
0.2
0.0
a
b
c
c
MDS *ad lib.*
MDD
MDS pair fed
MDD:MDS

intestines of the MDD:MDS mice (35%; P<0.01), indicating persistent changes to crypt cell homeostasis. MDD also reduced the fraction of cells undergoing mitosis in small intestinal tumors (**Figure 3-6B**). In the colon, methyl donor restriction caused a significant reduction in the numbers of $PHH3^+$ cells in both the MDD group (48%, P<0.01) and the MDD:MDS group (25%; P<0.05) (**Fig. 3-6C**).

Methyl donor restriction causes persistent depletion of $Dclk1^+$ intestinal stem cells

Immunohistology was used to examine cells expressing Doublecortin-like kinase 1 (Dclk1), a putative stem cell marker (197), in crypts of the small intestine and colon. $Dclk1^+$ cells contribute to the regulation of crypt homeostasis, as demonstrated by the fact that their ablation leads to a significant reduction in Ki-67^+ crypt epithelial cells (198). Importantly, it has also been suggested that $Dclk1^+$ cells can act as the initiating cell type for tumors in the $Apc^{Min/+}$ mouse (198). Consistent with previous reports (197), $Dclk1^+$ cells were observed scattered throughout the intestinal and colonic epithelium, but were concentrated in the lower portion of the crypt (**Figure 3-7A**). However, both methyl donor restriction and pair-feeding significantly reduced the number of $Dclk1^+$ cells within small intestinal crypts compared to Dclk1 staining in MDS controls (62%, P<0.01 and 36%, P<0.01, respectively, (**Figure 3-7A**). The frequency of $Dclk1^+$ cells remained suppressed in the MDD:MDS mice (32%, P<0.01), indicating a persistent depletion of this stem cell marker, even after methyl donor repletion (**Figure 3-7A**). A similar effect was observed in the colon; $Dclk1^+$ cells were reduced in both the MDD (41%; P<0.01), MDS-PF (26%; P<0.01) and MDD:MDS mice (25%; P<0.01) (**Figure 3-7B**). Since $Dclk1^+$ cells can serve as a cell type of origin for tumors formed in *Apc* mutant mice, the reduction in $Dclk1^+$ cell numbers associated with MDD may be related to the tumor-protective effects of the MDD diet.

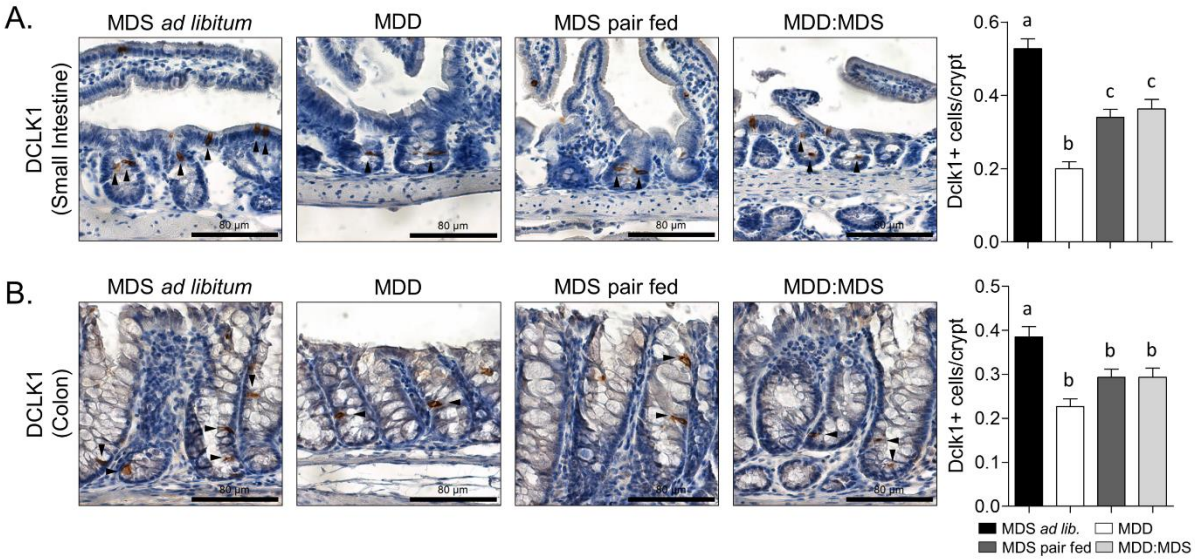

Figure 3-7. Immunohistochemical staining of Dclk1 in normal crypts and tumors of the small intestine. (A) Dietary MDD is associated with a reduction in the average number of Dclk1$^+$ cells per crypt is reduced in the small intestine (62% reduction, P<0.01). Importantly, Dclk1$^+$ cells are also reduced in the MDD:MDS mice (32% reduction, P<0.01), suggesting that this reduction is long-lasting. (B) Dietary MDD is associated with a reduction in the average number of DCLK1-positive cells per 40x field in tumors of the small intestine (74% reduction, P<0.01). (C) Dietary MDD is also associated with a significant reduction in the number of Dclk1+ cells in normal colonic crypts (41% reduction, P<0.01) in MDD mice. Dclk1 is a putative marker for intestinal tumor stem cells, and so the reduction of Dclk1$^+$ cell populations by dietary MDD may underlie its protective effects. Error bars indicate means ± SEM. Statistically significant differences (P<0.05) between groups, measured by ANOVA with Bonferroni's post-test, are indicated within bar graphs by differences in the letter placed above each group. Scale bars, 80 and 200 µm.

Adverse effects of methyl donor deficiency are reversed by methyl donor repletion

The dietary restriction of methyl donors can result in a number of pathologies (199–201). Consistent with our earlier study in *Apc*$^{Min/+}$ mice, MDD interfered with normal weight gain. At 22 weeks of age, body weights were significantly lower (45%, P<0.01) in the MDD and MDS-PF mice compared to the MDS mice (11.2 ± 2.1 g and 11.6 ± 1.38 g vs. 20.3 ± 3.3 g, respectively, P<0.01) (**Figure 3-8**). However, the inhibited body weight gain caused by 11 weeks of MDD was readily reversible upon methyl donor repletion, with normal body weights achieved within two weeks (**Figure 3-8**). Histological changes associated with MDD were also evaluated. As shown in **Figure 3-9A**, MDD caused significant hepatic steatosis, evidenced by the presence of clear vacuoles formed by excessive fat deposition (202). However, these fatty deposits were not present in the livers of MDD:MDS mice, indicating that the steatosis was readily reversible upon methyl donor repletion. Spleens harvested from mice maintained on the MDD diet showed evidence of depleted white pulp accompanied by a reduction in the size and number of splenic follicles, indicating a reduction in B lymphocyte populations (**Figure 3-9B**). These findings are consistent with reports that folate deficiency inhibits lymphocytic proliferation (200) and are consistent with our previous observations in *Apc*$^{Min/+}$ mice (122). Changes to the white pulp, however, were fully reversible in the MDD:MDS mice. Finally, hyperhomocysteinemia caused by choline or folate deficiency has been shown to induce renal fibrosis, particularly around glomeruli (201). However, using Masson's Trichrome staining to visualize collagen deposition, there was no evidence of renal fibrosis in any of the experimental groups (**Figure 3-9C**).

3.4 Discussion

This study expands upon our previous work (122) and demonstrates in a second *Apc*-mutant mouse model the adenoma-suppressive properties of dietary methyl donor restriction. The study further demonstrates that even a temporary period of dietary methyl donor restriction imparts long-lasting tumor

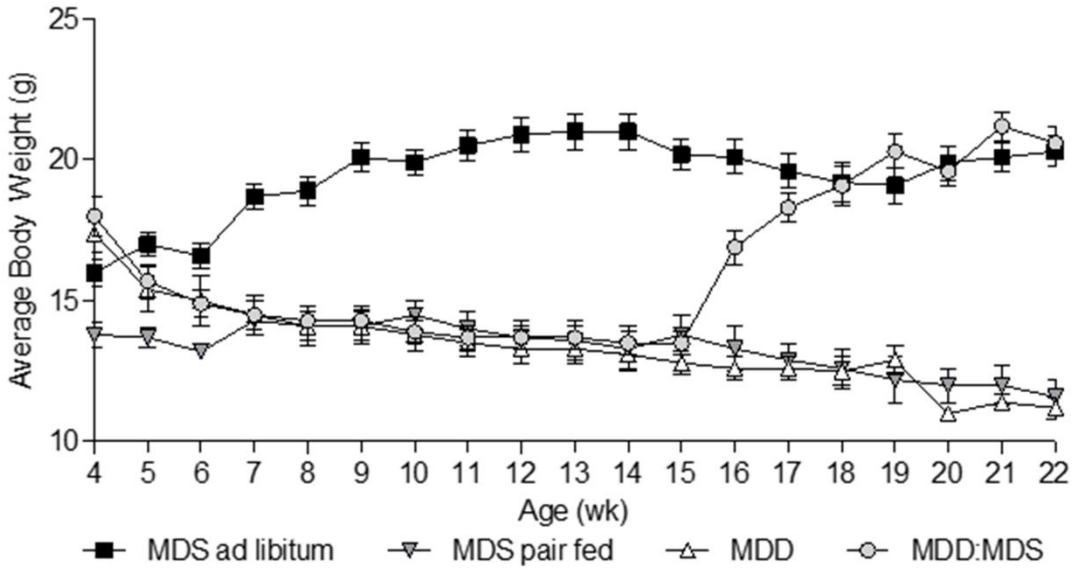

Figure 3-8. Body weight changes in $Apc^{\Delta 14/+}$ mice. Body weights of mice in each experimental group were recorded weekly throughout the study; each point represents average body weight ± SEM. At the end of the study, mice in groups 2 (MDS pair fed) and 3 (MDD) were reduced by approximately 45%. Mice in group 4 (MDD:MDS) initially failed to gain weight and at the time of transfer to MDS diet (15 weeks of age) weighed approximately 33% less than group 1 (MDS *ad lib.*) mice. However, following methyl donor repletion with the MDS diet, group 4 mice rapidly gained weight and had returned to a normal body weight by the end of the study. Error bars indicate means ± SEM.

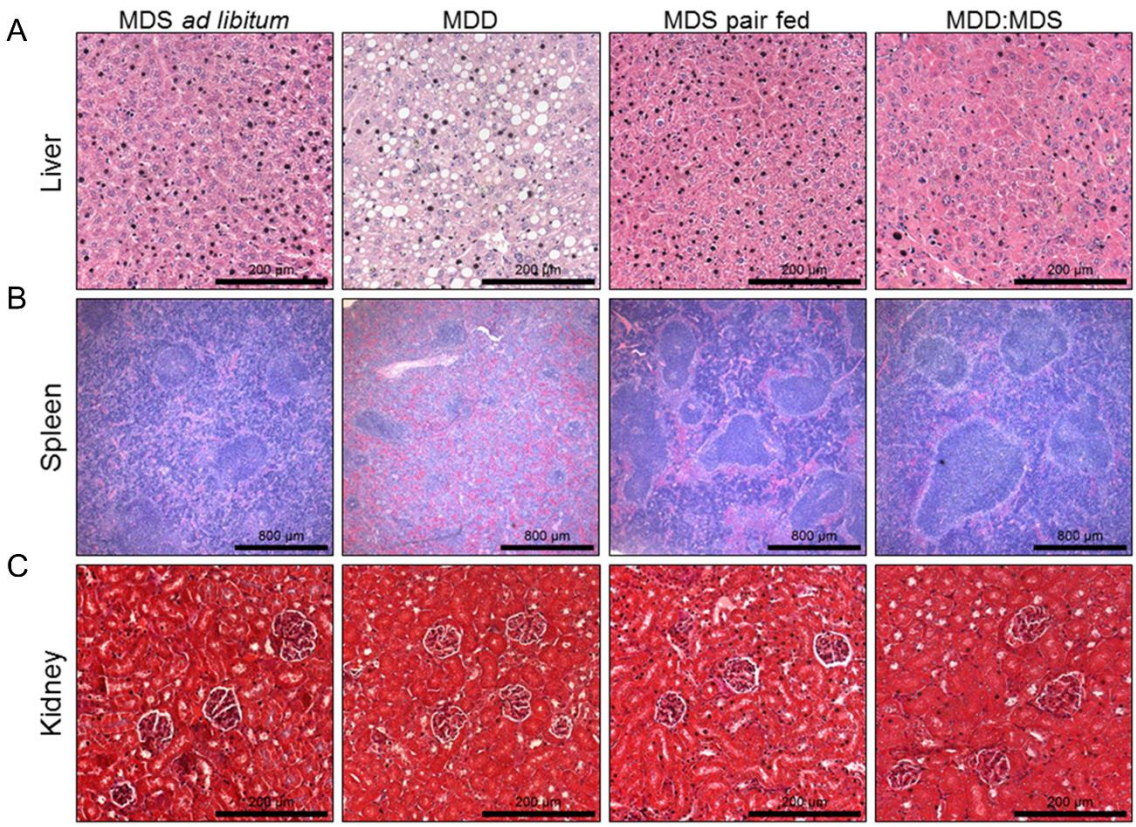

Figure 3-9. Adverse effects of dietary MDD. (A) Representative images of liver H&E staining from the four experimental groups. Mice maintained on MDD diet for 18 weeks develop hepatic steatosis, as evidenced by the presence of vacuoles formed by fat accumulation. These vacuoles are not present in the liver of MDD:MDS mice, indicating that hepatic steatosis is reversed after 7 weeks of methyl donor repletion. (B) Representative images of spleen H&E staining; MDD mice show a loss of white pulp (stained purple) and follicles, indicating a reduction in splenic lymphocyte populations. As before, spleens from MDD:MDS mice do not show evidence of lymphocytic depletion, indicating that this effect of the MDD diet is reversible by methyl donor repletion. (C) Chronic choline deficiency has been reported to cause renal fibrosis, particularly around glomeruli. Using Masson's Trichrome stain to visualize collagen deposition (blue), we did not find evidence of renal fibrosis in MDD mice. Scale bars, 200 and 800 µm.

protection to the intestine, an effect that persists for at least 7 weeks after mice have been returned to a methyl donor sufficient diet. While some reports have suggested that folic acid may have chemopreventive efficacy in the general population (203,204), data from recent studies suggest that high levels of folic acid intake may increase the likelihood of cancer development in certain populations by accelerating the progression of pre-existing lesions (118). The present study and our previous work (122) support these observations and suggest that short-term reduced intake of folic acid, methionine, choline and vitamin B12 may benefit those individuals at elevated risk of CRC. Furthermore, the sustained tumor protection described in this report, which persists beyond the period of active methyl donor restriction, implies that this dietary manipulation causes long-term changes to the intestinal mucosa that can impede tumor initiation.

Evidence from several studies suggests that the benefits of methyl donor-based chemoprevention strategies are heavily dependent upon the timing of administration (174). As shown by Song *et al.* (205), *Apc*$^{+/-}$*Msh2*$^{-/-}$ mice fed a folate-supplemented diet prior to the establishment of neoplastic foci benefit from significantly reduced intestinal adenoma multiplicity; however, a folate-supplemented diet initiated after the formation of neoplastic foci has the opposite effect. Furthermore, our previous work demonstrates that the tumor protective effects of dietary MDD are abrogated when dietary administration is delayed beyond 10 weeks of age in *Apc*$^{Min/+}$ mice (122). Thus, it will be important for future studies to examine how the timing of MDD with respect to age and neoplastic progression impacts long-term protection.

The tumor protection afforded by methyl donor restriction is associated with alterations to intestinal morphology and cell turnover, assessed by a morphometric analysis of cryptal structure, crypt fission rates and analysis of cell turnover characteristics. Importantly, many of these alterations were retained following methyl donor repletion. Specifically, MDD was associated with a reduction in crypt length and crypt branching, suggesting altered intestinal growth and homeostasis. Crypt branching is a

measure of the rate of crypt fission (195), a process that controls intestinal growth, in which crypts divide longitudinally, initiated by stem cells located at the crypt base (193). Crypt fission has recently been implicated in intestinal cancer progression, providing a mechanism for the occult expansion of mutant crypts (194). As shown by Fischer *et al.* (206), mutant intestinal crypts in *Apc*-deficient mice clonally expand *via* crypt fission, creating fields of normal-appearing mutant crypts that are poised for tumorigenesis. A follow-up study by the same investigators demonstrated that reduced crypt fission is associated with decreased tumor multiplicity in $Pms2^{Cre/Cre};Apc^{CKO/CKO}$ mice (194). Thus, our findings are consistent with a role for MDD in reducing adenoma risk by limiting crypt fission. As crypt fission is initiated by ISCs (193,195), this observation may reflect changes to the intestinal stem cell pool.

Tumor protection was also associated with altered crypt homeostasis, as evidenced by the reduced proliferation of cells within the crypt epithelium. In a comprehensive review, Lipkin (207) discussed the possibility that increased susceptibility to cancer may be related to the basal proliferative rate within the normal colonic mucosa. Several studies have demonstrated an association between increased proliferation of normal mucosa and the risk of developing cancer (207,208). In a case-control study by Mills et al. (209), samples of normal mucosa from individuals with FAP or sporadic CRC were shown to have a markedly increased fraction of mitotic cells compared to healthy controls. These findings suggest that elevated basal proliferation of normal gut mucosa may be an important early and predisposing factor in cancer development. As reviewed by Tammariello and Milner (210), a large number of dietary agents have been tested for their chemopreventive benefit in *Apc* mouse models; among the most effective cancer prevention strategies are those agents that target cell proliferation rates within morphologically normal, but at-risk mucosa (211,212). As discussed by Kim (213), folate restriction alone has the ability to reduce basal proliferation rates in animal tumor models. In addition, Crott et al. (214) showed that moderate folate restriction to colon cells affected several cancer-related pathways, including cell cycle checkpoints, cellular adhesion and migration, and Wnt signaling. Thus, our findings are

consistent with a role for MDD in modifying adenoma risk by influencing basal mucosal homeostasis. Furthermore, several recent studies have revealed an role for folate metabolism in the regulation of ISCs and other stem cells (215,216). These long-term alterations to intestinal epithelial homeostasis provide additional evidence that dietary MDD may induce changes to ISCs within the normal mucosa associated with tumor protection.

Dietary MDD caused a significant depletion of intestinal cells expressing Dclk1, a putative stem cell marker that has been the focus of recent interest (217). Giannakis *et al.* (217) originally proposed Dclk1 as a marker for intestinal stem cells after finding that Dclk1 expression was enriched in cells isolated from the progenitor cell compartment of intestinal crypts in C57Bl/6 mice. Nakanishi *et al.* (197) later demonstrated *via* a series of lineage-tracing experiments that Dclk1^{+} cells can act as the initiating cell for intestinal tumors in *Apc*$^{Min/+}$ mice and proposed that Dclk1 may represent a marker for "tumor stem cells". Importantly, these studies also demonstrated that genetic ablation of Dclk1^{+} cells dramatically reduced intestinal tumor burden, suggesting that Dclk1+ cells may provide a target for novel CRC therapies (197,218). Thus, the tumor protection afforded by dietary methyl donor restriction may be based in part on a selective reduction in Dclk1^{+} cell populations. Several recent studies by Westphalen *et al.* (198) have demonstrated that loss of *Apc* function within Dclk1^{+} stem cells is insufficient to drive tumor formation. Using *Dclk1-CreERT x Apc*$^{flox/flox}$ mice, they demonstrate that mice remain tumor-free for up to 18 months after *Apc* inactivation following tamoxifen injections. However, intermittent, short-term treatment with dextran sodium sulfate (DSS) subsequent to *Apc* loss leads to the formation of multiple intestinal tumors with 100% penetrance, indicating the requirement for a concomitant pro-inflammatory stimulus (198). Furthermore, in lineage tracing experiments using intestinal organoids cultured with Wnt3a-supplemented media, Westphalen *et al.* (198) also showed that treatment with either macrophage-conditioned media or IL-1β caused a 4-fold increase in Dclk1^{+} cell-derived crypts. In our previous study (122), we showed that dietary MDD significantly reduces the expression of a number of

pro-inflammatory cytokines in the intestine, including IL-1β. Thus, it is possible that dietary MDD inhibits Dclk1-mediated tumor development *via* several interrelated mechanisms. Under one scenario, by reducing the levels of a number of pro-inflammatory mediators within the intestinal mucosa, MDD may eliminate an important stimulus required for activation of mutated $Dclk1^{+}$ cells. In addition, the MDD diet may reduce the overall density of $Dclk1^{+}$ stem cells within the intestinal crypt compartment, thereby reducing the probability of *Apc* loss occurring within these tumor initiating stem cells in $Apc^{\Delta 14/+}$ mice.

FOCM is fundamental to cellular homeostasis and genomic integrity, and thus dietary MDD is unlikely to be applied to the general population as a primary prevention strategy. However, the present study suggests that even a short-term intervention with MDD diet may provide benefit to certain high-risk subpopulations. One group that may benefit is adolescent FAP patients, in which a defined period of MDD may suppress polyposis, thereby delaying the need for colectomy. Due to the potential risk associated with the dual-modulatory effect of folic acid on colorectal tumorigenesis (219), future clinical application of MDD should be combined with careful monitoring by colonoscopy, which is already used routinely for FAP patients (180). While most of the side effects of MDD are readily reversible upon methyl donor repletion, a thorough investigation of the potential effects of MDD on normal development and cardiovascular integrity will need to be undertaken prior to further clinical applications. However, due to the long-lasting protective effects of even temporary MDD, a strategy analogous to "short-term intermittent therapy to eliminate premalignancy" (SITEP) (53) may provide clinical benefit while minimizing unwanted side effects. By administering short pulses of dietary MDD, it may be possible to induce persistent changes to the intestinal epithelium that provide long-lasting tumor suppression, while minimizing exposure to nutritional deficiency. In the future, it will be important to evaluate how the timing of MDD administration can be modulated to provide an optimal balance between tumor protection and unwanted side effects. In addition, future efforts to identify specific metabolic and cell-signaling pathways that are affected by dietary MDD may yield novel targets for chemoprevention.

In summary, this study provides additional evidence that dietary methyl donor restriction may be a viable strategy for cancer prevention in high-risk individuals. Our previous study demonstrated that a diet deficient in methyl donors reduced intestinal tumor incidence by greater than 95% in *Apc*$^{Min/+}$ mice. The present study extends these promising results to a second *Apc*-dependent mouse tumor model, *Apc*$^{\Delta 14/+}$, and show that the tumor protection afforded by dietary methyl donor restriction is both effective and long-lasting. Tumor protection is accompanied by long-term changes to intestinal crypt morphology and cell turnover which may result from alterations to the intestinal stem cell pool, as evidenced by the depletion of Dclk1^{+} cells from the crypt base. Finally, several detrimental effects associated with methyl donor restriction (e.g., reduced body weight gain, hepatic steatosis) are shown to be transient and readily reversible following methyl donor repletion. Taken together, these results indicate that even temporary dietary methyl donor restriction in severely tumor-prone mice can induce persistent changes to the intestinal epithelium that provide long-lasting tumor protection in the adult.

Chapter 4: Metabolite profiling of mice maintained on a methyl donor deficient diet reveals metabolic changes associated with tumor protection

4.1 Introduction

Investigations into the effects of folate consumption on the risk of CRC have produced conflicting results. Early epidemiological studies suggested that folate deficiency increases the risk of CRC in the general population (173–176). However, a more recent meta-analysis of 50,000 individuals enrolled in 13 different folate supplementation trials found no effect on CRC incidence (115). In contrast to studies in the general population, studies of certain high-risk individuals suggest that elevated folate intake may actually *increase* CRC risk (116,117). This finding is consistent with the results of preclinical studies from our laboratory (122,220) showing that a diet deficient in the methyl donor nutrients folate, choline, methionine and Vitamin B12 inhibits tumor development in *Apc*-mutant mouse models of CRC. These studies suggest that reduced methyl donor intake may benefit individuals at elevated risk of CRC. Our most recent study (220) demonstrated that even temporary dietary methyl donor deficiency (MDD) provides long-lasting tumor protection that is associated with persistent changes to the intestinal epithelium.

At present, the metabolic pathways through which the MDD diet affects changes to the intestinal epithelium and reduces CRC risk are unknown. Because the methyl donor nutrients depleted from the MDD diet all play a role in FOCM, this pathway is predicted to be heavily impacted by MDD. FOCM is responsible for several fundamental biosynthetic processes including the production of nucleotides and the generation of SAM, the “universal methyl donor”, which is required for the methylation of DNA and histones (221). FOCM has also been shown to interact with many other metabolic systems, including lipid and energy metabolism (222). These functions make FOCM critical to cellular homeostasis; disruption of FOCM can compromise DNA stability, alter gene expression, and inhibit cellular proliferation and survival (223). Furthermore, methyl donor nutrients contribute to many metabolic functions independent of

FOCM, including the synthesis of phospho- and sphingolipids, proteins, hormones and other small molecules (222). While drugs that disrupt FOCM and downstream pathways have been used to successfully treat CRC for decades (223), there are currently no cancer *prevention* strategies based on the manipulation of these pathways.

Our previous studies (122,220) suggest that the manipulation of methyl donor metabolism is a promising approach to the prevention of CRC. However, the MDD diet was associated with a number of adverse effects that, while reversible, may limit its clinical efficacy. Investigating the specific metabolic pathways that are disrupted under conditions of dietary MDD may help to identify novel targets for safer and more effective CRC prevention strategies. To achieve this goal, the present study uses an untargeted metabolomic profiling platform to quantify ~400 biochemicals within samples of mouse colonic mucosa collected in our previous dietary study (220). Using this approach, we have shown that dietary MDD is associated with extensive metabolic changes, a subset of which persist following methyl donor repletion. These metabolic changes were enriched in several key pathways, including the methionine cycle, the transsulfuration pathway, secondary bile acid synthesis, and fatty acid β-oxidation. These observations provide clues to the molecular changes underlying MDD-induced tumor protection and identify metabolomic features of the MDD diet that may provide new targets for CRC prevention.

4.2 Materials and Methods

Animal Treatment and Sample Collection

Dietary experiments using *Apc*$^{\Delta 14/+}$ mice and collection of colonic tissue samples have previously been described in detail (220). Animal experiments were conducted with approval from the Institutional Animal Care and Use Committee, UConn Health. Briefly, dietary studies used two amino-acid defined experimental diets: the Methyl Donor Sufficient (MDS; TD.99366, Harlan Laboratories, Madison WI) diet and the Methyl Donor Deficient (MDD; TD.00605) diet, which was identical to the MDS diet except for the

depletion of folate, choline, methionine and vitamin B12, and the addition of homocysteine. Full details of MDS and MDD diet composition have previously been reported (220). *Apc*$^{\Delta 14/+}$ mice were randomized at 4 weeks of age and placed into four experimental groups; each group was placed on a specific dietary regimen for 18 weeks as previously reported (220). Briefly, group I (MDS *ad libitum*, "AL", n=28) mice were fed the MDS diet *ad libitum* for the entire 18-week period. Group II (MDD, n=19) mice were fed the MDD diet *ad libitum* for 18 weeks. Group III (MDS-PF, "PF", n=27) mice were pair-fed the MDS diet in an amount equivalent to levels consumed by Group II mice. Finally, mice in Group IV (MDD:MDS-Repletion, "R", n=28) were placed on the MDD diet for 11 weeks, and then switched to the MDS diet for the remaining 7 weeks. All mice were sacrificed at 22 weeks of age. Upon sacrifice, colons were harvested, flushed with ice-cold PBS and opened longitudinally. Normal-appearing mucosa was scraped from the distal 2-3 cm of the colon and immediately snap-frozen. Mucosa samples were stored at -80°C until analysis.

Metabolite Profiling

Fifty mg of snap-frozen, normal-appearing colonic mucosa was shipped to Metabolon, Inc. (Durham, NC) on dry ice for metabolite quantification. Upon receipt, samples were stored at -80°C until processing. The platform used for sample preparation and analysis has been previously described in detail (224,225). Briefly, tissue samples were mechanically disrupted and homogenized using a GenoGrinder 2000 (Glen Mills, Inc.) and metabolites were extracted using cold methanol precipitation. Tissue extracts were split into 3 aliquots: one for analysis by UPLC-MS/MS with positive ion electrospray ionization, one for analysis by UPLC-MS/MS with negative ion electrospray ionization, and one for analysis by GC-MS. For LC, the samples were stored overnight under nitrogen before preparation for analysis. For GC, each sample was dried under vacuum overnight before preparation for analysis. Reproducibility of the extraction and chromatography procedures was assessed by spiking in xenobiotic compounds at known

concentrations. GC/LC-MS parameters including column retention time, spectral peaks, and mass-to-charge ratio were compared to a proprietary reference chemical library to identify metabolites.

Bioinformatics and Biostatistics

MS peaks representing metabolites of interest were quantified by calculating the area under the curve. Missing values were assumed to be below the limit of detection and were imputed with the minimum observed value for each given compound. When necessary, biochemical data was normalized to total protein to account for differences in metabolite levels due to differences in the amount of material present in each sample. For analyses across multiple days, a data normalization step was performed to correct variation resulting from instrument inter-day variability. Each compound was corrected in run-day blocks by setting the medians equal to 1 and normalizing each data point proportionately (termed the "block correction"). Statistical analysis of mean metabolite levels was performed using Welch's two-sample *t*-test followed by false discovery rate (FDR) correction using the Benjamini-Hochberg procedure. Differences with an FDR-corrected P-value < 0.05 were considered to be statistically significant. Random Forest Analysis (RFA), an ensemble machine learning technique, was used to generate metabolite signatures that allowed accurate classification of de-identified samples into experimental groups. Mean Decrease Accuracy (MDA) analysis was used to quantify the importance of individual metabolites to accurate classification by RFA. Hierarchical clustering of samples was done by calculating Euclidean distance between samples, and dimensionality was reduced using Principal Component Analysis (PCA). RFA, MDA, clustering and PCA were done using the R programming language and software environment. Pathway analysis was done by calculating relative-betweenness centrality using MetaboAnalyst 3.0 (226).

4.3 Results

Dietary methyl donor deficiency is associated with a distinct colonic metabolite profile

Our recent study (220) demonstrated that *Apc*$^{\Delta 14/+}$ mice fed a diet deficient in methyl donor nutrients benefit from dramatic intestinal tumor protection that persists after mice are returned to a control diet. To explore the molecular changes associated with MDD that may underlie this protection, we conducted GC/LC-MS-based metabolite profiling of normal colonic mucosa harvested from mice in our previous study (220). Using a previously described metabolomics platform (224), 388 unique metabolites were quantified in 7 mice from each of the 4 experimental groups; these "metabolite profiles" were used for all subsequent analyses. As shown in **Figure 4-1A**, MDD samples are separated from MDS *ad libitum,* MDS pair-fed, and MDD:MDS-Repletion samples by PCA, indicating that MDD is associated with a distinct metabolic profile. Furthermore, PCA reveals that metabolite profiles of mice in the MDD:MDS-Repletion group only partially overlap with those from mice in the MDS *ad libitum* and MDS pair-fed groups, suggesting that some metabolic changes persist within the colonic mucosa after a return to the MDS control diet. The association of MDD with a unique metabolite signature was underscored by RFA, which was able to accurately distinguish between MDD and MDS-AL mice, as well as between MDD and MDS-PF mice, with 100% accuracy. By comparing the profiles of MDD and MDS-PF mice, it is possible to identify metabolic changes due specifically to deficiency in methyl donor nutrients. As shown in **Figure 4-1B**, the 30 metabolites most important to the accurate separation of MDD and MDS-PF samples by RFA were identified using MDA analysis. These 30 metabolites were classified into functional subgroups and were used as a starting point to identify the metabolic pathways most significantly affected by dietary MDD. Subgroup classifications for these metabolites, as well as their fold-changes in MDD samples relative to MDS-PF, are shown in **Table 4-1**. By manually investigating all metabolites within the subgroups identified in this way, we were able to identify the three metabolic pathways with the greatest number of MDD-

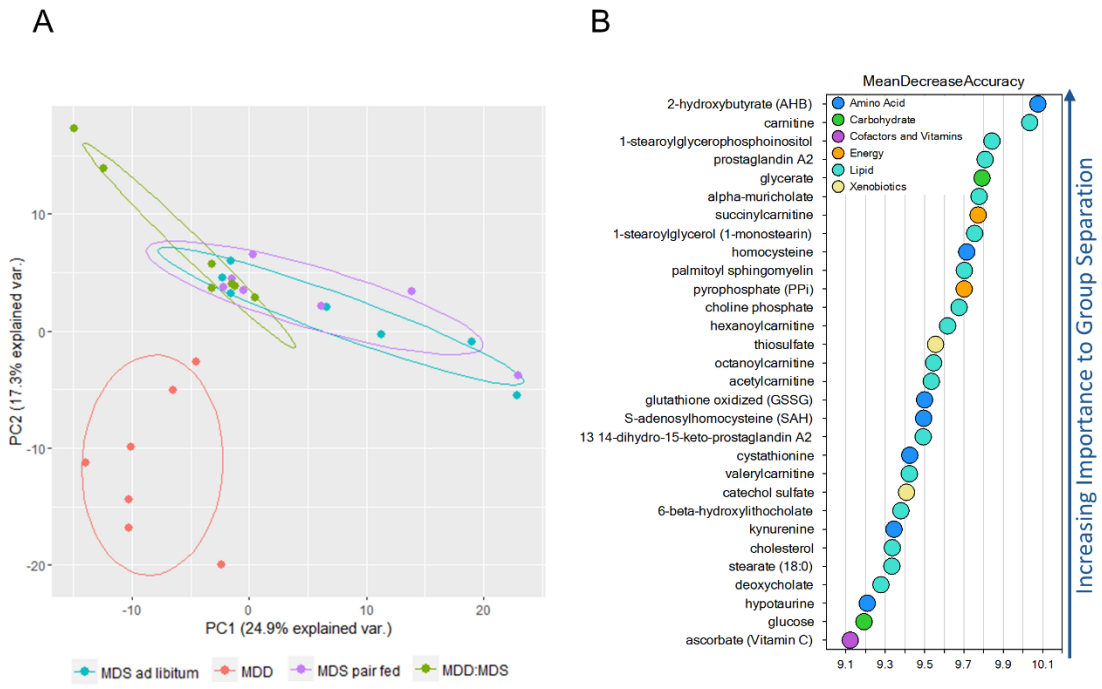

Figure 4-1. Identification of a metabolite profile associated with dietary MDD. (A) Principal component analysis (PCA) biplot showing separation of MDD samples from the other experimental groups, indicating a distinct metabolic profile. Partial overlap of MDD:MDS samples with both MDS *ad libitum* and MDS pair-fed controls suggests that some metabolic changes persist at least 7 weeks beyond methyl donor repletion. (B) Top 30 metabolites ranked by importance to separation of MDD and MDS-PF samples by Random Forest Analysis (RFA). These metabolites were used as a stating point in the identification of metabolic pathways most significantly affected by dietary MDD.

Metabolite	Platform	KEGG ID	Subgroup	Fold change (vs MDS PF)	q-value
ascorbate	GC/MS	C00072	Ascorbate and Aldarate Metabolism	1.6	2.9E-03
catechol sulfate	LC/MS (-)	C00090	Benzoate Metabolism	-12.5	1.0E-02
alpha-muricholate	LC/MS (+)	C17647	Bile Acid Metabolism	-10.0	2.5E-05
6-beta-hydroxylithocholate	LC/MS (-)	C15515	Bile Acid Metabolism	-7.1	2.7E-05
deoxycholate	LC/MS (-)	C04483	Bile Acid Metabolism	-10.0	1.9E-03
carnitine	LC/MS (+)	C00318	Carnitine-Dependent Fatty Acid Oxidation	-2.4	5.5E-07
hexanoylcarnitine	LC/MS (+)	--	Carnitine-Dependent Fatty Acid Oxidation	-2.6	4.0E-04
octanoylcarnitine	LC/MS (+)	C02838	Carnitine-Dependent Fatty Acid Oxidation	-2.6	7.6E-05
acetylcarnitine	LC/MS (+)	C02571	Carnitine-Dependent Fatty Acid Oxidation	-1.9	1.0E-04
valerylcarnitine	LC/MS (+)	--	Carnitine-Dependent Fatty Acid Oxidation	-4.2	5.0E-04
thiosulfate	GC/MS	C05529	Chemical	1.7	1.0E-03
prostaglandin A2	LC/MS (-)	C05953	Eicosanoid	3.1	6.5E-05
13,14-dihydro-15-keto-prostaglandin A2	LC/MS (-)	--	Eicosanoid	3.4	6.3E-05
glycerate	GC/MS	C00258	Glycolysis, Gluconeogenesis, and Pyruvate Metabolism	-1.7	4.7E-03
glucose	GC/MS	C00031	Glycolysis, Gluconeogenesis, and Pyruvate Metabolism	-12.5	8.3E-03
stearate	LC/MS (-)	C01530	Long Chain Fatty Acid	1.5	9.9E-03
1-stearoylglycerophosphoinositol	LC/MS (-)	--	Lysolipid	2.8	9.0E-05
2-hydroxybutyrate (AHB)	GC/MS	C05984	Methionine, Cysteine and Taurine Metabolism	6.1	5.0E-04
homocysteine	GC/MS	C00155	Methionine, Cysteine and Taurine Metabolism	111.2	6.3E-05
glutathione, oxidized (GSSG)	LC/MS (+)	C00127	Methionine, Cysteine and Taurine Metabolism	1.4	1.2E-02
S-adenosylhomocysteine (SAH)	LC/MS (-)	C00021	Methionine, Cysteine and Taurine Metabolism	14.5	2.7E-05
cystathionine	GC/MS	C02291	Methionine, Cysteine and Taurine Metabolism	12.7	1.9E-03
hypotaurine	GC/MS	C00519	Methionine, Cysteine and Taurine Metabolism	5.2	4.9E-05
1-stearoylglycerol (1-monostearin)	GC/MS	D01947	Monoacylglycerol	1.9	1.9E-03
pyrophosphate (PPi)	GC/MS	C00013	Oxidative Phosphorylation	1.9	9.0E-04
choline phosphate	LC/MS (+)	C00588	Phospholipid Metabolism	-2.4	8.1E-05
palmitoyl sphingomyelin	GC/MS	--	Sphingolipid Metabolism	3.7	4.0E-04
cholesterol	GC/MS	C00187	Sterol	1.6	2.1E-03
succinylcarnitine	LC/MS (+)	--	TCA Cycle	-2.2	4.9E-05
kynurenine	LC/MS (+)	C00328	Tryptophan Metabolism	3.1	7.9E-03

Table 4-1. Fold-changes and subgroup classification of Top 30 metabolites identified by RFA.

associated metabolic changes: Methionine and Cysteine Metabolism, Bile Acid Metabolism, and Carnitine-dependent Fatty Acid Oxidation (FAO).

MDD reduces methionine cycle flux and increases transsulfuration pathway flux

We predicted that mice fed the MDD diet would experience reduced levels of methyl donor nutrients within the colonic mucosa. As shown in **Figure 4-2A&B**, mice fed the MDD diet showed significant reductions in the levels of methionine (-2.9-fold, P<0.001) and betaine (-3.3-fold, P<0.001), the metabolite immediately downstream of choline, relative to MDS *ad libitum* control mice, validating our prediction. Furthermore, as shown in **Figure 4-2C**, MDD mice exhibited a dramatic increase in the level of homocysteine (109-fold, P<0.001) relative to control, again consistent with our prediction. This substantial increase in homocysteine was accompanied by an increase in S-adenosylhomocysteine (SAH) (17.1-fold, P<0.001) (**Figure 4-2D**), a metabolite normally produced by demethylation of the "universal methyl donor" S-adenosylmethionine (SAM) (221). As shown in **Figure 4-2E-G**, MDD was also associated with increases in cystathionine (11.5-fold, P<0.001), 2-hydroxybutyrate (3.5-fold, P<0.01) and cysteine (4.0-fold, P<0.05), suggesting increased flux through the cysteine-generating transsulfuration pathway (227). Cysteine produced *via* the transsulfuration pathway can be utilized in downstream pathways involved in the buffering of oxidative stress (227). As shown in **Figure 4-2H&I** MDD mice exhibited increases in hypotaurine (2.9-fold, P<0.01) and glutathione disulfide (1.3-fold, P<0.05) suggesting taurine and glutathione metabolism, two critical antioxidant mechanisms, are upregulated in MDD mice. A depiction of the methionine and cysteine metabolism changes associated with dietary MDD is shown in **Figure 4-3**.

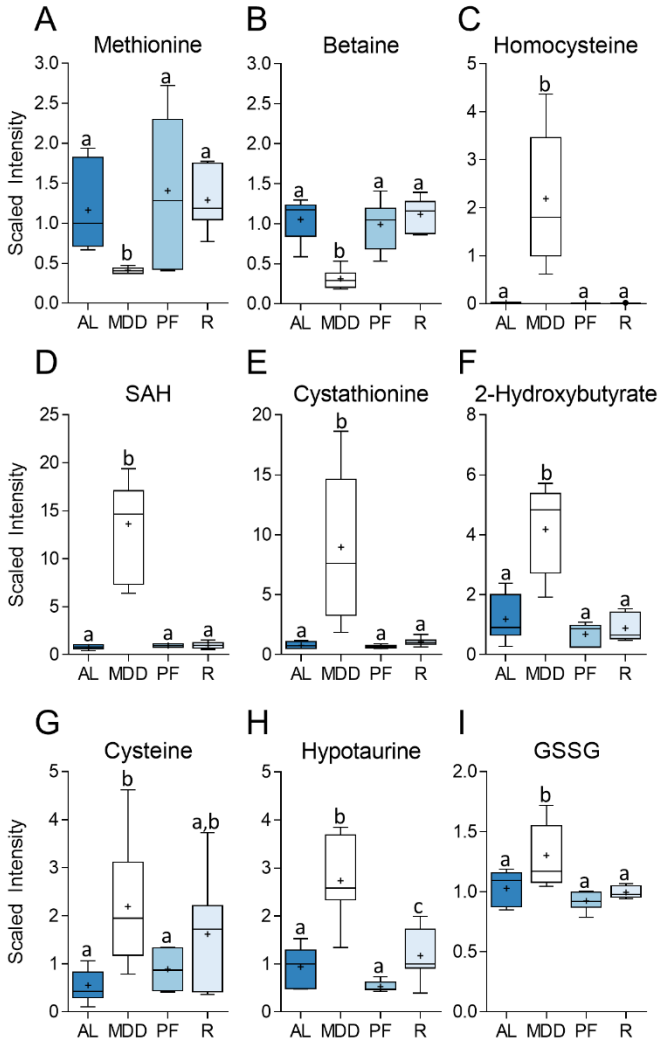

Figure 4-2. Changes in the levels of metabolites involved in the methionine cycle and the transsulfuration pathway. Levels of methionine (A; -2.9-fold, P<0.001), betaine (B; -3.3-fold, P<0.001), homocysteine (C; 109-fold, P<0.001), s-adenosylmethionine (D; 17.1-fold, P<0.001), cystathionine (E; 11.5-fold, P<0.001), 2-hydroxybutyrate (F; 3.5-fold, P<0.01), cysteine (G; 4.0-fold, P<0.05), hypotaurine (H; 2.9-fold, P<0.01), and glutathione disulfide (I; 1.3-fold, P<0.05) are all altered under conditions of dietary methyl donor restriction. Whiskers on Tukey's box plots represent Interquartile Range (IQR). Statistically significant differences (P<0.05) between groups, measured by ANOVA with Bonferroni's post-test, are indicated within bar graphs by differences in the letter placed above each group.

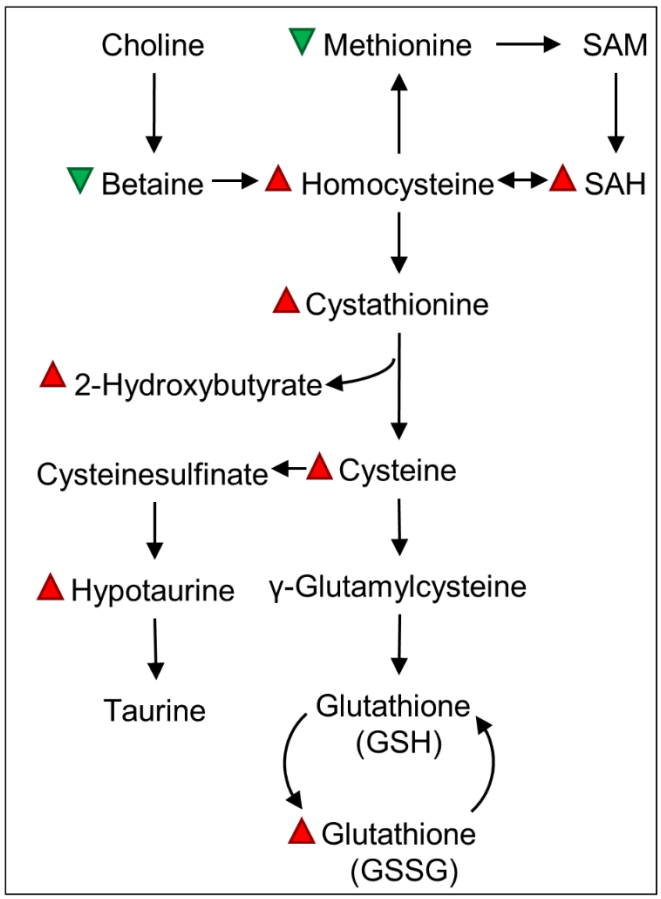

Figure 4-3. Schematic overview of metabolic changes to the methionine cycle and transsulfuration pathway under conditions of dietary MDD. Consistent with the composition of the MDD diet, levels of methionine and betaine in the colonic mucosa were significantly reduced. Furthermore, levels of homocysteine were significantly increased, leading to increased flux through the transsulfuration pathway.

MDD inhibits production of secondary bile acids (BAs)

Unexpectedly, metabolite profiling revealed reduced levels of secondary bile acids within the colonic mucosa of MDD mice. Secondary BAs have previously been suggested to promote colorectal carcinogenesis (228). As shown in **Figure 4-4A&B**, dietary MDD was associated with decreased levels of deoxycholate (-4.5-fold, $P<0.05$) and its taurine-conjugated bile salt taurodeoxycholate (-2.2-fold, $P<0.01$) within the colonic mucosa, relative to MDS *ad libitum* control. Furthermore, as shown in **Figure 4-4C-E**, dietary MDD was associated with reductions in levels of α-Muricholate (-3.8-fold, $P<0.005$), β-Muricholate (-2.2-fold, $P<0.05$), and Murideoxycholate (-2.6-fold, $P<0.05$), the predominant murine secondary bile acids. Together, these data suggest that dietary MDD inhibits the synthesis of secondary bile acids. A depiction of the changes to secondary bile acid metabolism is shown in **Figure 4-5**.

MDD inhibits carnitine-dependent FAO

A large number of metabolites identified by MDA analysis were classified as acylcarnitines. Acylcarnitines are fatty acid-derived acyl groups conjugated to the shuttle molecule carnitine that are transported into the mitochondrial matrix to be oxidized for energy production (66). As shown in **Figure 4-6A**, a panel of acylcarnitines was reduced within the colonic mucosa of MDD mice, including acetylcarnitine (-1.8-fold, $P<0.001$), propionylcarnitine (-2.0-fold, $P<0.05$), hydroxybutyrylcarnitine (-1.7-fold, $P<0.01$), valerylcarnitine (-3.4-fold, $P<0.001$), hexanoylcarnitine (-3.0-fold, $P<0.01$), octanoylcarnitine (-3.0-fold, $P<0.05$), palmitoylcarnitine (-2.1-fold, $P<0.05$), and oleoylcarntine (-2.2-fold, $P<0.05$). Decreased acylcarnitine levels are likely a consequence of limited availability of carnitine (-2.0-fold, $P<0.01$), which is synthesized from methionine (229) and was significantly reduced in the mucosa of MDD mice relative to MDS *ad libitum* control (**Figure 4-6B**). The oxidation of acylcarnitines within the mitochondrial matrix produces the critical energy metabolism cofactors Acetyl CoA (**Figure 4-6C**), which was also reduced in MDD mice (-2.5-fold, $P<0.05$). Together, these results suggest that dietary MDD

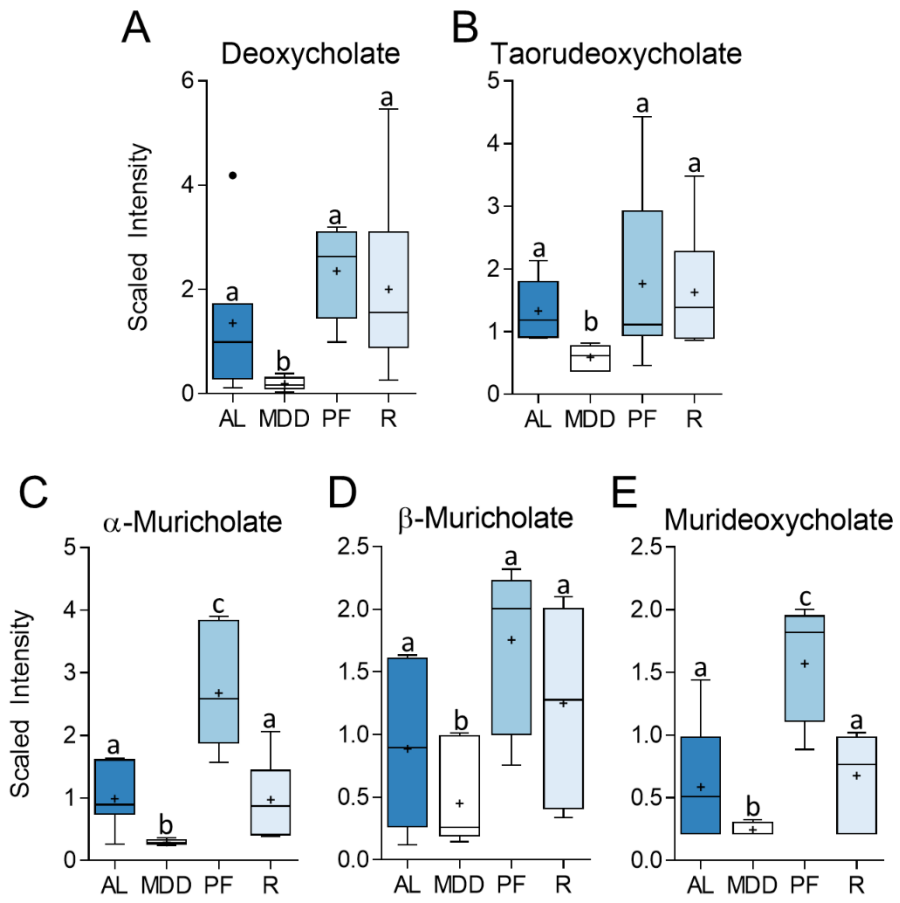

Figure 4-4. Changes in the levels of metabolites involved in secondary bile acid (BA) synthesis. Levels of deoxycholate (A; -4.5-fold, P<0.05), taurodeoxycholate (B; -2.2-fold, P<0.01), alpha-muricholate (C; -3.8-fold, P<0.005), beta-muricholate (D; -2.2-fold, P<0.05), and murideoxycholate (E; -2.6-fold, P<0.05) are altered under conditions of dietary methyl donor restriction, suggesting inhibition of secondary BA synthesis. Whiskers on Tukey's box plots represent Interquartile Range (IQR). Statistically significant differences (P<0.05) between groups, measured by ANOVA with Bonferroni's post-test, are indicated within bar graphs by differences in the letter placed above each group.

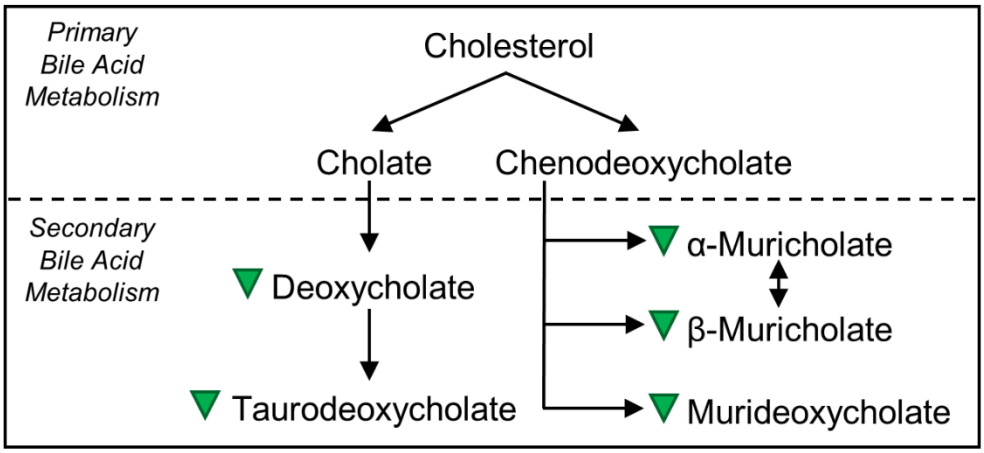

Figure 4-5. Schematic overview of the metabolic changes to secondary bile acid metabolism under conditions of dietary MDD. Dietary methyl donor deficiency significantly reduces levels of secondary bile acids, which are known to promote intestinal tumorigenesis, within the colonic mucosa.

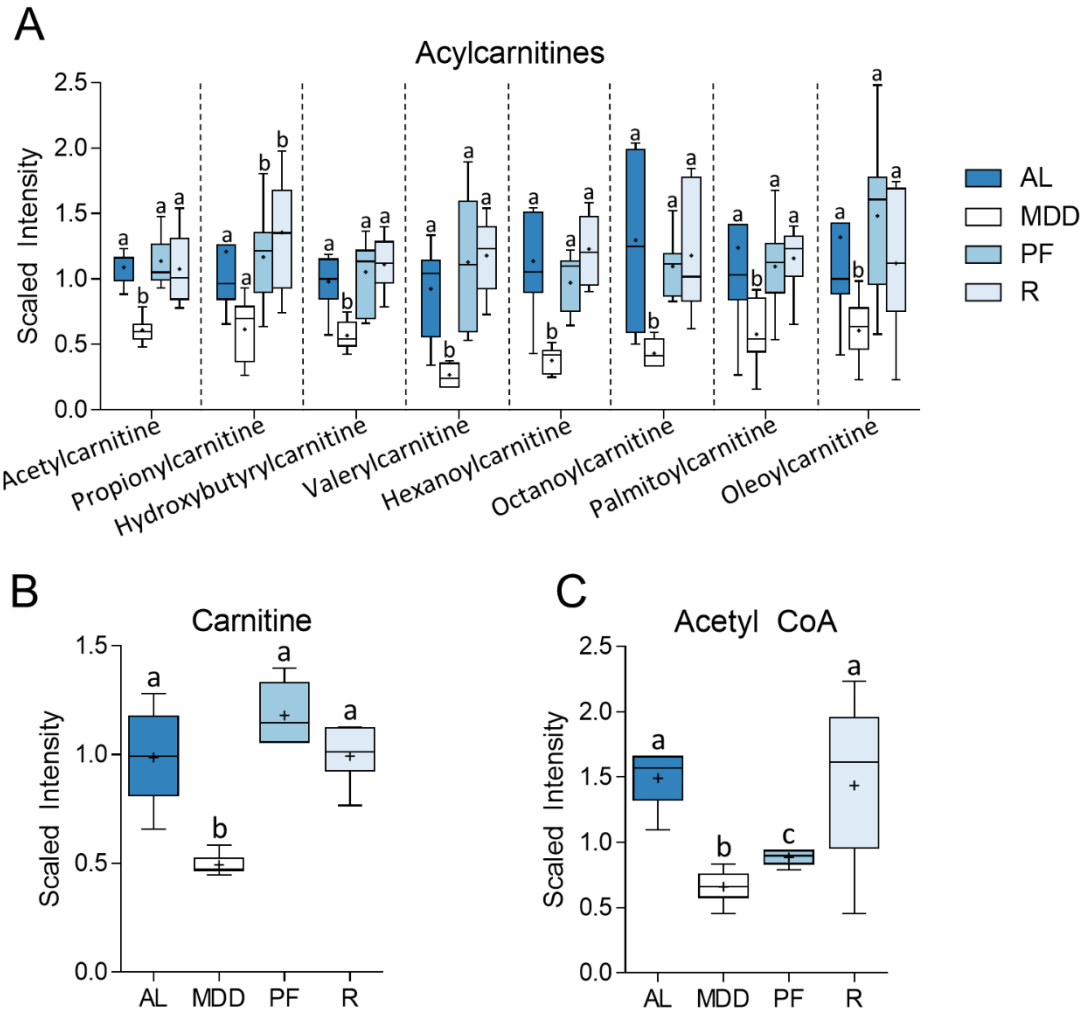

Figure 4-6. Changes in the levels of metabolites involved in fatty acid β-oxidation (FAO). (A) Levels of a panel of acylcarnitines, as well as carnitine (B; -2.0-fold, $P<0.01$) and acetyl CoA (C;-2.5-fold, $P<0.05$) are reduced under conditions of dietary methyl donor restriction, suggesting inhibition of FAO. Whiskers on Tukey's box plots represent Interquartile Range (IQR). Statistically significant differences ($P<0.05$) between groups, measured by ANOVA with Bonferroni's post-test, are indicated within bar graphs by differences in the letter placed above each group.

inhibits mitochondrial FAO, possibly leading to impaired Acetyl CoA-dependent energy metabolism. A depiction of the changes to carnitine-dependent FAO is shown in **Figure 4-7**.

MDD causes persistent changes to intestinal redox balance

As previously described (220), dietary MDD confers long-lasting tumor protection to *Apc*$^{\Delta 14/+}$ mice, which persists for at least 7 weeks beyond active deficiency. To determine whether persistent tumor protection is associated with persistent metabolic changes, we normalized MDD and MDD:MDS-Repletion metabolite profiles to MDS *ad libitum* control and compared the two normalized profiles to identify metabolite levels that were significantly altered in both groups. Metabolite changes identified in this way are referred to as "retained changes". As shown in **Figure 4-8A**, pathway analysis of retained changes using MetaboAnalyst 3.0 showed that these changes were enriched in several pathways involved in redox balance, including Taurine and Hypotaurine Metabolism, and Ascorbate Metabolism. As shown in **Figure 4-2H**, levels of hypotaurine, which are elevated in MDD mice, are also elevated in MDD:MDS-Repletion mice (1.3-fold, $P<0.05$) relative to MDS *ad libitum*. Similarly, as shown in **Figure 4-8B&C**, levels of ascorbate, a potent antioxidant (230), are elevated in both MDD (1.4-fold, $P<0.05$) and MDD:MDS-Repletion mice (1.2-fold, $P<0.05$), as are levels of UDP-glucuronate (MDD, 1.8-fold, $P<0.05$; MDD:MDS-R, 1.6-fold, $P<0.05$), an intermediate in ascorbate synthesis. Together, these results suggest that ascorbate metabolism is persistently upregulated following temporary MDD. Finally, levels of indoxyl sulfate, a pro-oxidant toxin produced by intestinal microbes (231), were reduced in both MDD (-2.1-fold, $P<0.05$) and MDD:MDS-Repletion mice (-1.3-fold, $P<0.05$) (**Figure 4-8D**). Together, these results suggest the that dietary MDD persistently alters multiple pathways involved in redox balance, possibly leading to reduced oxidative stress. To further investigate the effects of temporary MDD on oxidative stress, we used the Thiobarbituric acid reactive substances (TBARS) assay to quantify levels of malondialdehyde (MDA) within colonic mucosa samples. MDA is a product of lipid peroxidation that is frequently used as a marker for

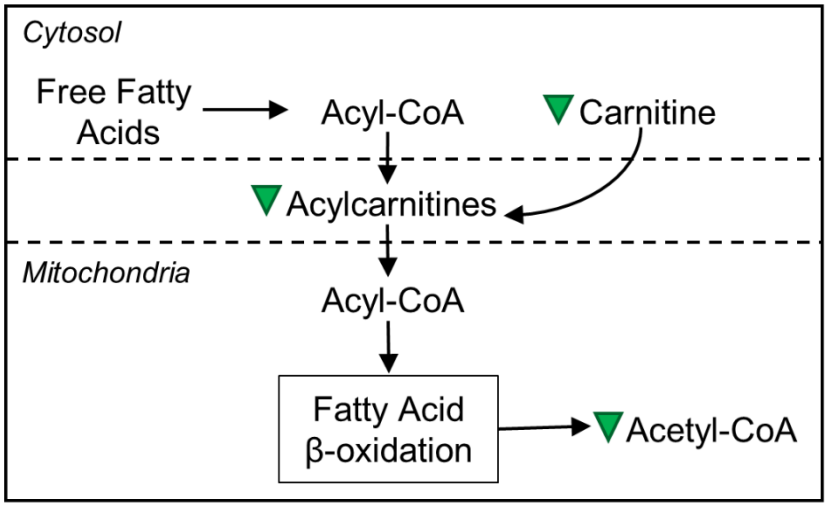

Figure 4-7. Schematic overview of the metabolic changes to mitochondrial fatty acid β-oxidation under conditions of dietary MDD. Levels of carnitine, which is synthesized from methionine, are significantly reduced within the colonic mucosa under conditions of dietary MDD. As a result, levels of a panel of acylcarnitines are reduced, inhibiting mitochondrial fatty acid beta oxidation and the production of Acetyl-CoA.

Figure 4-8. Identification of MDD-associated metabolic changes that persist during methyl donor repletion. (A) Biplot of metabolite set enrichment analysis (MSEA) depicting metabolic pathways significantly enriched for persistent changes. Three pathways involved in redox balance were observed to be significantly enriched for persistent changes: taurine and hypotaurine metabolism, pentose metabolism, and ascorbate metabolism. The size and color of each point represents the number of metabolites within the pathway and the p-value, respectively. Pathway Impact represents the number of unique metabolic pathways that interact with a given pathway. (B) Levels of ascorbate, a potent antioxidant, are increased in both MDD (1.4-fold, $P<0.05$) and MDD:MDS-Repletion mice (1.2-fold, $P<0.05$). (C) Levels of UDP-glucoronate, and intermediate in the synthesis of ascorbate are also elevated in MDD (1.8-fold, $P<0.05$) and MDD:MDS-Repletion mice (1.2-fold, $P<0.05$), suggesting persistent upregulation of ascorbate synthesis following temporary MDD. (D) Levels of indoxyl sulfate, a pro-oxidant bacterial toxin, are reduced in both MDD (-2.1-fold, $P<0.05$) and MDD:MDS-Repletion mice (-1.3-fold, $P<0.05$). (E) Levels of malondialdehyde (MDA), a marker of oxidative stress measured by the TBARS assay are significantly reduced in both MDD (-2.5-fold, $P<0.05$) and MDD:MDS-Repletion mice (-1.7-fold, $P<0.05$). Together, these results suggest oxidative stress is persistently reduced within the colonic mucosa following temporary MDD. Whiskers on Tukey's box plots represent Interquartile Range (IQR). Error bars in (E) represent SEM. Statistically significant differences ($P<0.05$) between groups, measured by ANOVA with Bonferroni's post-test, are indicated within bar graphs by differences in the letter placed above each group.

Figure 4-8

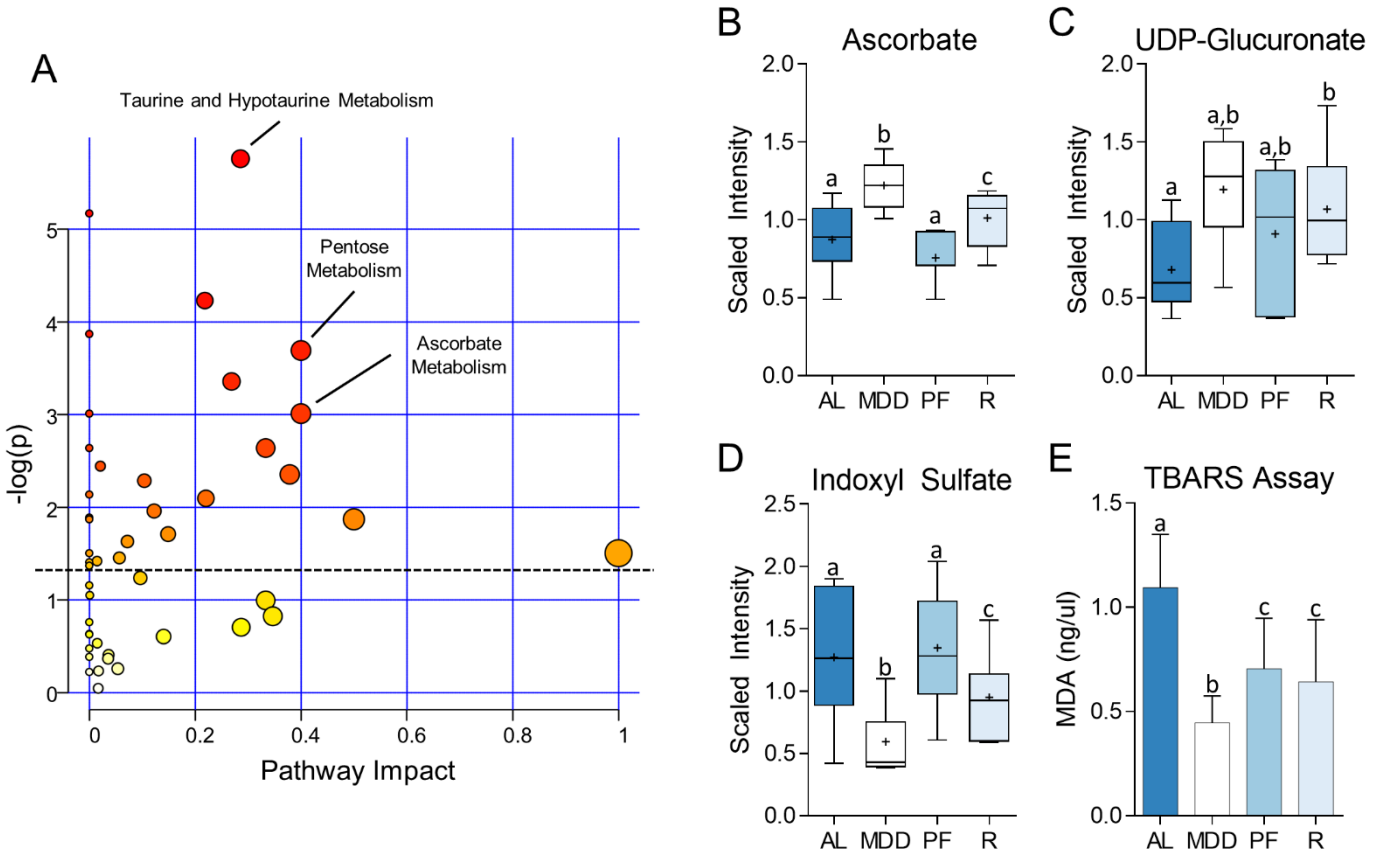
A
Taurine and Hypotaurine Metabolism
Pentose Metabolism
Ascorbate Metabolism
-log(p)
Pathway Impact
B
Ascorbate
Scaled Intensity
C
UDP-Glucuronate
Scaled Intensity
D
Indoxyl Sulfate
Scaled Intensity
E
TBARS Assay
MDA (ng/ul)
AL MDD PF R

oxidative stress (232). As shown in **Figure 4-8E**, MDA levels are significantly reduced in both MDD (-2.5-fold, P<0.05) and MDD:MDS-Repletion mice (-1.7-fold, P<0.05), suggesting that dietary MDD persistently reduces oxidative stress within the colonic mucosa.

4.4 Discussion

This study expands on our previous work (122,220) by identifying several metabolic pathways that are altered under conditions of dietary MDD and may contribute to tumor protection. Furthermore, this study provides clues about the molecular mechanisms underlying the long-lasting nature of MDD-associated tumor protection by identifying a subset of metabolic changes that persist at least 7 weeks beyond active MDD. The effects of methyl donor nutrient intake on colorectal carcinogenesis are unclear, with some studies suggesting that high intake of folic acid may be chemoprotective in the general population (173–176). In contrast, our previous studies (122,220) suggest that reduced intake of methyl donor nutrients may be a viable strategy for the prevention of CRC in certain high-risk populations. However, dietary MDD is associated with several unwanted side effects that may complicate the clinical translation of dietary MDD or limit its utility in the general population. By uncovering metabolic pathways that are perturbed under conditions of MDD, the present study has uncovered potential biomarkers of CRC risk and has identified targets for novel preventive interventions. Together, our findings may provide new avenues for the clinical implementation of chemoprevention strategies based on the manipulation of FOCM.

As predicted, dietary methyl donor deficiency was associated with extensive changes to FOCM within the colonic mucosa including reduced availability of methionine and choline and dramatically increased levels of homocysteine. Several studies have demonstrated that cancer cells have an increased demand for methionine and are more sensitive to the effects of methionine restriction (MR) than normal cells (233). As a result of these findings, dietary MR has been proposed as a strategy for CRC prevention.

As shown by Komninou *et al*. (234) dietary MR reduced the multiplicity of preneoplastic aberrant crypt foci (ACF) in F344 rats treated with azoxymethane, supporting this strategy. Our results provide additional evidence in a genetic model of CRC that MR is a viable strategy for the prevention of CRC, and suggest that it may be particularly effective in high-risk individuals, such as those with FAP.

MDD was also associated with increased levels of SAH, which is produced directly from homocysteine by the enzyme SAH hydrolase (235). SAH has previously been shown to inhibit the activity of DNA methyltransferase enzymes (236,237), and elevated levels of SAH are associated with widespread DNA hypomethylation (238). As shown by Eads *et al.* (34) and Weis *et al.* (35)*,* genetic ablation of DNMT1 and 3a, respectively, prevents the formation of tumors in *Apc*-mutant mice, indicating a requirement for *de novo* DNA methylation in the formation of intestinal polyps. Thus, elevated levels of SAH may contribute to tumor protection by inhibiting DNMTs and preventing the *de novo* DNA methylation associated with polyp formation. Furthermore, since epigenetic modifications to DNA can have long-term consequences for gene expression (239), it is possible that this metabolic change may contribute to the long-term tumor protection associated with MDD.

MDD was associated with reduced secondary BA levels within the colonic mucosa. In a seminal study, Cook *et al.* (240) demonstrated that prolonged exposure to high BA concentrations induced the formation of tumors in mice. Since that time, accumulated evidence has illustrated a role for BAs in the initiation and promotion of CRC (228). Exposure of intestinal epithelial cells to BAs can cause oxidative stress, DNA damage and apoptosis, with prolonged exposure leading to genomic instability and apoptotic resistance, two hallmarks of cancer (241). Reducing the level of secondary BAs within the colon may be a viable strategy for CRC chemoprevention. As shown by Khare *et al.* (242), treatment of AOM-treated mice with ursodeoxycholic acid, a synthetic BA that reduces colonic levels of toxic secondary BAs (243), significantly inhibited tumorigenesis. As reviewed by Payne *et al.* (241), secondary bile acids damage the intestinal epithelium, initiate inflammatory responses, and promote hyperproliferation of

undifferentiated stem and progenitor cells. We have previously reported that dietary MDD is associated with diminished populations of Dclk1$^+$ stem cells within the intestinal mucosa (220). Dclk1$^+$ cells, which normally contribute to epithelial repair after mucosal injury (244), are the putative cell-of-origin for tumors in *Apc*-mutant mice. Mutant Dclk1$^+$ cells can become activated and initiate tumorigenesis after exposure to an inflammatory stimulus (198), such as secondary BA exposure. Thus, reduced levels of secondary BAs within the mucosa may contribute to MDD tumor protection by minimizing oxidative damage and inflammation, thereby reducing the risk of mutant Dclk1$^+$ cells becoming activated (220). Together, our results support the use of intestinal BAs as biomarkers for CRC risk and reinforce the potential for secondary BA synthesis as a chemopreventive target. Furthermore, our studies suggest that future investigation of the relationship between BA exposure and the activation of tumor-initiating Dclk1$^+$ cells may be warranted.

Metabolite profiling revealed that MDD inhibits FAO by reducing the availability of carnitine, thereby restricting transport of fatty acids (FAs) into mitochondrial matrices. As reviewed by Carracedo *et al.* (66), several recent studies have suggested that cancer cells are dependent on FAO to meet their increased demands for energy and biosynthetic cofactors, such as Acetyl CoA. There is also growing evidence that inhibition of FAO is a viable strategy for cancer treatment. As shown by Samudio *et al.* (245), treatment of human leukemia cells with etomoxir, an irreversible FAO inhibitor, increases sensitivity to the induction of apoptosis. Furthermore, as shown by Schlaepfer *et al.* (68), treatment with etomoxir significantly inhibits tumor growth in a prostate cancer xenograft model. Thus, our results suggest that dietary MDD may protect against tumors by inhibiting mitochondrial FAO by impairing the proliferation and survival of initiated cells within the colonic mucosa. Our results provide additional evidence that FAO inhibition is a viable strategy for cancer treatment and suggest that a similar approach may be efficacious in treating CRC. Furthermore, our results extend the scope of possible applications for FAO inhibition by suggesting that this strategy might also be viable for the *prevention* of CRC.

Finally, a set of metabolic changes associated with MDD were also detected in the MDD:MDS-Repletion mice, suggesting that they are retained for at least 7 weeks beyond active methyl donor restriction. These changes predominantly affected pathways involved in managing oxidative stress, including hypotaurine synthesis, glutathione synthesis, and ascorbate metabolism (246–248). Several studies have demonstrated that oxidative stress enhances intestinal tumorigenesis in *Apc*-deficient mice (249,250). As shown by Cheung *et al.* (250), genetic deletion of *Nrf2*, the transcription factor that initiates glutathione synthesis in response to oxidative stress, leads to increased tumor incidence and multiplicity in $Apc^{Min/+}$ mice. The use of individual antioxidants for the prevention of CRC is controversial. A recent meta-analysis performed by Papaioannou *et al.* (251) failed to show chemopreventive efficacy for a large number of single agent interventions, casting doubt on the viability of this approach to cancer prevention. However, there is some recent evidence that diets which increase total antioxidant capacity (TAC), as opposed to any single antioxidant, may reduce incidence of CRC (252). The persistent increase in the levels of multiple antioxidants within the colonic mucosa as a result of MDD suggests that a methyl donor restricted diet may promote a sustained increase in TAC that reduces the risk of oncogenesis. This hypothesis is further supported by our observation that markers of oxidative stress are persistently reduced subsequent to temporary MDD. Together, these results suggest that measurements of TAC may be useful as a biomarker for CRC risk and suggest that augmenting intestinal TAC may be a viable strategy for CRC prevention.

In conclusion, this study extends our previous work (122,220) by identifying several metabolic pathways that are perturbed under conditions of dietary MDD, thereby providing clues to the molecular changes underlying of MDD-associated tumor protection. As predicted, dietary MDD is associated with inhibition of the methionine cycle and increased levels of homocysteine within the colonic mucosa, which led to increased flux through the transsulfuration pathway. Unexpectedly, MDD was also associated with inhibition of secondary bile acid synthesis and the generation of acetyl CoA *via* fatty acid β-oxidation.

Finally, levels of several metabolites involved in redox balance were persistently altered, even after 7 weeks of methyl donor repletion, suggesting tumor protection may be due, in part, to long term augmentation of colonic antioxidant capacity. Together, these observations identify several metabolic pathways that may serve as novel targets for CRC detection and chemoprevention.

Chapter 5: Summary, Conclusions, and Future Directions

CRC incidence and mortality have declined over the last several decades, in large part due to the increased utilization of screening colonoscopy (2). However, the 5-year survival rate for CRC is 65% overall, and just 11% for cancers identified in Stage IV (1). Combined with a rapidly aging US population, these low survival rates underscore the need for improved methods for CRC detection and prevention. FOCM controls the availability of biosynthetic building blocks and regulates gene expression *via* DNA methylation (107,108), making it central to the maintenance of cellular homeostasis. FOCM itself is known to be disrupted in CRC (128,253), as are many of the processes that it controls, including *de novo* nucleotide synthesis, the maintenance of genomic stability, and the regulation of gene expression *via* DNA methylation (27,31,254,255). Consistent with these roles in carcinogenesis, FOCM has been used successfully as a chemotherapeutic target for decades (223). However, less is known about the role of FOCM in early colonic neoplasia, or its potential as a target for novel CRC *prevention* strategies. Intriguingly, FOCM is sensitive to perturbation by environmental influences, especially changes in the dietary intake of the methyl donor nutrients folate, choline, methionine and vitamin B12 (256–258). Thus, manipulation of dietary intake of these nutrients represents a promising approach to the modulation of FOCM. The studies described herein seek to understand the role of FOCM-dependent mechanisms in early colonic neoplasia and investigate the ability of FOCM manipulation *via* dietary methyl donor deficiency (MDD) to disrupt intestinal tumorigenesis. We demonstrate for the first time the extensive disruption of patterns of DNA methylation, a critical FOCM-dependent mechanism, in the earliest stages of colorectal neoplasia. Furthermore, these studies demonstrate that manipulation of FOCM *via* dietary MDD is a viable strategy for CRC prevention and identify several molecular and cellular targets that may enable the clinical translation of a FOCM-based prevention strategy.

We report the use of a highly sensitive epigenomic profiling approach that combines LCM with RRBS and RNA-Seq to identify DNA methylation changes present in *KRAS*-mutant human ACF and Stage

III-IV CRCs. Consistent with previous reports of genome-wide methylation loss in a variety of human cancers (31,155), the majority of DMRs identified in advanced CRCs were globally hypomethylated. Unexpectedly, the majority of DMRs identified in ACF were *hypermethylated*, indicating a global gain of DNA methylation at the earliest stages of colonic tumor initiation. Since the majority of ACF are self-limiting and unlikely to progress to malignancy (93), genome-wide hypermethylation may provide a mechanism for restricting ACF progression, in part by reducing the risk of genomic instability that is associated with global loss of methylation (27). Furthermore, the present study uncovered extensive promoter and gene body hypermethylation of homeobox genes in both cancers and ACF, many of which belong to the HOX family. The expression of homeobox genes, which is regulated to a large extent by DNA methylation (164,165), contributes to the maintenance of cellular identity and adult tissue morphology (166). Aberrant hypermethylation of homeobox-containing genes has been described in breast and lung cancers, and several HOX genes (HOXA7, HOXA9, and HOXB13) are reportedly hypermethylated in CRC (158,167,168). However, the large number of differentially methylated homeobox genes identified in our panel of primary Stage III-IV cancers, and the identification of homeobox gene hypermethylation in ACF, is an unexpected result that implicates the dysregulation of cellular identity in the earliest stages of colonic neoplasia.

Promoter DMRs in both CRC and ACF were also enriched in genes known to be targeted by PRC2 in embryonic stem cells (ESCs). PRC2 is a histone-modifying complex expressed in embryonic stem cells that plays an important role in maintaining 'stemness' (150) by methylating histone H3K27 and repressing genes required for differentiation (157). Widschwendter *et al.* hypothesized that cancer-associated promoter hypermethylation of PRC2 targets originates in stem cells during the earliest stages of carcinogenesis, and predisposes these cells to neoplastic transformation by "locking in" a stem cell phenotype (159). Our data support the timing of this hypothesis by demonstrating that hypermethylation of PRC2 targets occurs as early as the ACF stage.

Finally, our results indicate that aberrant DNA methylation commonly occurs within intergenic transcription factor binding sites, especially those corresponding to members of the AP-1 transcription factor family. Recent evidence indicates that transcriptional activation by AP-1 is controlled, in part, by DNA methylation (171). As shown by Park *et al.* (171), the DNA binding activity of AP-1 is significantly reduced when CpGs in close proximity to its DNA binding motif are methylated. As shown by Berman *et al.* (172), intergenic AP-1 binding sequences undergo methylation loss in human CRC. Our data recapitulate this finding and suggest that loss of methylation at AP-1 sites occurs early in the neoplastic process.

DNA methylation changes identified within CRC and ACF samples were associated with a variety of genes and regulatory elements, but the effects of specific epigenetic phenotypes on CRC risk are currently unknown. In the future, data collected from ACF patients returning for follow-up colonoscopy, or acquired from The Cancer Genome Atlas (TCGA), could be used to examine the relationship between particular epigenomic aberrations (e.g. hypermethylation of one or more homeobox genes, AP-1 site hypomethylation) in precursor lesions and the incidence of advanced neoplasia. Furthermore, while all of the samples examined in this study harbored *KRAS* Exon 2 mutations ($KRAS^{G12D}$ or $KRAS^{G12V}$), it is unknown whether *KRAS* mutations the observed DNA methylation changes. Alternatively, DNA methylation changes precede the acquisition of somatic mutations and predispose a population of cells to neoplastic transformation, consistent with the "epigenetic progenitor model" of cancer (259). Recent advances in intestinal organoid culture technology (260) provide an elegant system for testing the hypothesis that *KRAS* mutations directly cause the DNA methylation changes detected in our study. By deriving organoids from transgenic mice that express Tamoxifen-inducible Cre recombinase and harbor a *KRAS* Exon 2 mutation downstream of a Lox-Stop-Lox (LSL) cassette, it would be possible to determine the effects of *KRAS* mutation acquisition on patterns of DNA methylation. If the induction of a *KRAS* mutation is found to cause DNA methylation changes analogous to those identified in human ACF, subsequent study of

organoid growth characteristics may help shed light on whether these epigenetic changes promote or prevent the progression of early neoplasia. Furthermore, these studies may serve as a starting point for chemoprevention studies targeting particular epigenomic features, such as AP-1 binding site hypomethylation or homeobox gene hypermethylation.

The studies contained herein also demonstrate that manipulation of FOCM *via* dietary restriction of the methyl donor nutrients folate, choline, methionine and vitamin B12 is a viable strategy for CRC prevention. Previously, we demonstrated that a diet deficient in methyl donor nutrients reduced intestinal tumor incidence by greater than 95% in $Apc^{Min/+}$ mice (122). The present study extends these promising results to a second *Apc*-dependent mouse tumor model, $Apc^{\Delta 14/+}$, and shows that the tumor protection afforded by dietary methyl donor restriction is long-lasting (220). Tumor formation in the $Apc^{\Delta 14/+}$ mouse is driven by an *Apc* deletion that results in the production of truncated, non-functional APC protein (190). This mutation is highly homologous to the mutant APC commonly found in FAP patients (261), making the $Apc^{\Delta 14/+}$ mouse a good model of human FAP. Our findings provide additional evidence that dietary MDD may be a viable strategy for CRC prevention in humans, and suggest that it may have particular efficacy in individuals with FAP. Furthermore, the observation that temporary MDD imparts persistent protection suggests that this diet may be amenable to a prevention strategy analogous to "short-term intermittent therapy to eliminate premalignancy" (SITEP), in which short pulses of an intervention are administered to clear the colon of premalignant lesions while minimizing unwanted side effects.

MDD tumor protection was associated with altered crypt homeostasis, as evidenced by alterations to crypt architecture and a reduced frequency of mitotic cells within the crypt epithelium. In a case-control study by Mills et al. (209), samples of normal mucosa from individuals with either FAP or sporadic CRC were shown to have an increased frequency of cells in M-phase compared to healthy controls, indicating a correlation between basal mitotic rate and CRC risk. The most common mechanism for colonic tumor initiation in *Apc*-mutant mice is known to be *Apc* LOH (262), which occurs most

frequently during mitosis (263). Thus, dietary MDD may protect against tumor initiation by reducing rates of mitosis, in turn reducing the probability of *Apc* LOH. Future studies should investigate this mechanism by measuring the effects of dietary MDD on rates of *Apc* LOH.

Notably, tumor protection was also associated with reduced rates of crypt fission. Studies by Fischer *et al.* (194,206) demonstrated that mutant intestinal crypts in *Apc*-deficient mice clonally expand *via* crypt fission, creating fields of normal-appearing *Apc*-null crypts that are poised for tumorigenesis. A follow-up study by the same investigators demonstrated that reduced crypt fission is associated with decreased tumor multiplicity in $Pms2^{Cre/Cre};Apc^{CKO/CKO}$ mice (194). Future studies should investigate the effects of dietary MDD on the occult expansion of *Apc*-deficient crypts to determine whether inhibition of this process might underlie tumor protection. Crypt fission is initiated by ISCs in the crypt base (193,195); thus, further characterization of the effects of dietary MDD on the crypt base ISC compartment may lead to the identification of cellular targets for novel prevention strategies.

Dietary MDD was also associated with significant depletion of intestinal cells expressing Dclk1, a putative stem cell marker that has been the focus of recent interest (217). Nakanishi *et al.* (197) demonstrated *via* a series of lineage-tracing experiments that $Dclk1^{+}$ cells can act as the progenitor for intestinal tumors in $Apc^{Min/+}$ mice. Furthermore, these studies showed that genetic ablation of $Dclk1^{+}$ cells reduced intestinal tumor burden, suggesting that these cells may provide a target for novel CRC therapies (197,218). Notably, a recent study by Westphalen *et al.* (198) demonstrated that loss of *Apc* function within $Dclk1^{+}$ stem cells is insufficient to drive tumor formation. Using *Dclk1-CreERT x* $Apc^{flox/flox}$ mice, the authors demonstrate that mice remain tumor-free for up to 18 months after *Apc* inactivation following tamoxifen injections. However, intermittent, short-term treatment with dextran sodium sulfate (DSS) subsequent to *Apc* loss leads to the formation of multiple intestinal tumors with 100% penetrance, indicating a requirement for a concomitant pro-inflammatory stimulus (198). We have previously shown that dietary MDD is associated with reduced intestinal inflammation (122),

suggesting a relationship between dietary MDD, reduced inflammation, and the inhibition of Dclk1$^+$ cell activation. Future studies should investigate the ability of other anti-inflammatory interventions, such as treatment with NSAIDs, on the frequency and activation of Dclk1$^+$ cells within the intestine.

Finally, these studies show that several adverse effects associated with methyl donor restriction (e.g., reduced body weight gain, hepatic steatosis, and splenic atrophy) are readily reversible by methyl donor repletion. Although the reversal of these effects is promising, a thorough characterization of the adverse effects associated with dietary MDD will need to be completed prior to its clinical translation. Because dietary MDD may be particularly useful for delaying polyposis in young FAP patients, a thorough investigation of the effects of MDD on normal development will need to be undertaken prior to clinical translation. Furthermore, because elevated levels of serum homocysteine, a known consequence of folate deficiency, increases the risk of cardiovascular disease (264), future studies should also investigate the effects of dietary MDD on cardiovascular integrity.

Subsequent to our investigation of dietary methyl donor restriction, we used broad-spectrum metabolite profiling to characterize metabolic changes within the colonic mucosa of mice maintained on a MDD diet. Using this approach, we identified several pathways that are affected by dietary MDD and may contribute to tumor protection. As expected, metabolomic analysis revealed extensive changes to FOCM within the colonic mucosa, including reduced levels of methionine and choline, and dramatically increased levels of homocysteine. MDD was also associated with increased levels of SAH, which has previously been shown to inhibit the activity of DNA methyltransferase enzymes (236,237). Consistent with this effect, Caudill *et al.* (238) have shown that elevated levels of SAH are associated with widespread DNA hypomethylation. Epigenetic modifications can have long-term consequences on gene expression (239), and so it is possible that SAH-mediated DNA methylation changes underlie the persistent alteration of intestinal homeostasis that is associated with dietary MDD. Future studies should investigate the relationship between dietary MDD, elevated SAH, DNMT activity, and alterations in DNA methylation.

Should changes in DNA methylation contribute to the tumor protective effects of dietary MDD, these results may suggest that SAH itself has potential as a chemopreventive agent in certain populations.

MDD was also associated with dramatically reduced levels of secondary bile acids, which have been shown by Cook *et al.* (240) to induce tumorigenesis in mice when administered in high concentrations. Secondary bile acids are known to initiate inflammatory responses and promote the proliferation and expansion of undifferentiated ISCs (241). We have previously described diminished populations of putative tumor-initiating $Dclk1^+$ ISCs under conditions of dietary methyl donor restriction (220) and hypothesized that the loss of these cells contributes to the tumor-protective effects of the MDD diet. Future studies should investigate the possibility that secondary bile acids contribute to intestinal tumor development by promoting the activation and expansion of $Dclk1^+$ cells.

Metabolite profiling also revealed that dietary MDD inhibits mitochondrial FAO by restricting availability of the shuttle molecule carnitine and inhibiting the synthesis of the metabolic cofactor acetyl CoA. As reviewed by Carracedo *et al.* (66), several recent studies have suggested that cancer cells are dependent on FAO to meet their increased demands for energy, acetyl CoA and other biosynthetic cofactors. There is also growing evidence that inhibition of FAO is a viable strategy for cancer treatment. As shown by Samudio *et al.* (245), treatment of human leukemia cells with etomoxir, an irreversible FAO inhibitor, increases sensitivity to the induction of apoptosis by genotoxic drugs. Furthermore, as shown by Schlaepfer *et al.* (68), treatment with etomoxir significantly inhibits tumor growth in a prostate cancer xenograft model. Our results extend the scope of possible applications for pharmacologic inhibition of FAO by suggesting that this strategy may also be efficacious in the prevention and treatment of CRC. Future studies should examine the ability of existing FAO inhibitors (e.g. etomoxir, perhexiline, and trimetazidine) to inhibit intestinal oncogenesis or treat existing cancers. Currently, no FAO inhibitors are approved for human use in the United States. However, successful proof of concept chemoprevention or

chemotherapeutic studies using the agents listed above may warrant the development of novel FAO inhibitors with more favorable safety profiles.

Finally, a set of metabolic changes associated with MDD were also detected in the MDD:MDS-Repletion mice, suggesting that these changes are retained for at least 7 weeks beyond active methyl donor restriction. These changes predominantly affected pathways involved in the management of oxidative stress including hypotaurine synthesis, glutathione synthesis, and ascorbate metabolism (246–248). Several studies have demonstrated that oxidative stress enhances intestinal tumorigenesis in *Apc*-deficient mice (249,250). However, the use of individual antioxidants for the prevention of CRC is controversial. A recent meta-analysis performed by Papaioannou *et al.* (251) showed that a large number of single-antioxidant interventions had no effect on colonic tumor incidence. In contrast, there is evidence to suggest that diets which increase total antioxidant capacity (TAC), as opposed to levels of any single antioxidant, may reduce incidence of CRC (252). Thus, our findings may warrant further study of the effects of dietary MDD on intestinal TAC. Furthermore, they suggest that treatment with a combination of antioxidants in doses sufficient to elevate TAC, rather than a single-agent intervention, may be a viable strategy for CRC chemoprevention.

In conclusion, the studies described herein advance our understanding of the role of FOCM, and the homeostatic processes that it controls, in colorectal tumor development. Our human studies have uncovered a role for aberrant DNA methylation, a gene-regulatory mechanism that is controlled by FOCM, in the earliest stages of colonic neoplasia. In addition, data from our preclinical dietary intervention studies provide considerable evidence supporting the use of FOCM inhibition as a strategy for CRC prevention. Furthermore, by beginning to unravel the molecular mechanisms underlying MDD-associated tumor protection, we have identified putative molecular and cellular targets for novel chemopreventive interventions. Together, these findings advance our efforts to develop clinically relevant strategies for the detection, prevention, and treatment of CRC based on the manipulation of one-carbon metabolism.

References

1. American Cancer Society. Cancer Facts & Figures 2016. Am Cancer Soc. 2016;

2. Welch HG, Robertson DJ. Colorectal Cancer on the Decline. N Engl J Med. 2016;375:804.

3. Howlander N, Noone AM, Krapcho M, Garshell J, Miller D, Altrekruse SF. Cancer Statistics Review, 1975-2012. Natl Cancer Inst [Internet]. 2014 [cited 2016 Oct 6]; Available from: http://seer.cancer.gov/archive/csr/1975_2012/

4. Jafari MD, Jafari F, Halabi WJ, Nguyen VQ, Pigazzi A, Carmichael JC, et al. Colorectal Cancer Resections in the Aging US Population: A Trend Toward Decreasing Rates and Improved Outcomes. JAMA Surg. 2014;149:557–64.

5. Tabarestani S, Ghafouri-Fard S. Cancer stem cells and response to therapy. Asian Pac J Cancer Prev APJCP. 2012;13:5951–8.

6. Cho KR, Vogelstein B. Genetic alterations in the adenoma--carcinoma sequence. Cancer. 1992;70:1727–31.

7. Bougatef K, Ouerhani S, Moussa A, Kourda N, Coulet F, Colas C, et al. Prevalence of mutations in APC, CTNNB1, and BRAF in Tunisian patients with sporadic colorectal cancer. Cancer Genet Cytogenet. 2008;187:12–8.

8. Galiatsatos P, Foulkes WD. Familial Adenomatous Polyposis. Am J Gastroenterol. 2006;101:385–98.

9. Gregorieff A, Clevers H. Wnt signaling in the intestinal epithelium: from endoderm to cancer. Genes Dev. 2005;19:877–90.

10. Rowan AJ, Lamlum H, Ilyas M, Wheeler J, Straub J, Papadopoulou A, et al. APC mutations in sporadic colorectal tumors: A mutational “hotspot” and interdependence of the “two hits.” Proc Natl Acad Sci. 2000;97:3352–7.

11. Iacopetta B. TP53 mutation in colorectal cancer. Hum Mutat. 2003;21:271–6.

12. Zilfou JT, Lowe SW. Tumor Suppressive Functions of p53. Cold Spring Harb Perspect Biol [Internet]. 2009 [cited 2016 Oct 6];1. Available from: http://www.ncbi.nlm.nih.gov/pmc/articles/PMC2773645/

13. Dhillon AS, Hagan S, Rath O, Kolch W. MAP kinase signalling pathways in cancer. Oncogene. 2007;26:3279–90.

14. Zhang W, Liu HT. MAPK signal pathways in the regulation of cell proliferation in mammalian cells. Cell Res. 2002;12:9–18.

15. Barras D. BRAF Mutation in Colorectal Cancer: An Update. Biomark Cancer. 2015;7:9–12.

16. Vogelstein B, Fearon ER, Hamilton SR, Kern SE, Preisinger AC, Leppert M, et al. Genetic alterations during colorectal-tumor development. N Engl J Med. 1988;319:525–32.

17. Prior IA, Lewis PD, Mattos C. A comprehensive survey of Ras mutations in cancer. Cancer Res. 2012;72:2457–67.

18. Ascierto PA, Kirkwood JM, Grob J-J, Simeone E, Grimaldi AM, Maio M, et al. The role of BRAF V600 mutation in melanoma. J Transl Med. 2012;10:85.

19. Armaghany T, Wilson JD, Chu Q, Mills G. Genetic Alterations in Colorectal Cancer. Gastrointest Cancer Res GCR. 2012;5:19–27.

20. Kemp Z, Rowan A, Chambers W, Wortham N, Halford S, Sieber O, et al. CDC4 mutations occur in a subset of colorectal cancers but are not predicted to cause loss of function and are not associated with chromosomal instability. Cancer Res. 2005;65:11361–6.

21. Fearon ER, Pierceall WE. The deleted in colorectal cancer (DCC) gene: a candidate tumour suppressor gene encoding a cell surface protein with similarity to neural cell adhesion molecules. Cancer Surv. 1995;24:3–17.

22. Vogelstein B, Papadopoulos N, Velculescu VE, Zhou S, Diaz LA, Kinzler KW. Cancer Genome Landscapes. Science. 2013;339:1546–58.

23. Jones PA, Baylin SB. The epigenomics of cancer. Cell. 2007;128:683–92.

24. Kawakami K, Ruszkiewicz A, Bennett G, Moore J, Grieu F, Watanabe G, et al. DNA hypermethylation in the normal colonic mucosa of patients with colorectal cancer. Br J Cancer. 2006;94:593–8.

25. Silviera ML, Smith BP, Powell J, Sapienza C. Epigenetic differences in normal colon mucosa of cancer patients suggest altered dietary metabolic pathways. Cancer Prev Res Phila Pa. 2012;5:374–84.

26. Ehrlich M. DNA hypomethylation in cancer cells. Epigenomics. 2009;1:239–59.

27. Eden A, Gaudet F, Waghmare A, Jaenisch R. Chromosomal instability and tumors promoted by DNA hypomethylation. Science. 2003;300:455.

28. Sunami E, de Maat M, Vu A, Turner RR, Hoon DSB. LINE-1 Hypomethylation During Primary Colon Cancer Progression. PLoS ONE [Internet]. 2011 [cited 2016 Oct 6];6. Available from: http://www.ncbi.nlm.nih.gov/pmc/articles/PMC3077413/

29. Esteller M. CpG island hypermethylation and tumor suppressor genes: a booming present, a brighter future. Oncogene. 2002;21:5427–40.

30. Sakai E, Nakajima A, Kaneda A. Accumulation of aberrant DNA methylation during colorectal cancer development. World J Gastroenterol. 2014;20:978–87.

31. Ehrlich M. DNA methylation in cancer: too much, but also too little. Oncogene. 2002;21:5400–13.

32. Newell-Price J, Clark AJ, King P. DNA methylation and silencing of gene expression. Trends Endocrinol Metab TEM. 2000;11:142–8.

33. Waldron D. Epigenetics: A three-state model for epigenetic silencing. Nat Rev Genet. 2016;17:192–3.

34. Eads CA, Nickel AE, Laird PW. Complete genetic suppression of polyp formation and reduction of CpG-island hypermethylation in Apc(Min/+) Dnmt1-hypomorphic Mice. Cancer Res. 2002;62:1296–9.

35. Weis B, Schmidt J, Maamar H, Raj A, Lin H, Tóth C, et al. Inhibition of intestinal tumor formation by deletion of the DNA methyltransferase 3a. Oncogene. 2015;34:1822–30.

36. Leick MB, Shoff CJ, Wang EC, Congress JL, Gallicano GI. Loss of imprinting of IGF2 and the epigenetic progenitor model of cancer. Am J Stem Cells. 2011;1:59–74.

37. Issa J-P. CpG island methylator phenotype in cancer. Nat Rev Cancer. 2004;4:988–93.

38. Tanaka H, Deng G, Matsuzaki K, Kakar S, Kim GE, Miura S, et al. BRAF mutation, CpG island methylator phenotype and microsatellite instability occur more frequently and concordantly in mucinous than non-mucinous colorectal cancer. Int J Cancer. 2006;118:2765–71.

39. Yang H-M, Mitchell JM, Sepulveda JL, Sepulveda AR. Molecular and histologic considerations in the assessment of serrated polyps. Arch Pathol Lab Med. 2015;139:730–41.

40. Mojarad EN, Kuppen PJ, Aghdaei HA, Zali MR. The CpG island methylator phenotype (CIMP) in colorectal cancer. Gastroenterol Hepatol Bed Bench. 2013;6:120–8.

41. Kim MS, Lee J, Sidransky D. DNA methylation markers in colorectal cancer. Cancer Metastasis Rev. 2010;29:181–206.

42. Jass JR, Whitehall VLJ, Young J, Leggett BA. Emerging concepts in colorectal neoplasia. Gastroenterology. 2002;123:862–76.

43. Toyota M, Ahuja N, Ohe-Toyota M, Herman JG, Baylin SB, Issa JP. CpG island methylator phenotype in colorectal cancer. Proc Natl Acad Sci U S A. 1999;96:8681–6.

44. Lee S, Cho N-Y, Yoo EJ, Kim JH, Kang GH. CpG island methylator phenotype in colorectal cancers: comparison of the new and classic CpG island methylator phenotype marker panels. Arch Pathol Lab Med. 2008;132:1657–65.

45. Luo Y, Wong C-J, Kaz AM, Dzieciatkowski S, Carter KT, Morris SM, et al. Differences in DNA methylation signatures reveal multiple pathways of progression from adenoma to colorectal cancer. Gastroenterology. 2014;147:418–429.e8.

46. Inoue A, Okamoto K, Fujino Y, Nakagawa T, Muguruma N, Sannomiya K, et al. B-RAF mutation and accumulated gene methylation in aberrant crypt foci (ACF), sessile serrated adenoma/polyp (SSA/P) and cancer in SSA/P. Br J Cancer. 2015;112:403–12.

47. Greenspan EJ, Jablonski MA, Rajan TV, Levine J, Belinsky GS, Rosenberg DW. Epigenetic alterations in RASSF1A in human aberrant crypt foci. Carcinogenesis. 2006;27:1316–22.

48. Chan AO-O, Broaddus RR, Houlihan PS, Issa J-PJ, Hamilton SR, Rashid A. CpG island methylation in aberrant crypt foci of the colorectum. Am J Pathol. 2002;160:1823–30.

49. Suzuki H, Watkins DN, Jair K-W, Schuebel KE, Markowitz SD, Dong Chen W, et al. Epigenetic inactivation of SFRP genes allows constitutive WNT signaling in colorectal cancer. Nat Genet. 2004;36:417–22.

50. Pavlova NN, Thompson CB. The Emerging Hallmarks of Cancer Metabolism. Cell Metab. 2016;23:27–47.

51. Hagland HR, Søreide K. Cellular metabolism in colorectal carcinogenesis: Influence of lifestyle, gut microbiome and metabolic pathways. Cancer Lett. 2015;356:273–80.

52. Vander Heiden MG, Cantley LC, Thompson CB. Understanding the Warburg effect: the metabolic requirements of cell proliferation. Science. 2009;324:1029–33.

53. Chen X, Qian Y, Wu S. The Warburg Effect: Evolving Interpretations Of An Established Concept. Free Radic Biol Med. 2015;0:253–63.

54. Berg JM, Tymoczko JL, Stryer L. The Glycolytic Pathway Is Tightly Controlled. Biochemistry (Mosc). 5th edition. New York: W H Freeman; 2002.

55. Fang S, Fang X. Advances in glucose metabolism research in colorectal cancer. Biomed Rep. 2016;5:289–95.

56. Patra KC, Hay N. The pentose phosphate pathway and cancer. Trends Biochem Sci. 2014;39:347–54.

57. Shibuya N, Inoue K, Tanaka G, Akimoto K, Kubota K. Augmented pentose phosphate pathway plays critical roles in colorectal carcinomas. Oncology. 2015;88:309–19.

58. Locasale JW, Grassian AR, Melman T, Lyssiotis CA, Mattaini KR, Bass AJ, et al. Phosphoglycerate dehydrogenase diverts glycolytic flux and contributes to oncogenesis. Nat Genet. 2011;43:869–74.

59. Mattaini KR, Sullivan MR, Vander Heiden MG. The importance of serine metabolism in cancer. J Cell Biol. 2016;214:249–57.

60. Chiang PK, Gordon RK, Tal J, Zeng GC, Doctor BP, Pardhasaradhi K, et al. S-Adenosylmethionine and methylation. FASEB J Off Publ Fed Am Soc Exp Biol. 1996;10:471–80.

61. Maddocks ODK, Labuschagne CF, Adams PD, Vousden KH. Serine Metabolism Supports the Methionine Cycle and DNA/RNA Methylation through De Novo ATP Synthesis in Cancer Cells. Mol Cell. 2016;61:210–21.

62. Nilsson R, Jain M, Madhusudhan N, Sheppard NG, Strittmatter L, Kampf C, et al. Metabolic enzyme expression highlights a key role for MTHFD2 and the mitochondrial folate pathway in cancer. Nat Commun. 2014;5:3128.

63. Ookhtens M, Kannan R, Lyon I, Baker N. Liver and adipose tissue contributions to newly formed fatty acids in an ascites tumor. Am J Physiol. 1984;247:R146-153.

64. Williams MD, Zhang X, Park J-J, Siems WF, Gang DR, Resar LMS, et al. Characterizing metabolic changes in human colorectal cancer. Anal Bioanal Chem. 2015;407:4581–95.

65. Holla VR, Wu H, Shi Q, Menter DG, DuBois RN. Nuclear orphan receptor NR4A2 modulates fatty acid oxidation pathways in colorectal cancer. J Biol Chem. 2011;286:30003–9.

66. Carracedo A, Cantley LC, Pandolfi PP. Cancer metabolism: fatty acid oxidation in the limelight. Nat Rev Cancer. 2013;13:227–32.

67. Schafer ZT, Grassian AR, Song L, Jiang Z, Gerhart-Hines Z, Irie HY, et al. Antioxidant and oncogene rescue of metabolic defects caused by loss of matrix attachment. Nature. 2009;461:109–13.

68. Schlaepfer IR, Rider L, Rodrigues LU, Gijón MA, Pac CT, Romero L, et al. Lipid catabolism via CPT1 as a therapeutic target for prostate cancer. Mol Cancer Ther. 2014;13:2361–71.

69. Chao A, Thun MJ, Jacobs EJ, Henley SJ, Rodriguez C, Calle EE. Cigarette smoking and colorectal cancer mortality in the cancer prevention study II. J Natl Cancer Inst. 2000;92:1888–96.

70. Fedirko V, Tramacere I, Bagnardi V, Rota M, Scotti L, Islami F, et al. Alcohol drinking and colorectal cancer risk: an overall and dose-response meta-analysis of published studies. Ann Oncol Off J Eur Soc Med Oncol ESMO. 2011;22:1958–72.

71. Frezza EE, Wachtel MS, Chiriva-Internati M. Influence of obesity on the risk of developing colon cancer. Gut. 2006;55:285–91.

72. Slattery ML. Physical activity and colorectal cancer. Sports Med Auckl NZ. 2004;34:239–52.

73. Giovannucci E, Willett WC. Dietary factors and risk of colon cancer. Ann Med. 1994;26:443–52.

74. Doll R, Peto R. The causes of cancer: quantitative estimates of avoidable risks of cancer in the United States today. J Natl Cancer Inst. 1981;66:1191–308.

75. Adlercreutz H. Phytoestrogens: epidemiology and a possible role in cancer protection. Environ Health Perspect. 1995;103:103–12.

76. Bingham SA, Day NE, Luben R, Ferrari P, Slimani N, Norat T, et al. Dietary fibre in food and protection against colorectal cancer in the European Prospective Investigation into Cancer and Nutrition (EPIC): an observational study. The Lancet. 2003;361:1496–501.

77. Pericleous M, Mandair D, Caplin ME. Diet and supplements and their impact on colorectal cancer. J Gastrointest Oncol. 2013;4:409–23.

78. Garland CF, Garland FC, Gorham ED, Lipkin M, Newmark H, Mohr SB, et al. The Role of Vitamin D in Cancer Prevention. Am J Public Health. 2006;96:252–61.

79. Connelly-Frost A, Poole C, Satia JA, Kupper LL, Millikan RC, Sandler RS. Selenium, folate, and colon cancer. Nutr Cancer. 2009;61:165–78.

80. Gescher AJ, Sharma RA, Steward WP. Cancer chemoprevention by dietary constituents: a tale of failure and promise. Lancet Oncol. 2001;2:371–9.

81. Rex DK, Johnson DA, Anderson JC, Schoenfeld PS, Burke CA, Inadomi JM, et al. American College of Gastroenterology guidelines for colorectal cancer screening 2009 [corrected]. Am J Gastroenterol. 2009;104:739–50.

82. Zauber AG, Winawer SJ, O'Brien MJ, Lansdorp-Vogelaar I, van Ballegooijen M, Hankey BF, et al. Colonoscopic polypectomy and long-term prevention of colorectal-cancer deaths. N Engl J Med. 2012;366:687–96.

83. Lieberman DA, Rex DK, Winawer SJ, Giardiello FM, Johnson DA, Levin TR, et al. Guidelines for colonoscopy surveillance after screening and polypectomy: a consensus update by the US Multi-Society Task Force on Colorectal Cancer. Gastroenterology. 2012;143:844–57.

84. Nelson RL, Schwartz A. A survey of individual preference for colorectal cancer screening technique. BMC Cancer. 2004;4:76.

85. Achkar E, Moayyedi P. Colorectal cancer screening with fecal occult blood testing (FOBT): an international perspective. Am J Gastroenterol. 2006;101:212.

86. A stool DNA test (Cologuard) for colorectal cancer screening. JAMA. 2014;312:2566.

87. Anderson JC, Swede H, Rustagi T, Protiva P, Pleau D, Brenner BM, et al. Aberrant crypt foci as predictors of colorectal neoplasia on repeat colonoscopy. Cancer Causes Control CCC. 2012;23:355–61.

88. Drew DA, Devers TJ, O'Brien MJ, Horelik NA, Levine J, Rosenberg DW. HD chromoendoscopy coupled with DNA mass spectrometry profiling identifies somatic mutations in microdissected human proximal aberrant crypt foci. Mol Cancer Res MCR. 2014;12:823–9.

89. Mo A, Jackson S, Varma K, Carpino A, Giardina C, Devers TJ, et al. Distinct Transcriptional Changes and Epithelial-Stromal Interactions Are Altered in Early-Stage Colon Cancer Development. Mol Cancer Res MCR. 2016;14:795–804.

90. Bird RP. Observation and quantification of aberrant crypts in the murine colon treated with a colon carcinogen: preliminary findings. Cancer Lett. 1987;37:147–51.

91. Nascimbeni R, Villanacci V, Mariani PP, Di Betta E, Ghirardi M, Donato F, et al. Aberrant crypt foci in the human colon: frequency and histologic patterns in patients with colorectal cancer or diverticular disease. Am J Surg Pathol. 1999;23:1256–63.

92. Ochiai M, Ushigome M, Fujiwara K, Ubagai T, Kawamori T, Sugimura T, et al. Characterization of Dysplastic Aberrant Crypt Foci in the Rat Colon Induced by 2-Amino-1-Methyl-6-Phenylimidazo[4,5-b]Pyridine. Am J Pathol. 2003;163:1607–14.

93. Rosenberg DW, Yang S, Pleau DC, Greenspan EJ, Stevens RG, Rajan TV, et al. Mutations in BRAF and KRAS differentially distinguish serrated versus non-serrated hyperplastic aberrant crypt foci in humans. Cancer Res. 2007;67:3551–4.

94. Takayama T, Ohi M, Hayashi T, Miyanishi K, Nobuoka A, Nakajima T, et al. Analysis of K-ras, APC, and beta-catenin in aberrant crypt foci in sporadic adenoma, cancer, and familial adenomatous polyposis. Gastroenterology. 2001;121:599–611.

95. Anderson JC, Pleau DC, Rajan TV, Protiva P, Swede H, Brenner B, et al. Increased frequency of serrated aberrant crypt foci among smokers. Am J Gastroenterol. 2010;105:1648–54.

96. Cooper K, Squires H, Carroll C, Papaioannou D, Booth A, Logan RF, et al. Chemoprevention of colorectal cancer: systematic review and economic evaluation. Health Technol Assess Winch Engl. 2010;14:1–206.

97. US Preventive Services Task Force. Final Recommendation Statement: Aspirin Use to Prevent Cardiovascular Disease and Colorectal Cancer. 2016 Sep.

98. Potter JD. The failure of cancer chemoprevention. Carcinogenesis. 2014;35:974–82.

99. Adhami VM, Bailey HH, Mukhtar H. Cancer chemoprevention is not a failure. Carcinogenesis. 2014;35:2154–5.

100. Freudenheim JL, Graham S, Marshall JR, Haughey BP, Cholewinski S, Wilkinson G. Folate intake and carcinogenesis of the colon and rectum. Int J Epidemiol. 1991;20:368–74.

101. Meyer F, White E. Alcohol and nutrients in relation to colon cancer in middle-aged adults. Am J Epidemiol. 1993;138:225–36.

102. White E, Shannon JS, Patterson RE. Relationship between vitamin and calcium supplement use and colon cancer. Cancer Epidemiol Biomarkers Prev. 1997;6:769–74.

103. Giovannucci E, Rimm EB, Ascherio A, Stampfer MJ, Colditz GA, Willett WC. Alcohol, low-methionine - low-folate diets, and risk of colon cancer in men. J Natl Cancer Inst. 1995;87:265–73.

104. Bird CL, Swendseid ME, Witte JS, Shikany JM, Hunt IF, Frankl HD, et al. Red cell and plasma folate, folate consumption, and the risk of colorectal adenomatous polyps. Cancer Epidemiol Biomarkers Prev. 1995;4:709–14.

105. Kim Y-I, Fawaz K, Knox T, Lee YM, Norton R, Arora S, et al. Colonic mucosal concentrations of folate correlate well with blood measurements of folate status in persons with colorectal polyps. Am J Clin Nutr. 1998;68:866–72.

106. Health claims and label statements; folate and neural tube defects. Final rule. (Codified in Section 101.79, Title 21, Code of Federal Regulations). Federal Register, 61 , 8752-878.

107. Shane B. Folylpolyglutamate Synthesis and Role in the Regulation of One-Carbon Metabolism. In: G.D. Aurbach and Donald B. McCormick, editor. Vitam Horm [Internet]. Academic Press; 1989 [cited 2014 Jul 4]. page 263–335. Available from: http://www.sciencedirect.com/science/article/pii/S0083672908603970

108. Hanley MP, Rosenberg DW. One-Carbon Metabolism and Colorectal Cancer: Potential Mechanisms of Chemoprevention. Curr Pharmacol Rep. 2015;1:197–205.

109. Benito E, Stiggelbout A, Bosch FX, Obrador A, Kaldor J, Mulet M, et al. Nutritional factors in colorectal cancer risk: A case-control study in majorca. Int J Cancer. 1991;49:161–7.

110. Glynn SA, Albanes D, Pietinen P, Brown CC, Rautalahti M, Tangrea JA, et al. Colorectal cancer and folate status: a nested case-control study among male smokers. Cancer Epidemiol Biomark Prev Publ Am Assoc Cancer Res Cosponsored Am Soc Prev Oncol. 1996;5:487–94.

111. Paspatis GA, Karamanolis DG. Folate supplementation and adenomatous colonic polyps. Dis Colon Rectum. 1994;37:1340–1.

112. Su LJ, Arab L. Nutritional status of folate and colon cancer risk: evidence from NHANES I epidemiologic follow-up study. Ann Epidemiol. 2001;11:65–72.

113. Wei EK, Giovannucci E, Wu K, Rosner B, Fuchs CS, Willett WC, et al. Comparison of risk factors for colon and rectal cancer. Int J Cancer J Int Cancer. 2004;108:433–42.

114. Razzak AA, Oxentenko AS, Vierkant RA, Tillmans LS, Wang AH, Weisenberger DJ, et al. Associations between intake of folate and related micronutrients with molecularly defined colorectal cancer risks in the Iowa Women's Health Study. Nutr Cancer. 2012;64:899–910.

115. Vollset SE, Clarke R, Lewington S, Ebbing M, Halsey J, Lonn E, et al. Effects of folic acid supplementation on overall and site-specific cancer incidence during the randomised trials: meta-analyses of data on 50,000 individuals. Lancet Lond Engl. 2013;381:1029–36.

116. Ebbing M, Bønaa KH, Nygård O, Arnesen E, Ueland PM, Nordrehaug JE, et al. Cancer incidence and mortality after treatment with folic acid and vitamin B12. JAMA. 2009;302:2119–26.

117. Figueiredo JC, Grau MV, Haile RW, Sandler RS, Summers RW, Bresalier RS, et al. Folic acid and risk of prostate cancer: results from a randomized clinical trial. J Natl Cancer Inst. 2009;101:432–5.

118. Cole BF, Baron JA, Sandler RS, Haile RW, Ahnen DJ, Bresalier RS, et al. Folic acid for the prevention of colorectal adenomas: a randomized clinical trial. JAMA J Am Med Assoc. 2007;297:2351–9.

119. Baggott JE, Oster RA, Tamura T. Meta-analysis of cancer risk in folic acid supplementation trials. Cancer Epidemiol. 2012;36:78–81.

120. Le Leu RK, Young GP, McIntosh GH. Folate deficiency reduces the development of colorectal cancer in rats. Carcinogenesis. 2000;21:2261–5.

121. Song J, Medline A, Mason JB, Gallinger S, Kim YI. Effects of dietary folate on intestinal tumorigenesis in the apcMin mouse. Cancer Res. 2000;60:5434–40.

122. Kadaveru K, Protiva P, Greenspan EJ, Kim Y-I, Rosenberg DW. Dietary methyl donor depletion protects against intestinal tumorigenesis in Apc(Min/+) mice. Cancer Prev Res Phila Pa. 2012;5:911–20.

123. Kim Y-I. Folate: a magic bullet or a double edged sword for colorectal cancer prevention? Gut. 2006;55:1387–9.

124. Carreras CW, Santi DV. The catalytic mechanism and structure of thymidylate synthase. Annu Rev Biochem. 1995;64:721–62.

125. Zhang Y, Morar M, Ealick SE. Structural biology of the purine biosynthetic pathway. Cell Mol Life Sci CMLS. 2008;65:3699–724.

126. Bulock KG, Beardsley GP, Anderson KS. The Kinetic Mechanism of the Human Bifunctional Enzyme ATIC (5-Amino-4-imidazolecarboxamide Ribonucleotide Transformylase/Inosine 5'-Monophosphate Cyclohydrolase) A SURPRISING LACK OF SUBSTRATE CHANNELING. J Biol Chem. 2002;277:22168–74.

127. Hartman SC, Buchanan JM. Nucleic Acids, Purines, Pyrimidines (Nucleotide Synthesis). Annu Rev Biochem. 1959;28:365–410.

128. Odin E, Wettergren Y, Carlsson G, Gustavsson B. Determination of reduced folates in tumor and adjacent mucosa of colorectal cancer patients using LC-MS/MS. Biomed Chromatogr BMC. 2013;27:487–95.

129. Das SK, Kunkel TA, Loeb LA. Effects of altered nucleotide concentrations on the fidelity of DNA replication. Basic Life Sci. 1985;31:117–26.

130. Mathews CK. DNA precursor metabolism and genomic stability. FASEB J Off Publ Fed Am Soc Exp Biol. 2006;20:1300–14.

131. Witherspoon M, Chen Q, Kopelovich L, Gross SS, Lipkin SM. Unbiased metabolite profiling indicates that a diminished thymidine pool is the underlying mechanism of colon cancer chemoprevention by alpha-difluoromethylornithine. Cancer Discov. 2013;3:1072–81.

132. Stead LM, Au KP, Jacobs RL, Brosnan ME, Brosnan JT. Methylation demand and homocysteine metabolism: effects of dietary provision of creatine and guanidinoacetate. Am J Physiol Endocrinol Metab. 2001;281:E1095-1100.

133. Hoffman DR, Marion DW, Cornatzer WE, Duerre JA. S-Adenosylmethionine and S-adenosylhomocystein metabolism in isolated rat liver. Effects of L-methionine, L-homocystein, and adenosine. J Biol Chem. 1980;255:10822–7.

134. Wasson GR, McGlynn AP, McNulty H, O'Reilly SL, McKelvey-Martin VJ, McKerr G, et al. Global DNA and p53 region-specific hypomethylation in human colonic cells is induced by folate depletion and reversed by folate supplementation. J Nutr. 2006;136:2748–53.

135. Jhaveri MS, Wagner C, Trepel JB. Impact of Extracellular Folate Levels on Global Gene Expression. Mol Pharmacol. 2001;60:1288–95.

136. Chai H, Brown RE. Field effect in cancer-an update. Ann Clin Lab Sci. 2009;39:331–7.

137. Campbell JD, Mazzilli SA, Reid ME, Dhillon SS, Platero S, Beane J, et al. The Case for a Pre-Cancer Genome Atlas (PCGA). Cancer Prev Res Phila Pa. 2016;9:119–24.

138. Gu H, Smith ZD, Bock C, Boyle P, Gnirke A, Meissner A. Preparation of reduced representation bisulfite sequencing libraries for genome-scale DNA methylation profiling. Nat Protoc. 2011;6:468–81.

139. Hahn MA, Li AX, Wu X, Pfeifer GP. Single base resolution analysis of 5-methylcytosine and 5-hydroxymethylcytosine by RRBS and TAB-RRBS. Methods Mol Biol Clifton NJ. 2015;1238:273–87.

140. Huang DW, Sherman BT, Lempicki RA. Systematic and integrative analysis of large gene lists using DAVID bioinformatics resources. Nat Protoc. 2009;4:44–57.

141. Subramanian A, Tamayo P, Mootha VK, Mukherjee S, Ebert BL, Gillette MA, et al. Gene set enrichment analysis: a knowledge-based approach for interpreting genome-wide expression profiles. Proc Natl Acad Sci U S A. 2005;102:15545–50.

142. Heinz S, Benner C, Spann N, Bertolino E, Lin YC, Laslo P, et al. Simple combinations of lineage-determining transcription factors prime cis-regulatory elements required for macrophage and B cell identities. Mol Cell. 2010;38:576–89.

143. Amann JM, Chyla BJI, Ellis TC, Martinez A, Moore AC, Franklin JL, et al. Mtgr1 is a transcriptional corepressor that is required for maintenance of the secretory cell lineage in the small intestine. Mol Cell Biol. 2005;25:9576–85.

144. Pabst O, Zweigerdt R, Arnold HH. Targeted disruption of the homeobox transcription factor Nkx2-3 in mice results in postnatal lethality and abnormal development of small intestine and spleen. Dev Camb Engl. 1999;126:2215–25.

145. VanDussen KL, Carulli AJ, Keeley TM, Patel SR, Puthoff BJ, Magness ST, et al. Notch signaling modulates proliferation and differentiation of intestinal crypt base columnar stem cells. Dev Camb Engl. 2012;139:488–97.

146. Hill ME, Asa SL, Drucker DJ. Essential requirement for Pax6 in control of enteroendocrine proglucagon gene transcription. Mol Endocrinol Baltim Md. 1999;13:1474–86.

147. Ormestad M, Astorga J, Landgren H, Wang T, Johansson BR, Miura N, et al. Foxf1 and Foxf2 control murine gut development by limiting mesenchymal Wnt signaling and promoting extracellular matrix production. Dev Camb Engl. 2006;133:833–43.

148. Karlsson L, Lindahl P, Heath JK, Betsholtz C. Abnormal gastrointestinal development in PDGF-A and PDGFR-(alpha) deficient mice implicates a novel mesenchymal structure with putative instructive properties in villus morphogenesis. Dev Camb Engl. 2000;127:3457–66.

149. Ben-Porath I, Thomson MW, Carey VJ, Ge R, Bell GW, Regev A, et al. An embryonic stem cell-like gene expression signature in poorly differentiated aggressive human tumors. Nat Genet. 2008;40:499–507.

150. Margueron R, Reinberg D. The Polycomb complex PRC2 and its mark in life. Nature. 2011;469:343–9.

151. Enroth S, Rada-Iglesisas A, Andersson R, Wallerman O, Wanders A, Påhlman L, et al. Cancer associated epigenetic transitions identified by genome-wide histone methylation binding profiles in human colorectal cancer samples and paired normal mucosa. BMC Cancer. 2011;11:450.

152. Bhatlekar S, Fields JZ, Boman BM. HOX genes and their role in the development of human cancers. J Mol Med Berl Ger. 2014;92:811–23.

153. Fluge Ø, Gravdal K, Carlsen E, Vonen B, Kjellevold K, Refsum S, et al. Expression of EZH2 and Ki-67 in colorectal cancer and associations with treatment response and prognosis. Br J Cancer. 2009;101:1282–9.

154. Sarabi MM, Naghibalhossaini F. Association of DNA methyltransferases expression with global and gene-specific DNA methylation in colorectal cancer cells. Cell Biochem Funct. 2015;33:427–33.

155. Beggs AD, Jones A, El-Bahrawy M, El-Bahwary M, Abulafi M, Hodgson SV, et al. Whole-genome methylation analysis of benign and malignant colorectal tumours. J Pathol. 2013;229:697–704.

156. Bariol C, Suter C, Cheong K, Ku S-L, Meagher A, Hawkins N, et al. The relationship between hypomethylation and CpG island methylation in colorectal neoplasia. Am J Pathol. 2003;162:1361–71.

157. Benoit YD, Lepage MB, Khalfaoui T, Tremblay E, Basora N, Carrier JC, et al. Polycomb repressive complex 2 impedes intestinal cell terminal differentiation. J Cell Sci. 2012;125:3454–63.

158. Rauch T, Wang Z, Zhang X, Zhong X, Wu X, Lau SK, et al. Homeobox gene methylation in lung cancer studied by genome-wide analysis with a microarray-based methylated CpG island recovery assay. Proc Natl Acad Sci U S A. 2007;104:5527–32.

159. Widschwendter M, Fiegl H, Egle D, Mueller-Holzner E, Spizzo G, Marth C, et al. Epigenetic stem cell signature in cancer. Nat Genet. 2007;39:157–8.

160. Ohm JE, McGarvey KM, Yu X, Cheng L, Schuebel KE, Cope L, et al. A stem cell-like chromatin pattern may predispose tumor suppressor genes to DNA hypermethylation and heritable silencing. Nat Genet. 2007;39:237–42.

161. Schlesinger Y, Straussman R, Keshet I, Farkash S, Hecht M, Zimmerman J, et al. Polycomb-mediated methylation on Lys27 of histone H3 pre-marks genes for de novo methylation in cancer. Nat Genet. 2007;39:232–6.

162. Rada-Iglesias A, Enroth S, Andersson R, Wanders A, Påhlman L, Komorowski J, et al. Histone H3 lysine 27 trimethylation in adult differentiated colon associated to cancer DNA hypermethylation. Epigenetics. 2009;4:107–13.

163. Hahn MA, Li AX, Wu X, Yang R, Drew DA, Rosenberg DW, et al. Loss of the polycomb mark from bivalent promoters leads to activation of cancer-promoting genes in colorectal tumors. Cancer Res. 2014;74:3617–29.

164. Noordermeer D, Leleu M, Splinter E, Rougemont J, De Laat W, Duboule D. The dynamic architecture of Hox gene clusters. Science. 2011;334:222–5.

165. Haberland M, Mokalled MH, Montgomery RL, Olson EN. Epigenetic control of skull morphogenesis by histone deacetylase 8. Genes Dev. 2009;23:1625–30.

166. Freschi G, Taddei A, Bechi P, Faiella A, Gulisano M, Cillo C, et al. Expression of HOX homeobox genes in the adult human colonic mucosa (and colorectal cancer?). Int J Mol Med. 2005;16:581–7.

167. Ahlquist T, Lind GE, Costa VL, Meling GI, Vatn M, Hoff GS, et al. Gene methylation profiles of normal mucosa, and benign and malignant colorectal tumors identify early onset markers. Mol Cancer. 2008;7:94.

168. Tommasi S, Karm DL, Wu X, Yen Y, Pfeifer GP. Methylation of homeobox genes is a frequent and early epigenetic event in breast cancer. Breast Cancer Res BCR. 2009;11:R14.

169. Shaulian E, Karin M. AP-1 as a regulator of cell life and death. Nat Cell Biol. 2002;4:E131-136.

170. Ashida R, Tominaga K, Sasaki E, Watanabe T, Fujiwara Y, Oshitani N, et al. AP-1 and colorectal cancer. Inflammopharmacology. 2005;13:113–25.

171. Kong HK, Yoon S, Park JH. The regulatory mechanism of the LY6K gene expression in human breast cancer cells. J Biol Chem. 2012;287:38889–900.

172. Berman BP, Weisenberger DJ, Aman JF, Hinoue T, Ramjan Z, Liu Y, et al. Regions of focal DNA hypermethylation and long-range hypomethylation in colorectal cancer coincide with nuclear lamina-associated domains. Nat Genet. 2012;44:40–6.

173. Mason JB. Folate, cancer risk, and the Greek god, Proteus: a tale of two chameleons. Nutr Rev. 2009;67:206–12.

174. Ulrich CM, Potter JD. Folate and cancer--timing is everything. JAMA J Am Med Assoc. 2007;297:2408–9.

175. Giovannucci E. Epidemiologic studies of folate and colorectal neoplasia: a review. J Nutr. 2002;132:2350S–2355S.

176. Harnack L, Jacobs DR, Nicodemus K, Lazovich D, Anderson K, Folsom AR. Relationship of folate, vitamin B-6, vitamin B-12, and methionine intake to incidence of colorectal cancers. Nutr Cancer. 2002;43:152–8.

177. Sanjoaquin MA, Allen N, Couto E, Roddam AW, Key TJ. Folate intake and colorectal cancer risk: a meta-analytical approach. Int J Cancer. 2005;113:825–8.

178. Centers for Disease Control and Prevention (CDC). Spina bifida and anencephaly before and after folic acid mandate--United States, 1995-1996 and 1999-2000. MMWR Morb Mortal Wkly Rep. 2004;53:362–5.

179. McDowell MA, Lacher DA, Pfeiffer CM, Mulinare J, Picciano MF, Rader JI, et al. Blood folate levels: the latest NHANES results. NCHS Data Brief. 2008;1–8.

180. Kim G, Baik SH, Lee KY, Hur H, Min BS, Lyu CJ, et al. Colon carcinoma in childhood: review of the literature with four case reports. Int J Colorectal Dis. 2013;28:157–64.

181. Boroff ES, Gurudu SR, Hentz JG, Leighton JA, Ramirez FC. Polyp and adenoma detection rates in the proximal and distal colon. Am J Gastroenterol. 2013;108:993–9.

182. Drew DA, Goh G, Mo A, Grady JJ, Forouhar F, Egan G, et al. Colorectal polyp prevention by daily aspirin use is abrogated among active smokers. Cancer Causes Control CCC. 2015;

183. Hemmasi G, Sohrabi M, Zamani F, Ajdarkosh H, Rakhshani N, Khoonsari M, et al. Prevalence of colorectal adenoma in an average-risk population aged 40-50 versus 50-60 years. Eur J Cancer Prev Off J Eur Cancer Prev Organ ECP. 2015;24:386–90.

184. Choumenkovitch SF, Selhub J, Wilson PWF, Rader JI, Rosenberg IH, Jacques PF. Folic acid intake from fortification in United States exceeds predictions. J Nutr. 2002;132:2792–8.

185. Wagner C. Biochemical role of folate in cellular metabolism. Folate Health Dis. Second Edition. New York: Marcel Dekker; 1995. page 23–42.

186. Kräutler B. Vitamin B12: chemistry and biochemistry. Biochem Soc Trans. 2005;33:806–10.

187. Kelemen LE. The role of folate receptor alpha in cancer development, progression and treatment: cause, consequence or innocent bystander? Int J Cancer J Int Cancer. 2006;119:243–50.

188. Bulgar AD, Weeks LD, Miao Y, Yang S, Xu Y, Guo C, et al. Removal of uracil by uracil DNA glycosylase limits pemetrexed cytotoxicity: overriding the limit with methoxyamine to inhibit base excision repair. Cell Death Dis. 2012;3:e252.

189. Moser AR, Luongo C, Gould KA, McNeley MK, Shoemaker AR, Dove WF. ApcMin: a mouse model for intestinal and mammary tumorigenesis. Eur J Cancer Oxf Engl 1990. 1995;31A:1061–4.

190. Colnot S, Niwa-Kawakita M, Hamard G, Godard C, Le Plenier S, Houbron C, et al. Colorectal cancers in a new mouse model of familial adenomatous polyposis: influence of genetic and environmental modifiers. Lab Invest. 2004;84:1619–30.

191. Nakanishi M, Montrose DC, Clark P, Nambiar PR, Belinsky GS, Claffey KP, et al. Genetic deletion of mPGES-1 suppresses intestinal tumorigenesis. Cancer Res. 2008;68:3251–9.

192. Janakiram NB, Rao CV. Molecular markers and targets for colorectal cancer prevention. Acta Pharmacol Sin. 2008;29:1–20.

193. St Clair WH, Osborne JW. Crypt fission and crypt number in the small and large bowel of postnatal rats. Cell Tissue Kinet. 1985;18:255–62.

194. Fischer JM, Schepers AG, Clevers H, Shibata D, Liskay RM. Occult progression by Apc-deficient intestinal crypts as a target for chemoprevention. Carcinogenesis. 2014;35:237–46.

195. Berlanga-Acosta J, Playford RJ, Mandir N, Goodlad RA. Gastrointestinal cell proliferation and crypt fission are separate but complementary means of increasing tissue mass following infusion of epidermal growth factor in rats. Gut. 2001;48:803–7.

196. Takahashi H, Hosono K, Endo H, Nakajima A. Colon epithelial proliferation and carcinogenesis in diet-induced obesity. J Gastroenterol Hepatol. 2013;28 Suppl 4:41–7.

197. Nakanishi Y, Seno H, Fukuoka A, Ueo T, Yamaga Y, Maruno T, et al. Dclk1 distinguishes between tumor and normal stem cells in the intestine. Nat Genet. 2013;45:98–103.

198. Westphalen CB, Asfaha S, Hayakawa Y, Takemoto Y, Lukin DJ, Nuber AH, et al. Long-lived intestinal tuft cells serve as colon cancer-initiating cells. J Clin Invest. 2014;124:1283–95.

199. Buchman AL, Dubin MD, Moukarzel AA, Jenden DJ, Roch M, Rice KM, et al. Choline deficiency: a cause of hepatic steatosis during parenteral nutrition that can be reversed with intravenous choline supplementation. Hepatol Baltim Md. 1995;22:1399–403.

200. Courtemanche C, Elson-Schwab I, Mashiyama ST, Kerry N, Ames BN. Folate deficiency inhibits the proliferation of primary human CD8+ T lymphocytes in vitro. J Immunol Baltim Md 1950. 2004;173:3186–92.

201. Keith MO, Tryphonas L. Choline deficiency and the reversibility of renal lesions in rats. J Nutr. 1978;108:434–46.

202. Brunt EM. Pathology of fatty liver disease. Mod Pathol. 2007;20:S40–8.

203. Kim Y-I. Folate and colorectal cancer: an evidence-based critical review. Mol Nutr Food Res. 2007;51:267–92.

204. Ericson U, Sonestedt E, Gullberg B, Olsson H, Wirfält E. High folate intake is associated with lower breast cancer incidence in postmenopausal women in the Malmö Diet and Cancer cohort. Am J Clin Nutr. 2007;86:434–43.

205. Song J, Sohn KJ, Medline A, Ash C, Gallinger S, Kim YI. Chemopreventive effects of dietary folate on intestinal polyps in Apc+/-Msh2-/- mice. Cancer Res. 2000;60:3191–9.

206. Fischer JM, Miller AJ, Shibata D, Liskay RM. Different phenotypic consequences of simultaneous versus stepwise Apc loss. Oncogene. 2012;31:2028–38.

207. Lipkin M. Biomarkers of increased susceptibility to gastrointestinal cancer: new application to studies of cancer prevention in human subjects. Cancer Res. 1988;48:235–45.

208. Lasko CM, Bird RP. Modulation of aberrant crypt foci by dietary fat and caloric restriction: the effects of delayed intervention. Cancer Epidemiol Biomark Prev Publ Am Assoc Cancer Res Cosponsored Am Soc Prev Oncol. 1995;4:49–55.

209. Mills SJ, Mathers JC, Chapman PD, Burn J, Gunn A. Colonic crypt cell proliferation state assessed by whole crypt microdissection in sporadic neoplasia and familial adenomatous polyposis. Gut. 2001;48:41–6.

210. Tammariello AE, Milner JA. Mouse models for unraveling the importance of diet in colon cancer prevention. J Nutr Biochem. 2010;21:77–88.

211. Lin CC, Lu YP, Lou YR, Ho CT, Newmark HH, MacDonald C, et al. Inhibition by dietary dibenzoylmethane of mammary gland proliferation, formation of DMBA-DNA adducts in mammary glands, and mammary tumorigenesis in Sencar mice. Cancer Lett. 2001;168:125–32.

212. Barone M, Notarnicola M, Caruso MG, Scavo MP, Viggiani MT, Tutino V, et al. Olive oil and omega-3 polyunsaturated fatty acids suppress intestinal polyp growth by modulating the apoptotic process in ApcMin/+ mice. Carcinogenesis. 2014;35:1613–9.

213. Kim Y-I. Folate and carcinogenesis: evidence, mechanisms, and implications. J Nutr Biochem. 1999;10:66–88.

214. Crott JW, Liu Z, Keyes MK, Choi S-W, Jang H, Moyer MP, et al. Moderate folate depletion modulates the expression of selected genes involved in cell cycle, intracellular signaling and folate uptake in human colonic epithelial cell lines. J Nutr Biochem. 2008;19:328–35.

215. Yu D-H, Gadkari M, Zhou Q, Yu S, Gao N, Guan Y, et al. Postnatal epigenetic regulation of intestinal stem cells requires DNA methylation and is guided by the microbiome. Genome Biol. 2015;16:211.

216. Shyh-Chang N, Locasale JW, Lyssiotis CA, Zheng Y, Teo RY, Ratanasirintrawoot S, et al. Influence of threonine metabolism on S-adenosylmethionine and histone methylation. Science. 2013;339:222–6.

217. Giannakis M, Stappenbeck TS, Mills JC, Leip DG, Lovett M, Clifton SW, et al. Molecular properties of adult mouse gastric and intestinal epithelial progenitors in their niches. J Biol Chem. 2006;281:11292–300.

218. Kwatra D, Subramaniam D, Ramamoorthy P, Standing D, Moran E, Velayutham R, et al. Methanolic extracts of bitter melon inhibit colon cancer stem cells by affecting energy homeostasis and autophagy. Evid-Based Complement Altern Med ECAM. 2013;2013:702869.

219. Kim Y-I. Role of folate in colon cancer development and progression. J Nutr. 2003;133:3731S–3739S.

220. Hanley MP, Kadaveru K, Perret C, Giardina C, Rosenberg DW. Dietary Methyl Donor Depletion Suppresses Intestinal Adenoma Development. Cancer Prev Res Phila Pa. 2016;9:812–20.

221. Mentch SJ, Locasale JW. One-carbon metabolism and epigenetics: understanding the specificity. Ann N Y Acad Sci. 2016;1363:91–8.

222. Obeid R. The metabolic burden of methyl donor deficiency with focus on the betaine homocysteine methyltransferase pathway. Nutrients. 2013;5:3481–95.

223. Gonen N, Assaraf YG. Antifolates in cancer therapy: structure, activity and mechanisms of drug resistance. Drug Resist Updat Rev Comment Antimicrob Anticancer Chemother. 2012;15:183–210.

224. Evans AM, DeHaven CD, Barrett T, Mitchell M, Milgram E. Integrated, nontargeted ultrahigh performance liquid chromatography/electrospray ionization tandem mass spectrometry platform for the identification and relative quantification of the small-molecule complement of biological systems. Anal Chem. 2009;81:6656–67.

225. Ohta T, Masutomi N, Tsutsui N, Sakairi T, Mitchell M, Milburn MV, et al. Untargeted metabolomic profiling as an evaluative tool of fenofibrate-induced toxicology in Fischer 344 male rats. Toxicol Pathol. 2009;37:521–35.

226. Xia J, Sinelnikov IV, Han B, Wishart DS. MetaboAnalyst 3.0--making metabolomics more meaningful. Nucleic Acids Res. 2015;43:W251-257.

227. McBean GJ. The transsulfuration pathway: a source of cysteine for glutathione in astrocytes. Amino Acids. 2012;42:199–205.

228. Ajouz H, Mukherji D, Shamseddine A. Secondary bile acids: an underrecognized cause of colon cancer. World J Surg Oncol. 2014;12:164.

229. Vaz FM, Wanders RJA. Carnitine biosynthesis in mammals. Biochem J. 2002;361:417–29.

230. Beyer RE. The role of ascorbate in antioxidant protection of biomembranes: interaction with vitamin E and coenzyme Q. J Bioenerg Biomembr. 1994;26:349–58.

231. Bolati D, Shimizu H, Yisireyili M, Nishijima F, Niwa T. Indoxyl sulfate, a uremic toxin, downregulates renal expression of Nrf2 through activation of NF-κB. BMC Nephrol. 2013;14:56.

232. Gaweł S, Wardas M, Niedworok E, Wardas P. [Malondialdehyde (MDA) as a lipid peroxidation marker]. Wiad Lek Wars Pol 1960. 2004;57:453–5.

233. Cellarier E, Durando X, Vasson MP, Farges MC, Demiden A, Maurizis JC, et al. Methionine dependency and cancer treatment. Cancer Treat Rev. 2003;29:489–99.

234. Komninou D, Leutzinger Y, Reddy BS, Richie JP. Methionine restriction inhibits colon carcinogenesis. Nutr Cancer. 2006;54:202–8.

235. Kusakabe Y, Ishihara M, Umeda T, Kuroda D, Nakanishi M, Kitade Y, et al. Structural insights into the reaction mechanism of S-adenosyl-L-homocysteine hydrolase. Sci Rep. 2015;5:16641.

236. Deguchi T, Barchas J. Inhibition of transmethylations of biogenic amines by S-adenosylhomocysteine. Enhancement of transmethylation by adenosylhomocysteinase. J Biol Chem. 1971;246:3175–81.

237. Oliva A, Galletti P, Zappia V, Paik WK, Kim S. Studies on substrate specificity of S-adenosylmethionine: protein-carboxyl methyltransferase from calf brain. Eur J Biochem FEBS. 1980;104:595–602.

238. Caudill MA, Wang JC, Melnyk S, Pogribny IP, Jernigan S, Collins MD, et al. Intracellular S-adenosylhomocysteine concentrations predict global DNA hypomethylation in tissues of methyl-deficient cystathionine beta-synthase heterozygous mice. J Nutr. 2001;131:2811–8.

239. Feil R. Environmental and nutritional effects on the epigenetic regulation of genes. Mutat Res. 2006;600:46–57.

240. I. W. Cook, E. L. Kennaway, N. M. Kennaway. Production of tumors in mice by deoxycholic acid. Nature. 1940;145.

241. Payne CM, Bernstein C, Dvorak K, Bernstein H. Hydrophobic bile acids, genomic instability, Darwinian selection, and colon carcinogenesis. Clin Exp Gastroenterol. 2008;1:19–47.

242. Khare S, Mustafi R, Cerda S, Yuan W, Jagadeeswaran S, Dougherty U, et al. Ursodeoxycholic acid suppresses Cox-2 expression in colon cancer: roles of Ras, p38, and CCAAT/enhancer-binding protein. Nutr Cancer. 2008;60:389–400.

243. Rodrigues CM, Kren BT, Steer CJ, Setchell KD. The site-specific delivery of ursodeoxycholic acid to the rat colon by sulfate conjugation. Gastroenterology. 1995;109:1835–44.

244. May R, Qu D, Weygant N, Chandrakesan P, Ali N, Lightfoot SA, et al. Brief report: Dclk1 deletion in tuft cells results in impaired epithelial repair after radiation injury. Stem Cells Dayt Ohio. 2014;32:822–7.

245. Samudio I, Harmancey R, Fiegl M, Kantarjian H, Konopleva M, Korchin B, et al. Pharmacologic inhibition of fatty acid oxidation sensitizes human leukemia cells to apoptosis induction. J Clin Invest. 2010;120:142–56.

246. Aruoma OI, Halliwell B, Hoey BM, Butler J. The antioxidant action of taurine, hypotaurine and their metabolic precursors. Biochem J. 1988;256:251–5.

247. Wu G, Fang Y-Z, Yang S, Lupton JR, Turner ND. Glutathione metabolism and its implications for health. J Nutr. 2004;134:489–92.

248. Bánhegyi G, Braun L, Csala M, Puskás F, Mandl J. Ascorbate metabolism and its regulation in animals. Free Radic Biol Med. 1997;23:793–803.

249. Woo DK, Green PD, Santos JH, D'Souza AD, Walther Z, Martin WD, et al. Mitochondrial genome instability and ROS enhance intestinal tumorigenesis in APC(Min/+) mice. Am J Pathol. 2012;180:24–31.

250. Cheung KL, Lee JH, Khor TO, Wu T-Y, Li GX, Chan J, et al. Nrf2 knockout enhances intestinal tumorigenesis in Apc(min/+) mice due to attenuation of anti-oxidative stress pathway while potentiates inflammation. Mol Carcinog. 2014;53:77–84.

251. Papaioannou D, Cooper KL, Carroll C, Hind D, Squires H, Tappenden P, et al. Antioxidants in the chemoprevention of colorectal cancer and colorectal adenomas in the general population: a systematic review and meta-analysis. Colorectal Dis Off J Assoc Coloproctology G B Irel. 2011;13:1085–99.

252. Vece MM, Agnoli C, Grioni S, Sieri S, Pala V, Pellegrini N, et al. Dietary Total Antioxidant Capacity and Colorectal Cancer in the Italian EPIC Cohort. PloS One. 2015;10:e0142995.

253. Locasale JW. Serine, glycine and the one-carbon cycle: cancer metabolism in full circle. Nat Rev Cancer. 2013;13:572–83.

254. Jonges GN, Vogels IM, Bosch KS, Dingemans KP, Van Noorden CJ. Experimentally induced colon cancer metastases in rat liver increase the proliferation rate and capacity for purine catabolism in liver cells. Histochemistry. 1993;100:41–51.

255. Ong ES, Zou L, Li S, Cheah PY, Eu KW, Ong CN. Metabolic profiling in colorectal cancer reveals signature metabolic shifts during tumorigenesis. Mol Cell Proteomics MCP. 2010;

256. Shinohara Y, Hasegawa H, Ogawa K, Tagoku K, Hashimoto T. Distinct effects of folate and choline deficiency on plasma kinetics of methionine and homocysteine in rats. Metabolism. 2006;55:899–906.

257. Selhub J, Seyoum E, Pomfret EA, Zeisel SH. Effects of choline deficiency and methotrexate treatment upon liver folate content and distribution. Cancer Res. 1991;51:16–21.

258. Lu SC, Alvarez L, Huang ZZ, Chen L, An W, Corrales FJ, et al. Methionine adenosyltransferase 1A knockout mice are predisposed to liver injury and exhibit increased expression of genes involved in proliferation. Proc Natl Acad Sci U S A. 2001;98:5560–5.

259. Feinberg AP, Ohlsson R, Henikoff S. The epigenetic progenitor origin of human cancer. Nat Rev Genet. 2006;7:21–33.

260. Sato T, Vries RG, Snippert HJ, van de Wetering M, Barker N, Stange DE, et al. Single Lgr5 stem cells build crypt-villus structures in vitro without a mesenchymal niche. Nature. 2009;459:262–5.

261. Nielsen M, Bik E, Hes FJ, Breuning MH, Vasen HFA, Bakker E, et al. Genotype–phenotype correlations in 19 Dutch cases with APC gene deletions and a literature review. Eur J Hum Genet. 2007;15:1034–42.

262. Møllersen L, Paulsen JE, Alexander J. Loss of heterozygosity and nonsense mutation in Apc in azoxymethane-induced colonic tumours in min mice. Anticancer Res. 2004;24:2595–9.

263. Thiagalingam S, Laken S, Willson JKV, Markowitz SD, Kinzler KW, Vogelstein B, et al. Mechanisms underlying losses of heterozygosity in human colorectal cancers. Proc Natl Acad Sci. 2001;98:2698–702.

264. Durand P, Prost M, Blache D. Folate deficiencies and cardiovascular pathologies. Clin Chem Lab Med. 1998;36:419–29.